2021

Real time adaptive relay settings for Microgrid protection verified using Hardware in Loop

Aadam Harnekar
Michigan Technological University, aharneka@mtu.edu

REAL-TIME ADAPTIVE RELAY SETTINGS FOR MICROGRID PROTECTION VERIFIED USING HARDWARE IN LOOP

By

Aadam Ismail Harnekar

A REPORT

Submitted in partial fulfillment of the requirements for the degree of

MASTER OF SCIENCE

In Electrical Engineering

MICHIGAN TECHNOLOGICAL UNIVERSITY

2021

This report has been approved in partial fulfillment of the requirements for the Degree of MASTER OF SCIENCE in Electrical Engineering.

Department of Electrical and Computer Engineering

Thesis Advisor:	*Dr. Bruce A. Mork*
Committee Member:	*Dr. Glen Archer*
Committee Member:	*Dr. Leonard Bohmann*
Department Chair:	*Dr. Glen Archer*

Dedication

To my Father who had a dream to see me achieve great heights and always pushed me forward. I lost him in the midst of this project, but he will be very happy to see me complete his dream from wherever he is! Mother, who motivates me to never look back, whatever happens in life and whose hope for life is my success.

Teachers and friends who always had my back and didn't hesitate to criticize my work at every stage - without which I would neither be who I am nor would this work be what it is today.

Contents

List of Figures

List of Tables

Preface

I present here a masters report on "Real time adaptive relay settings using OPAL-RT for microgrid protection." It has been written to fulfill the graduation requirements of Master of Science in Electrical Engineering program at Michigan Technological University. I was engaged in researching and writing this report from January 2020 to April 2021.

The need for this research arose when I came across microgrid protection issues and the benefits of testing a protection system in real time using OPAL-RT. It was a long journey through the global pandemic which forced me to get the whole system remotely accessible. I had to learn from scratch about OPAL-RT and build the whole system through a lot of troubleshooting.

I would like to thank my colleagues Aamir, Joel, Gaurish and Justin for helping me throughout this research to setup the remotely accessible lab.

I hope you find the work an interesting read and that you enjoy it!

Acknowledgments

I would like to thank all those who have helped me learn, understand and appreciate this subject as well as those who helped me with the research ideas on this project. I would like especially thank Dr. Bruce A. Mork for giving me this opportunity to research under his guidance. Dr. Mork has always been open to new ideas and supported me with the necessary guidance and resources.

This project would not have been a success without the help of my collegues Aamir, Joel, Gaurish and Justin. They helped me setup the hardware and troubleshoot issues that arose at various stage of this project. I would also like to thank all of them for all the time and effort they put in to help me.

List of Abbreviations

AI	Analog Input
AO	Analog Output
DI	Digital Input
DO	Digital Output
RTS	Real Time Simulation
SLG	Single Line to Ground
PCC	Point of Common Coupling
SER	Sequential Event Record
DG	Distributed Generator

Abstract

Microgrids with penetration of renewables is imposing new challenges for system protection. Renewables are characterized with high source impedance which limit the short circuit current. The value of short-circuit current is limited due to converters used which limit the current to a maximum of 1.1 to 1.5 times maximum rated load current. This can result in faults during the islanded mode of microgrid to go unnoticed if the relay settings are not adapted to account for it. The presence of such uncleared faults in the microgrid can result in exposing it to overcurrent for a long time which can damage the equipment. One solution is to have different protection element pickup settings for different modes of operation. This report discusses the development of an algorithm to switch these settings upon microgrid state changes and test the algorithm using OPAL-RT hardware in loop real-time testing with SEL-351S relay as the hardware.

Adaptive settings group change algorithm depending on the microgrid state is the base case that this project is build on. A novel algorithm approach for dynamic settings change is developed which doesn't require a settings group change. This algorithm overcomes the drawback of settings group change method. The algorithm was developed on SEL-351S Relay and tested in real time using OPAL-RT on an IEEE 5-bus system which was modified into a microgrid. The algorithm implemented here using SEL-351S relay is limited to only four group settings. Thus, an algorithm for SEL-451 relay is also discussed as a future implementation which is limited to number of input contacts if hardwired or limited to bits if remote bits are used.

Chapter 1

Introduction

An increase in demand for energy due to industrial development, rise in population, and other factors has resulted in an increased load factor. Power system reliability issues arise from this high load demand which is a big issue. Gap between supply and demand of electricity results in large number of outages and blackouts in the grid all over the world which has a huge impact on the economy [1]. The rising cost of fuel, low generation efficiency and environmental pollution have forced the governments and other private agencies all over the world to increase the penetration of Distributed Energy Resources(DER) in the power grid to meet the rising demand of energy. Solar, Wind, Energy Storage,etc. are considered as the main DER's. Intermittent operation and low power generation capacity per unit of these DER's has motivated to combine them to form small grids called as 'Microgrids' [1].

1.1 Problem Statement

A microgrid is similar to a traditional distribution system but has DER added to it. Microgrids can operate in grid-connected or islanded modes depending on the power demand and local source generation. The conventional distribution systems can be converted into microgrids by adding DER and a circuit breaker with protection and control to serve as a Point of Common Coupling. Since the system is no longer passive and radical, these microgrids come with their set of protection challenges and conventional protection strategies become inadequate.

A typical microgrid is shown in Figure 1.1 which depicts the common microgrid components. When Circuit Breaker at Point of Common Coupling (PCC) opens, Microgrid goes in islanded mode. If the relay settings in this mode are still the same (not adapted); the microgrid is rendered without protection during islanded mode.

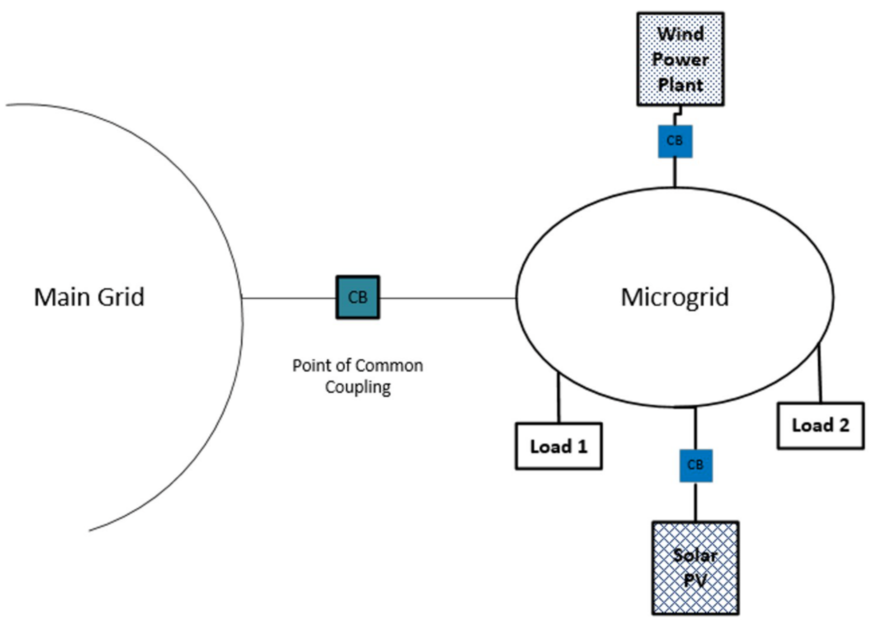

Figure 1.1: Typical Microgrid

It is then imperative to develop protection strategies that are robust for microgrid protection in grid-connected as well as islanded mode of operation. Various authors have worked on this issue and come up with promising protection strategies which are discussed in detail in Chapter 2. The implications of their research is studied and a justifiable protection strategy is selected as a base case scenario. The protection strategy is developed by considering different operating scenarios and implementing an algorithm for adaptive overcurrent protection of microgrid feeders. The developed algorithm is validated on actual hardware by testing it before it is implemented for real world application.

1.2 Scope of Research

The scope of this research involves developing an adaptive overcurrent protection algorithm for microgrid protection and testing it on standard test buses as recommended by IEEE. The algorithm is implemented on an SEL-351S relay which is a popular protective relay for distribution systems. The implementation is then tested on OPAL-RT to perform real-time simulation and test the adaptive settings change in real time.

IEEE 5 bus is used as a base case scenario. This system is further modified to include distributed generators. It is tested to mimic grid connected as well as islanded mode of operation. The protection settings developed are tested for both modes of operation and also verified for presence of different distributed generators. The development of protection settings involved selecting a load and a line as test location. Primary and backup protection for relays at those locations during various modes of microgrid is done by conducting coordination studies.

Chapter 2

Background

The protection of microgrids has become a challenge due to various issues that have arisen from the inverters having high source impedance and low short circuit sourcing currents. Various researchers have made considerable progress in developing protection schemes for it. This chapter walks through the different issues in microgrid protection, contributions of various authors in microgrid protection, advantages of adaptive over-current protection. Further it discusses the work of different authors on developing adaptive overcurrent protection algorithms to protect microgrids in both modes of operation.

2.1 Microgrids

The Department of Energy defines a "microgrid" as follows[2]

"a group of interconnected loads and distributed energy resources within clearly defined electrical boundaries that acts as a single controllable entity with respect to the grid. A microgrid can connect and disconnect from the grid to enable it to operate in both grid-connected or islanded mode."

Microgrids usually have distributed generators that can feed the local loads and supply power onto the main grid when there is an excess generation. The distributed generators in a microgrid consists of numerous independently controlled power generating sources for reliable and flexible grid infrastructure [3]. Microgrids have installed capacity of few kilowatts to megawatts. The prime objective of a microgrid is to add flexibility and reliability to distribution system, provide power to consumers at remote areas, critical industrial and military infrastructure. The fundamental microgrid components are protection and isolation devices at the point of common coupling (PCC), Distributed Generators (DG) which include rotating machines and Renewable Energy Sources (RES) such as solar, wind, fuel cell and Combined Heat Power (CHP), and local load to be fed by these DG's. In addition, a microgrid also includes controllers that are responsible for local and distributed control operations [3].

Microgrids can function in two modes: independently of the network called "Islanded mode", or connected to the network, know as "Grid-connected mode." Microgrids have all the fundamental components of a conventional grid such as power plant and loads; with the difference that its a scaled down model and has very short lengths of line connecting the loads to the source [3]. Microgrids can be considered as a system to integrate distributed generators at consumer end on low-voltage side to make the customer an active participant in the grid [4], thus making them a "Prosumer" of electricity instead of just being a consumer. Microgrid offers numerous benefits such as better system efficiency, reduced cost of generation, transmission and distribution, improved power quality and added system reliability. Its also makes the grid more resilient. Despite the numerous advantages microgrid offers, it comes with its own challenges in terms of implementation, operation, control and more specifically protection [4]. The conventional distribution system can be converted to a microgrid by adding some distributed generators and some controllers to control the power flow. These distributed generators meet the power requirements of local load and export the power to main grid if it is in excess, as well as import the power from main grid when required. Doing so results in bidirectional power flow in the system. This bidirectional power flow makes the conventional radial protection systems inadequate [4]. The operating times of protecting devices become unpredictable due to DG's contributing to the fault current and the lack of directionality leads to loss of protection coordination. Also, in the case of microgrids with different DG capacities and types the fault current will be of varied levels resulting in more degradation of protection coordination. "Blinding" and "Sympathetic tripping" are the expected events that result due to loss of protection coordination [4].

2.2 Microgrid Protection issues

Integration of microgrid to existing grid gives rise to major protection issues for the classical protection techniques implemented for conventional grid and demands an adaptive, smart and upgraded protection system [5]. Following are some of the major issues that require immediate attention and resolution.

2.2.1 Bidirectional Power flow

Microgrid integration to distribution network converts it from passive to an active network. Microgrid feeds the local load and when it has excess generation; it is required to export power to the main grid in reverse direction. This makes the power flow of microgrid bidirectional in nature which affects the magnitude and direction of fault current; thus affecting protection coordination [5]. Traditional overcurrent element without sense of directionality cannot distinguish between forward and reverse faults and thus can result in undesired tripping [6].

2.2.2 Reduction in short circuit fault current level

The fault current sourced by distributed generators is very low as compared to those one sourced by main grid, thus reducing the expected overall short circuit fault current level when connected to main grid. Moreover, in the case of islanded mode of operation and microgrid with inverter-based generators; the short-circuit fault current level is reduced drastically as the power electronic converters limit the short circuit current in order to protect the thyristors from thermal damage due to high currents. It is to detect the faults in such a system with low fault currents [5] [6].

2.2.3 Frequent Change in Microgrid configuration

Frequent changing of microgrid states from islanded to grid connected and vice-versa results in changes in short-circuit fault current capacity of the system. This frequent change in short circuit fault current level complicates overcurrent protection [5].

2.2.4 Selectivity and Sensitivity of an Overcurrent Relay

Selectivity is a very important characteristic of a protection system. Protection must be able to distinguish between the faults and isolate only the section of the system which has the fault. Protection system for microgrid must be able to differentiate between the faults occurring on main grid and microgrid. For the faults on main grid, isolation of microgrid must be done to protect the microgrid. On the other hand, for faults on microgrid, only the faulted section must be isolated. The relays should be sensitive enough without compromising the selectivity of the protection system [5].

2.2.5 Protection Blinding

Protection blinding results due to current infeed from the microgrid to the main grid. Figure 2.1 shows a simplified depiction to describe protection blinding. It is evident from the figure that for the fault shown in the system; relay R1 may not be able to detect due to the infeed current from the microgrid and will become blind for these faults. Relay R1 is required to detect this fault as a backup for relay R2. But due to protection blinding, Relay R2 loses its backup protection [6].

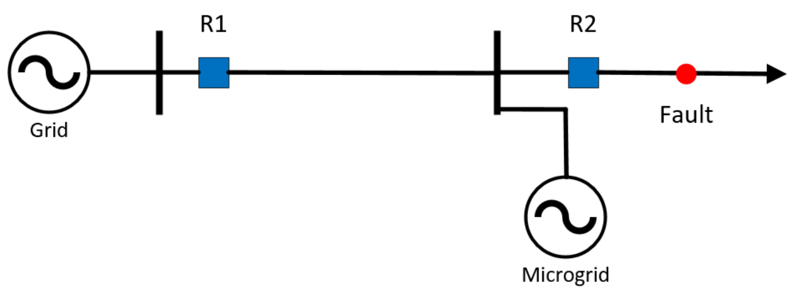

Figure 2.1: Protection Blinding

2.2.6 Sympathetic Tripping

If a relay in a healthy feeder trips falsely due to back-flow of current from the connected microgrid; this is called Sympathetic Tripping. In Figure 2.2 the fault will also be fed by microgrid M2; this fault current will flow through R3 and result in tripping

R3 for a fault which is on another line. The probability of such sympathetic tripping will increase as the microgrid approaches the relay R3 [6].

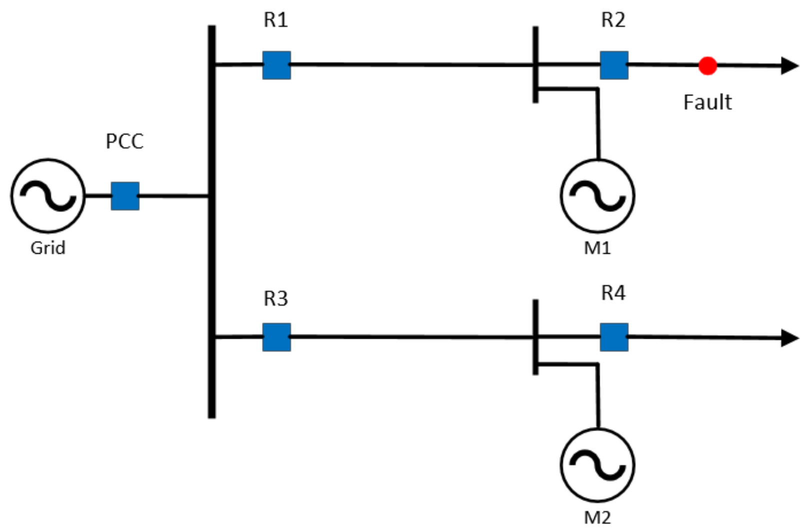

Figure 2.2: Sympathetic Tripping

2.3 Microgrid Protection Methods

Microgrid protection requires different protection schemes as compared to the conventional schemes due to the issues discussed in the preceding section. Many such protection schemes have been proposed for AC microgrid. These schemes can be grouped based on their fundamental operating mechanisms as adaptive protection based, differential protection based, travelling wave based and other protective methods [6]. Following section describes these methods in details and uses the background search done by [6] as a base for literature review on microgrid protection methods.

2.3.1 Adaptive Protection Based Methods

The process of changing the relay settings automatically as per the system conditions is called Adaptive Protection. Adaptive Protection helps in modification of the relay settings for a system to work in an optimal condition. The adaptive protection can be categorized as off-line or online protection as per the protection logic. In the off-line method, the fault analysis would be performed off-line and all the DG status as well as all the possible system configurations will be recorded for performing the analysis whose result would be used to generate an event table. The relay settings would be calculated by using the generated event table. Practically, it is very difficult to forecast all the possible fault cases in a microgrid due to the intermittent nature of renewable energy sources. This makes it really difficult to implement the off-line adaptive protection in a practical scenario. The online method makes use of Equation 2.1 wherein "mode of operation" decides the fault contribution from main grid. The value of 'mode of operation' is 1 for grid connected mode and is 0 for islanded mode which is the first part of the equation. The second part of the equation uses a number of parameters such as DG status, type of DG's (inverter or synchronous based) and quantity of DG's. These status are used dynamically and are fed in real time to the protection system to adapt it logic depending on the system condition. Thus, it is called online adaptive protection [6].

$$\begin{aligned} \mathrm{I_{relay\_set}} &= \mathrm{I_{Fault\_Grid}} \times \mathrm{Mode\,of\,operation} + \\ &\sum\nolimits_{\mathrm{i=1}}^{\mathrm{n}} \left(\mathrm{Impact\,factor(K_i)} \times \mathrm{I_{Faultt-DG_i}} \times \mathrm{DG_i\,status}\right) \end{aligned} \tag{2.1}$$

2.3.2 Differential Protection Based methods

Differential protection is one of the popular method of protection used in power system at various stages. It is also a popular method utilized for microgrid protection. The implementation of differential protection applied to microgrid is explained in [7] which gives insight into the basic operating fundamentals and tests the protection for grid connected as well as islanded mode. Fault current variation, bi-directional power flow, DG status and changes in system configuration do not have much impact on current differential protection as shown in [8]. As per the protection scheme presented in [9], all the relays are digital which can sample currents at more than 16 samples per cycle and are equipped with communication capability. In the presented scheme, relays are implemented at both end of the protected line and the sampled current data flows over communication channel installed between them. If the difference of current is greater than the set threshold limit, the relays operates and send a signal to respective circuit breaker to open up. The main drawback of this scheme is the cost of implementation as this scheme requires use of synchronous measurement and communication channel. An optimal differential protection scheme to reduce the cost of implementation is presented by the author in [10]. In this scheme, the relay at remote end is replaced by a cheap sensor due to which the cost of implementation is almost reduced by half. This scheme has no supported result evidence and cannot be relied on. Furthermore, there are certain schemes which use the concept of spectral energy at both ends as shown in [11]. The tripping logic is similar to current differential but is based on energy difference being greater than the set threshold. The issue with this scheme is setting a proper threshold as it depends on various factors such as fault impedance and operating mode of the microgrid.

2.3.3 Travelling Wave Based methods

Traveling wave-based methods have become popular with the advent of traveling wave relays which are very fast and operate within a half-power cycle as discussed in [12]. The traveling wave method has emerged as a popular one for protecting EHV and UHV transmission lines as well as HVDC systems [13]. In the case of microgrids, this method is rarely being used due to the limitation factors such as high sampling frequency, noise disturbance and short length of line [14]. Some researchers have developed improved traveling wave-based fault detection algorithms for converter-dominated microgrids based on mathematical morphology which captures the initial polarity of the initial current traveling wave as discussed by the author in [15]. The details on this morphology is can be found in [16]. This protection scheme has a good performance and is not affected by noise, high fault impedance, switching of grid states as well as transient microgrid conditions. However, even this scheme has the limitation of high requirement of sampling frequency which is an issue with short lines of feeder in the case of microgrids.

2.3.4 Other Protective methods

There are other protection methods apart from the above-mentioned ones and are described in detail in [6]. These methods are Voltage based methods, total harmonic based methods, and phasor based methods. Voltage based method is based on the Park transform of voltages and uses a threshold for making a trip decision similar to the differential energy-based method. This method is threshold dependent and setting up the value of the threshold is a very critical task. The total harmonic based method is also a threshold-based method that faces the same drawback as the voltage-based method. The phasor-based method uses the information on pre-fault and post-fault phase angles and has an advantage over other methods but it can only be implemented in grid-connected mode as the angle variation cannot be relied upon during islanded mode.

2.4 Literature Survey on Adaptive Protection methods

From the above discussion, it is evident that adaptive protection is a justifiable solution for microgrid protection. This research work involves dwelling further into adaptive overcurrent protection, developing protection logic, and testing the same on modified IEEE test buses using OPAL-RT as a real-time digital simulator.

[17] performed a detailed literature survey for adaptive protective schemes for microgrids till the year 2014. The following section gives a summary of his literature survey.

Adaptive protection can be broadly classified into overcurrent and multi-function protection groups. The use of overcurrent protection is more than distance and differential protection in the distribution system, hence there are more publications in the overcurrent protection group[17].

2.4.1 Adaptive Multifunction Protection System

[18] included an algorithm to achieve voltage control, grid reconfiguration, and protection applications which need further consideration for solving multi-objective optimization. [19] protection design executed the unification of modern digital substations, de-risking schemes, and self-contained modules. [20] discussed adaptive distance relaying scheme which attenuated the adverse effects of STATCOM in transmission lines. [21] put forward the use of central control and monitoring system as an adaptive relay setting strategy, wherein an investigation of protection strategies for adaptive safety protection in grid-connected and islanded modes at different faults was done. [22] worked out an online adaptive technique that helped in the setting of overcurrent relays in high voltage substations which eliminated the employment of communication infrastructure. Based on a centralized controller, [23] proposed adaptive multi-function protection system addressed issues such as selection of alternative setting groups, components, and system architecture; system configuration; and programmed logic.

2.4.2 Adaptive over-current protection

[24] proposed an algorithm that facilitated the self-adaptive response of relays to the changing conditions. [25] developed a topology detection technique with acceptable execution times for topology identification. [26] setting group method allowed comparison of the magnitude of the relay input current and the threshold value for verification of the fault status in the power system. [27] lodged a protection system which upon the need of a change of the distribution system conditions into grid, island, and losing generator modes, updated the trip characteristics of relays. Rather than

using communication to adapt the protection settings to the changes in the grid, [28] measured only local information. In this method, the relay settings were calculated offline and updated online according to the detections. Hierarchically Coordinated Protection (HCP) approach provided intelligence to directional overcurrent relays in [29], improved protection system tripping dependability, and mitigate effects of the complex grid. [30] was concerned with the adaptation of numerical relay settings to the microgrid status. Overcurrent relaying scheme in [31] detected the microgrid's mode of operation with no delay time. A self-adaptive algorithm for remote setup of any overcurrent devices was suggested by in [32]. [33] used inverse time overcurrent relay, re-closer, and sectionalized to present protection of overhead distribution feeder system. Unlike traditional distribution networks, whose protection system was based on time and current coordination of inverse time overcurrent protection devices, protection scheme in [34] demonstrated a self-adaptive method. The under-reach fault currents and the faults were detected and compensated by relays to adapt to the overcurrent protection scheme. A protection coordination approach in [35] allowed restoring of directional and inverse time overcurrent relay coordination concerning the varying fault current.

Adaptive overcurrent protection evolved much further after 2014 and the following section dwells into the work done by various authors on adaptive overcurrent protection, This literature survey was done on IEEE exploration from 2013 to the present date.

[36] reviewed the available adaptive protection schemes till the year 2013 and elaborated on the sustainability of operation in smart grid.

[37] presented a fault analysis of a practical university campus microgrid and proposed a method using information sharing technique through communication channels to protect the microgrid.

[38] proposed optional relay coordination method with adaptive protection scheme. He tested it on two different DG penetrated networks on a HIL testbed and suggested implementing these algorithms to achieve a high rate of convergence.

[39] employed a dual simplex algorithm to evaluate time multiplier setting and time of operation of relay for any microgrid topology using a lookup table which facilitated appropriate relay coordination.

[40] proposed standardization of exchanged data in the microgrid using IEC61850. It lets the user define a new logical node and does not have any limitation on relay type. This paper elaborated on the usage of IEC61850 for adaptive relay settings considering all the grid dynamic scenarios.

[41] treated the protection coordination problem as a linear programming problem considering different operating states and trains an artificial neural network with real-time measurements to detect a fault on the line. The testing performed suggested usage of estimation model along with adaptive overcurrent protection scheme that can modify relay setting for new state accurately.

[42] proposed a hybrid adaptive overcurrent and differential protection scheme for grid-connected and island mode. This scheme implements adaptive overcurrent relays to protect individual feeders whereas differential relays protect load buses. The scheme is validated in the time domain using a microgrid on EMTP.

[43] presented an adaptive protection scheme based on a modified particle swarm optimization algorithm is tested on IEEE 14 Bus system by adding distributed generators.

[44] proposed an adaptive overcurrent protection scheme based on fuzzy logic decision

making and tests the same in a modified CIGRE test microgrid using a real-time digital simulator.

[45] presented an automatic adaptive protection strategy for the microgrid. The proposed strategy uses pre-calculated settings for overcurrent protection developed in DigSILENT. The setting adjustment is performed to keep coordination time interval the same in grid-connected as well as islanded mode.

[46] demonstrates an adaptive protection scheme for inverter interfaced distributed generators in MATLAB Simulink for the microgrid.

[47] proposed an adaptive overcurrent protection scheme to protect the entire microgrid without modifying the existing protection scheme of the main grid. This scheme was based on data collected from a microgrid central controller.

[48] proposed a hybrid adaptive protection strategy which involved adaptive overcurrent as primary scheme backed up by total harmonic distortion detection method which takes over in case of failure of the primary scheme. The author also proposed an additional non-communication backup algorithm based on voltage measurement.

[49] proposed an adaptive overcurrent protection scheme for a microgrid with continuous monitoring, identification of states, and relay setting updates based on information collected from the microgrid control center.

[50] developed an adaptive overcurrent protection scheme for a grid integrated solar PV microgrid. Author also performed the coordination of primary and backup relay for three fault scenarios in a microgrid.

2.4.3 Adaptive Protection Algorithms

[49] proposed an algorithm for grid-connected and islanded mode in which the voltages and currents are constantly monitored and sent to Microgrid Control Center (MGCC). The MGCC monitors positive sequence components for 3 phase faults whereas it detects negative and zero sequence components for phase and ground faults. At the instant of fault, the MGCC communicates with the respective feeder to clear the fault and monitors whether it clears the fault. If it is unable to clear the fault then it waits for the specified time delay and opens up the main breaker at PCC to bring the microgrid in islanded mode. Now the algorithm for islanded mode comes into play and trips the breaker. In this state rest of the sources should be able to feed the local load. if the microgrid is stable, the MGCC sends a close command to the breaker at PCC when the re-connection conditions are satisfied.

In the case of grid integrated solar PV microgrid, [50] proposed an adaptive overcurrent protection scheme in which the pickup value for phase overcurrent element is based on the state of the microgrid. This method was designed and tested in Matlab. The method was tested for two modes of operation, grid-connected and islanded. The pickup values depend upon the state of the grid and as per the simulations, the fault current in islanded mode was very less as compared to grid-connected mode. This adaptive algorithm is used as a basis to develop an adaptive logic for this project. Although this method was not tested by the author on the actual relays, the same is tested with SEL-351S relay in real-time using OPAL-RT for this project.

2.5 Summary of Literature Survey

The literature survey conducted gave an insight into different adaptive methodologies currently available for microgrid protection. These methods address the problem by implementing different strategies. Some of these methods are practically implemented while others are just simulation-based and are not tested on actual relays. The adaptive settings group change method is the most popular method to perform adaptive settings on SEL relays. This methodology is not exhaustively tested in real time using hardware in loop techniques as seen from the literature survey performed. Also, the shortcomings of adaptive settings group change method are not looked into by researchers. Specifically, time delays in group changes are not addressed.

Thus, there is a need to test this adaptive method in real time using hardware in loop techniques and analyze the shortcomings of this method. This project tests the performance of the group change algorithm and then develops a unique algorithm that avoids the drawback of the group settings change algorithm. The hardware used and methodology development are discussed in the next chapter.

Chapter 3

Methodology

In this chapter, the hardware used to perform the research is described in sufficient depths. It starts with the description of OPAL-RT as a real-time digital simulator and then describes the SEL-351S relay along with its application in the power system. Further, this chapter explains the methodology used to interface the SEL-351S relay with OPAL-RT analog and digital input/output cards to connect the SEL-351S relay in the loop. It further describes the protection issue under study, the test setup, and adaptive settings change algorithm development.

3.1 OPAL-RT

It is always beneficial to test and evaluate the system's performance before it is implemented. There are systems already available that test the algorithms or device settings on a software platform. But these tests don't validate the performance of the equipment on which it will be implemented. Thus full-fledged testing is not possible with the software platform. To overcome this drawback of software testing, real-time testing was developed which would test the equipment along with its setting parameters before it is implemented in real practice. Real-time simulation refers to a computer powerful and capable enough of executing a simulated model on the actual system with the reflection of changes in the actual physical system in synchronized time. In the case of the Power system to observe, study and control the behavior of actual equipment such as a numerical protection relay in a complex power system, real time digital simulators can be implemented which are known to provide a safe, accurate and efficient environment to test the system before implementation [51].

There are few real-time simulators available in the market but OPAL-RT is one of the world leaders in real-time digital simulators which are based on FPGA (Field Programmable Gate Arrays) models. It is more technically viable and is known for its fast reliable operation and performance [51] [52]. OPAL-RT has multi-core computers which are optimized for parallel computing and are based on FPGA chips that can achieve maximum accuracy. There is a range of portable, high-performing real-time simulators which is developed by OPAL-RT specifically designed for power system protection engineers. The simulation environment is capable of performing complex model-based test scenarios as well as basic functional tests and can provide input-output arrays for connecting numerical relays for real-time testing. Apart from hardware packages, OPAL-RT offers software packages that come along such as RT-Lab, eMEGAsim, HYPERsim, ePHASORsim, and eFPGAsim [53].

3.1.1 Hardware Description

The hardware that is being used in this research is OP5600 which is an OPAL-RT Versatile simulator. It is a complete simulation system that contains a powerful target computer, a re-configurable FPGA along signal conditioning for up to 256 I/Os which operates on Spartan 3 or Virtex 6 FPGA platform. Figure 3.1 shows the front view of OP5600 Chassis whereas Figure 3.2 shows the rear-view. The front side consists of RJ45 Monitoring interfaces and monitoring connectors, whereas the rear side of the chassis provides access to the FPGA monitoring connections and all I/O connectors, power cable, and main power switch. The interfacing ports are divided into groups 1 to 4 and each group further is subdivided into A and B subsections. Rear ports have DB37 pin connectors which are used to interface the hardware with OP5600. The front RJ45 ports are only used for monitoring purposes.

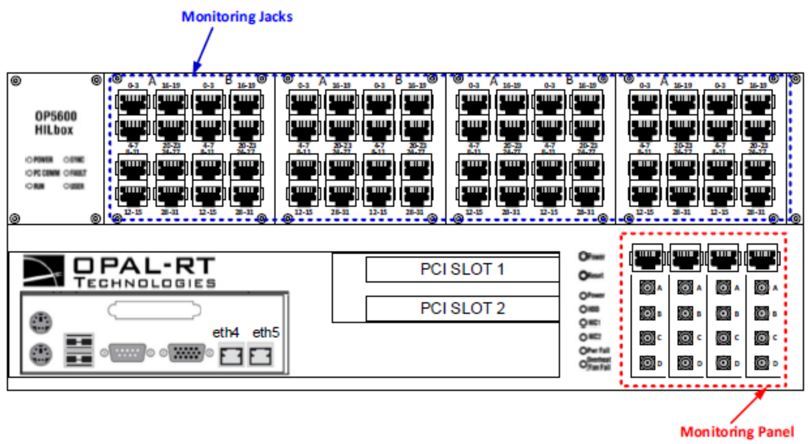

Figure 3.1: OPAL-RT Chassis Front View

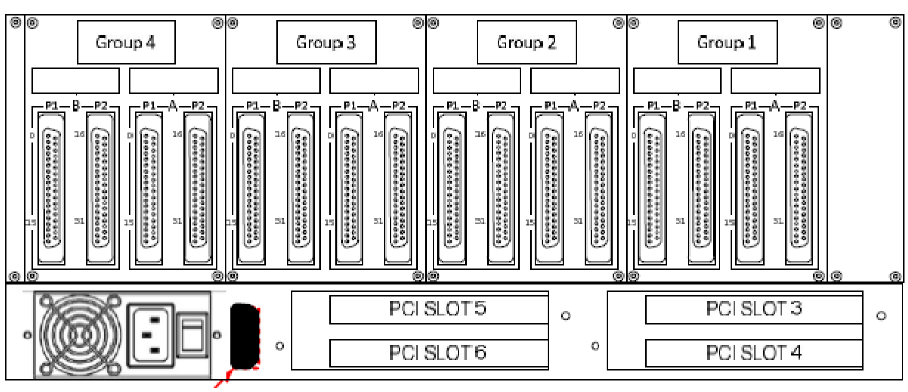

Figure 3.2: OPAL-RT Chassis Rear View

3.1.2 RT-Lab

RT-Lab is the software interface that allows models developed in MATLAB Simulink to be executed on OPAL-RT core and the resultant signals sent or received from actual hardware that is connected to OP5600 Analog or Digital Input/ Output ports. RT-Lab is fully integrated with MATLAB Simulink which makes it ideal for engineers for developing their systems rapidly and validating their application in real-time irrespective of the complexity in the system. RT-Lab allows better control, visualization, access, and customization of simulation projects in real-time [53].

RT-Lab has customizable dashboards, which indicate system behavior at a glance. RT-Lab also has a wonderful feature called parallelization which allows the distribution of complex models involving complex calculation over different cores of the target computer resulting in faster simulation response times. RT-Lab offers a rich array of communication protocols as well as Input-output flexibility for easy and quick interfacing with test equipment [53].

Figure 3.3 shows the home-screen of RT-Lab. Real-time testing using RT-Lab requires a user to follow four steps: Edit, Compile, Execute and Interact. Different sections of the screen and different tabs in the particular section of the screen are used to perform the above-mentioned steps in RT-Lab. Each of these steps is very crucial to the successful implementation of real-time testing and is described below.

Edit

During the editing phase, the model is either made from scratch on a blank MATLAB Template opened through RT-Lab or imported into RT-Lab from MATLAB Simulink file. The model has to be made RT-Lab compatible which is very important

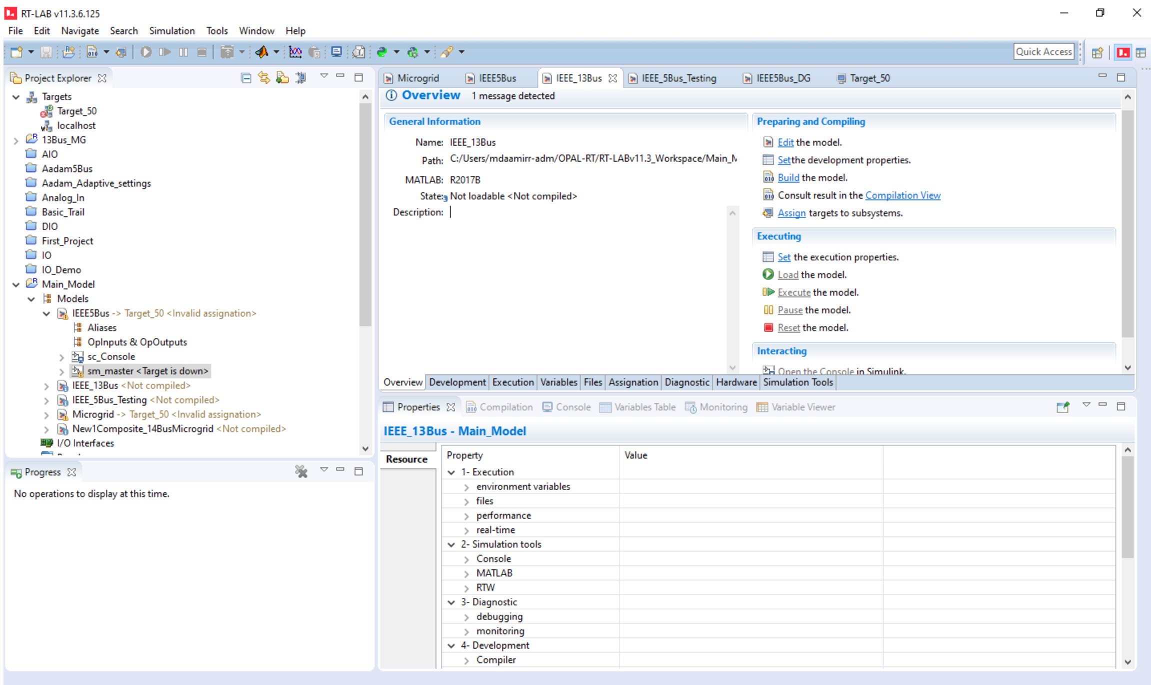

Figure 3.3: RT-Lab Home-screen

for a model to run in RT-Lab. To do this, the model is broken down into two main subsections called master and console. The master subsection has to be named as sm_Master which contains the part of the model that involves computation of actual system parameters. The console subsection is to be named as sc_console which contains the part of the model which has scopes and control parameters that can be changed while the simulation is running in RT-Lab. In this mode, the model is checked for any errors while in MATLAB so that errors don't get carried over to RT-Lab. It is also crucial in this mode to modify the model following RT-Lab guidelines for including interfacing blocks from the RT-Lab toolbox.

Compile

The model compilation is done after the editing phase has no errors in MATLAB Simulink. The model is built in RT-Lab once the development parameters are set in RT-Lab. The target PC is assigned to the model in this step. The build command generates a C code from the MATLAB model. This code is then sent onto the target computer and assigned to its CPU core.

Execute

To execute the model on the target PC it is important to set the Execution parameters. Figure 3.4 shows the tab in RT-Lab where the execution parameters are to be set. There are two main modes of execution; Software Synchronized and Hardware Synchronized. Software synchronized mode doesn't require hardware to be in the loop and is mainly done to test the model before interfacing it with real hardware. Hardware synchronized is the mode where actual hardware is present in the system. This mode requires the MATLAB model to have correct input-output blocks assigned to respective input-output cards of OPAL-RT.

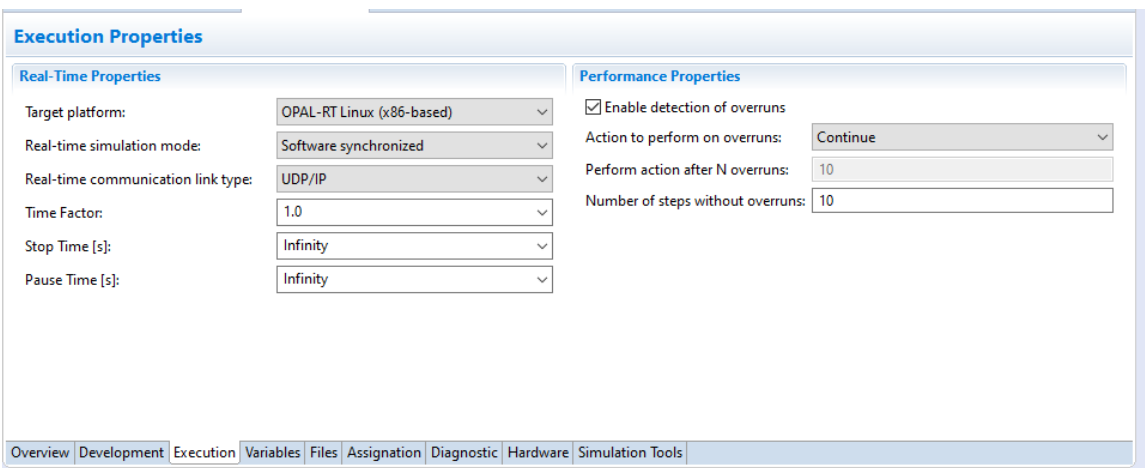

Figure 3.4: RT-Lab Execution Parameters

Interact

After the model has successfully executed, a console window of MATLAB Simulink will open up. This window will show the scopes and control inputs. The user can vary the control parameters in real-time and see the effects of it on actual hardware in real-time.

3.2 SEL-351S Relay

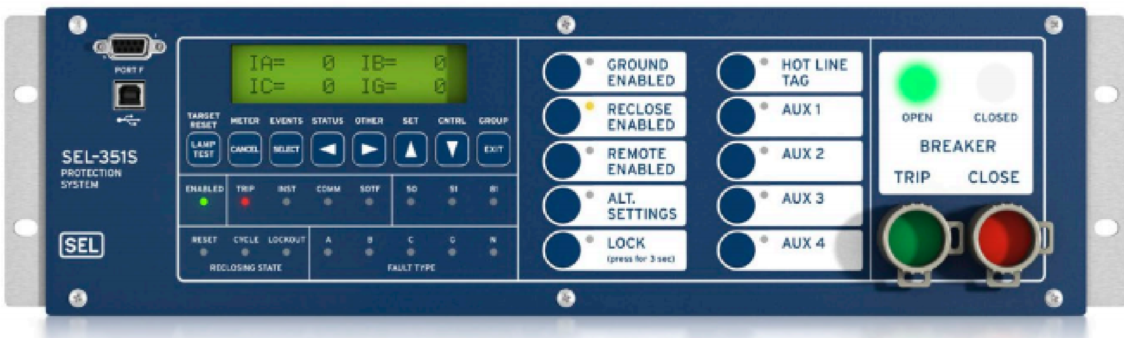

Figure 3.5: SEL-351S Relay

SEL-351S Relay is an advanced distributed feeder solution with integrated protection, monitoring, and control. It is a complete distribution protection system that is implemented to protect lines and equipment using phase, negative sequence, residual-ground, and neutral-ground overcurrent elements with directional control [54].

SEL-351S relay is best suitable for distribution system protection, monitoring, and control. Its overcurrent functions with the availability of directionality can be implemented to protect any power system circuit like lines, feeders, breakers, transformer, even generators. Directional power elements in the relay make it suitable for utility and customer interface protection where customer generation is present; also known as distributed generation. Figure 3.6 shows different applications of SEL-351S relay [55].

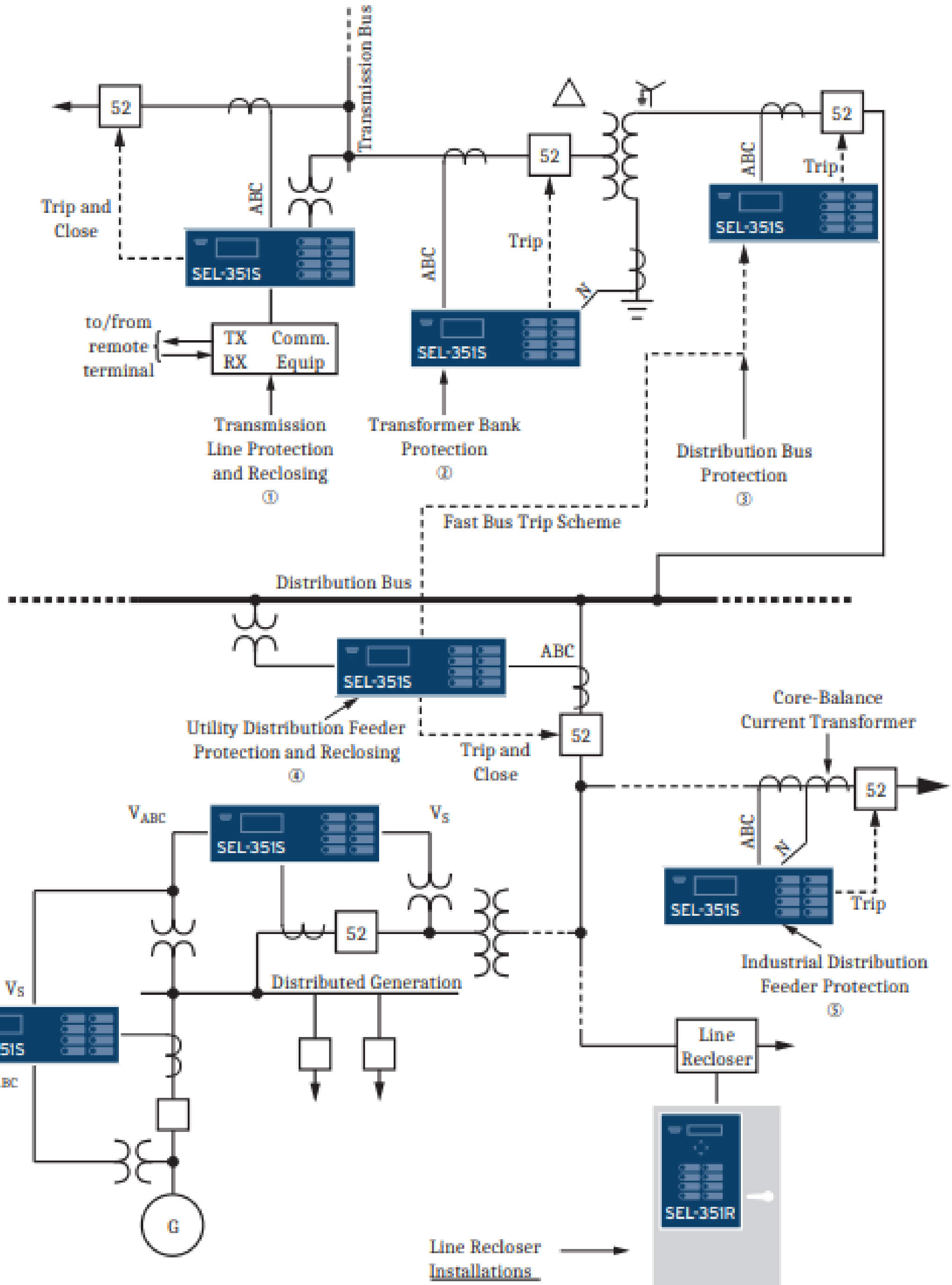

Figure 3.6: SEL-351S Relay: Application in Distribution System

3.2.1 Protection Functions

SEL-351S has different protection functions which make it a popular relay among protection engineers. Figure 3.7 shows the ANSI device numbers associated with the protection and control functions that are available on the SEL-351S Protection System. It also shows a list of the standard and optional monitoring and communications features. The relay has various protection functions and each function takes input for its operating quantity from the respective instrument transformer as shown in Figure 3.7 [55].

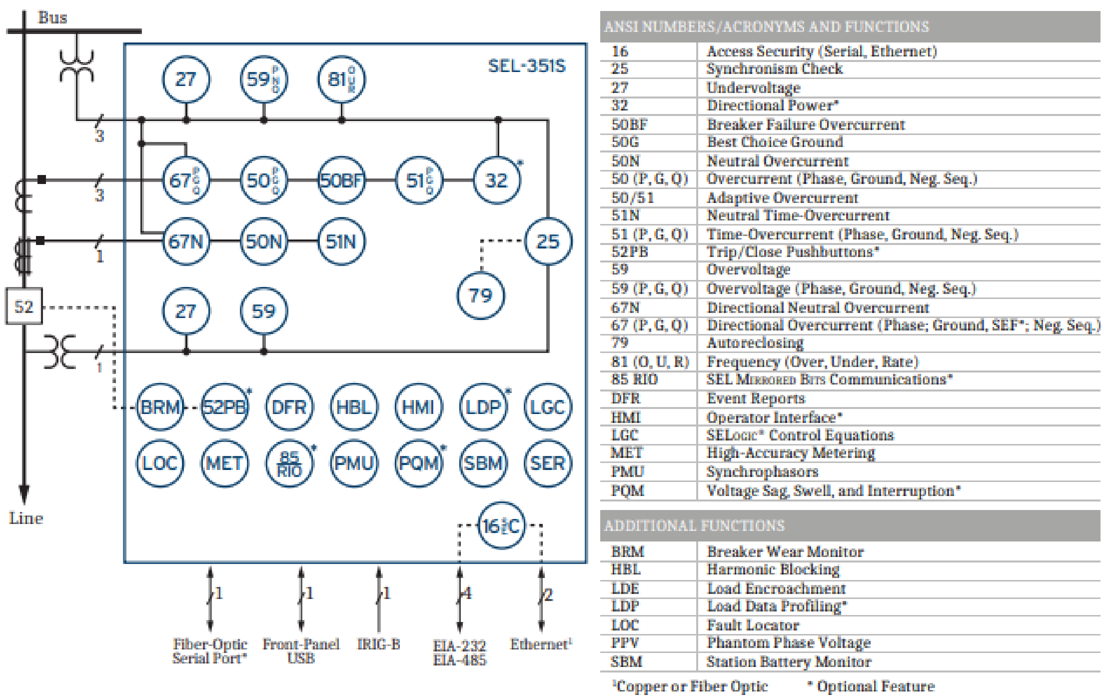

Figure 3.7: SEL-351S Relay: Protection Functions

3.2.2 Relay Hardware

Figure 3.8 shows the front and rear views of the SEL-351S relay. It has user-configurable push buttons and LED's in the front and multiple input-output contacts in the rear which can be used to create tripping/ closing logic in the relay. The status of breakers and other devices can be interfaced through the input contacts whereas the output contacts can be used to trip the associated circuit breakers. Apart from that, it has different communication channels such as serial, Ethernet, fiber [56].

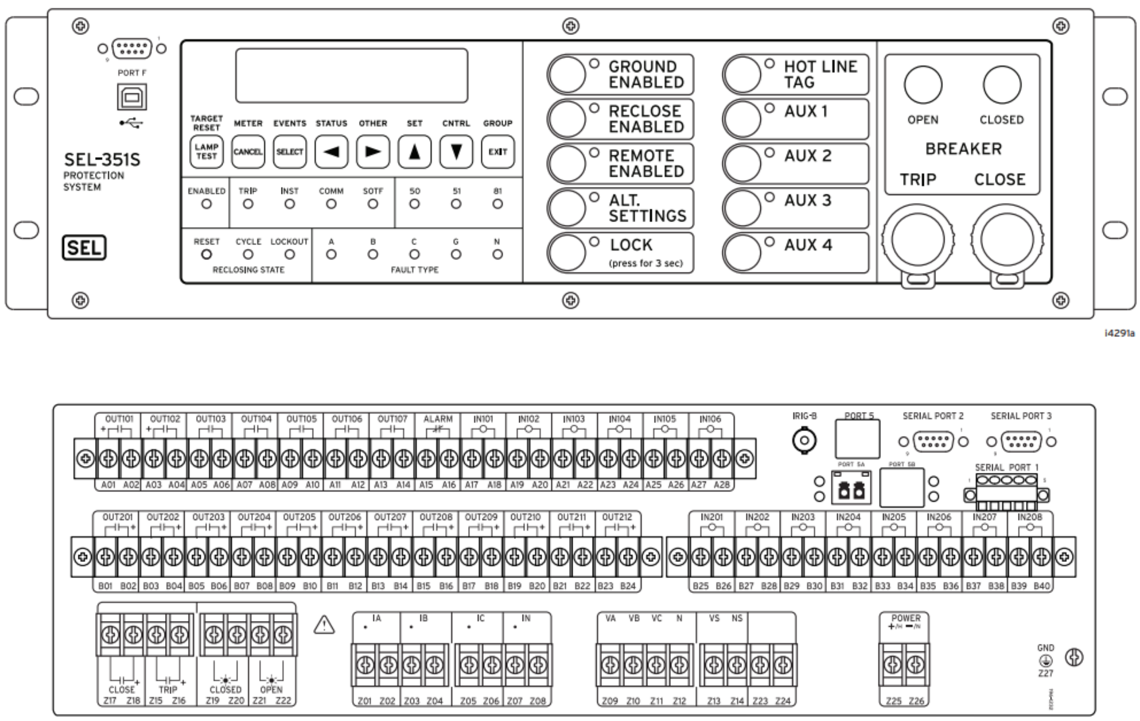

Figure 3.8: SEL-351S Relay: Front and rear view drawings

Figure 3.9 shows the typical wiring diagram for interfacing the instrument transformers and breaker coils with the relay. The external CT outputs are fed to internal CT inputs within the relay and external PT outputs are connected to internal PT inputs. The output contacts need external wetting voltage whereas the input contacts have internal wetting voltage.

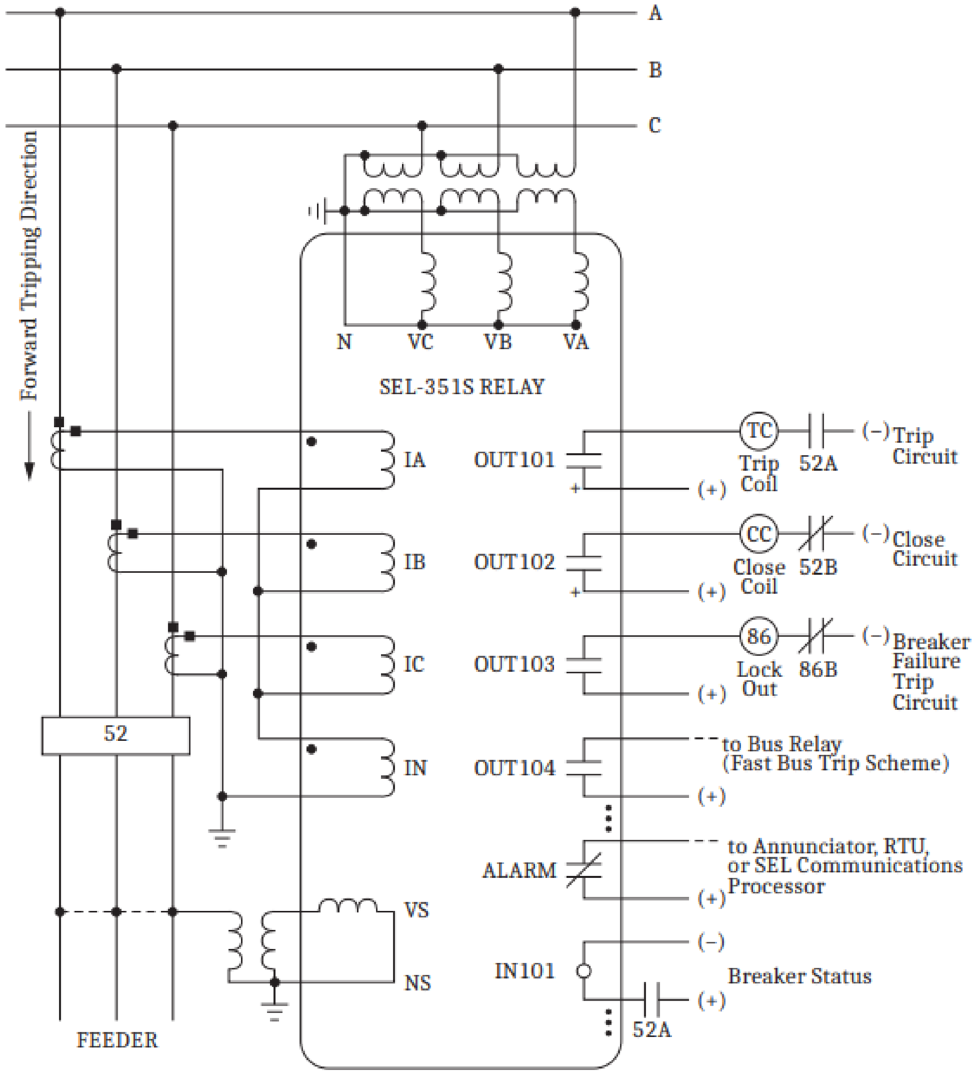

Figure 3.9: SEL-351S Relay: Typical Wiring Diagram

3.2.3 AcSELerator Quickset

SEL has its software package that comes along with all of the relays. This software is used to perform the relay settings, monitor the operation, and control the relay outputs. 'AcSELerator Quickset' is the software created by SEL and is user-friendly software. Figure 3.10 shows the homepage of AcSELerator Quickset. The relay is to be connected through the front serial port or Ethernet ports at the rear using the communication tab and setting the serial, network, or modem setting parameters. Once connected, the settings can be read from the relay, modified, and then sent back to the relay.

Figure 3.10: SEL-5030 AcSELerator Quickset Homepage

3.2.4 Relay Testing Methods

After developing the relay settings, it has to be tested before it is implemented in the system. This is done to ensure its operation during an event on the actual system. There are different testing devices available on market today out of which 'Doble' and 'Omicron' are the most popular ones. These testing devices are used to inject currents and voltages into the relay to simulate a faulty condition and observe the relay operation under these conditions. The outputs of these testing devices are connected to the CT/ PT input terminals of the relay designated as Ia, Ib, Ic, In; Va, Vb, Vc, Vn. The values of currents and voltage to be injected are either calculated manually or found out from short circuit studies software like ASPEN or ETAP. These are to be entered manually into the Doble and Omicron interface software to be injected into the relay.

SEL relays have one more feature called low-level testing interface which was developed by SEL for relay testing at low values of voltages and currents. SEL Adaptive Multi-channel source (AMS) is used to test the relays through a low-Level test interface. The low-level test interface bypasses the CT, PT board in the relay which is used to step down the voltages and currents to very small magnitudes. This bypassing facilitates relay testing at very low voltages of the order of millivolts. This is a very important advantage for testing the relays in real-time as OPAL-RT can only output voltages up to a maximum of 16 Volts. This interface allows injection of up to 9 volts peak to peak voltage. The values of voltages and currents are manually entered into the AMS test software and the software internally steps down the values by using a scaling factor provided in the relay instruction manual. These scaling factors vary with the relay model being used and are to be entered into AMS test software before testing.

3.3 SEL-351S Relay in loop with OPAL-RT

Interfacing OPAL-RT with the SEL-351S relay requires opening the relay front panel and disconnect the ribbon cable coming out from CT/PT board to the main-board and connect the ribbon cable from OPAL-RT directly to the main board of the relay. The relay has pins of ribbon cable termination as shown in Figure 3.11 [56].

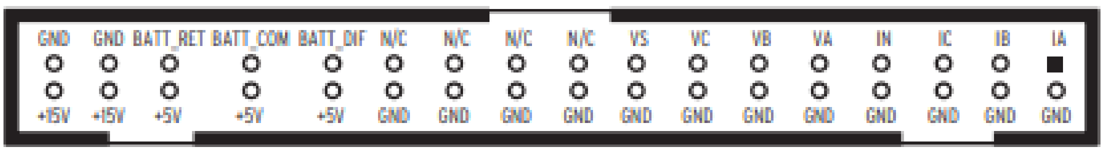

Figure 3.11: Low level interface of SEL-351S relay

The outputs from the OPAL-RT analog channel have to be interfaced with the respective input pins on the low-level interface of SEL-351S. Figure 3.12 shows the interfacing diagram that is required to be followed to interface SEL-351S relay with OPAL-RT. There are two parts of interfacing, the analog channel interface, and the digital channel interface. The analog outputs from OPAL-RT analog output channel are interfaced with the low-level voltage and current input signal interface on the relay main-board as in Figure 3.11. The details on interfacing is discussed in sections 4.1.2 and 4.1.3. The digital outputs from OPAL-RT are required to be input into the relay to switch the relay settings during different operating modes. The digital output contacts of OPAL-RT do not output voltage, thus a voltage source is to be connected in series with the contacts so that the relay can detect this input signal. For this model 24V, DC source was connected in series as shown in Figure 3.12.

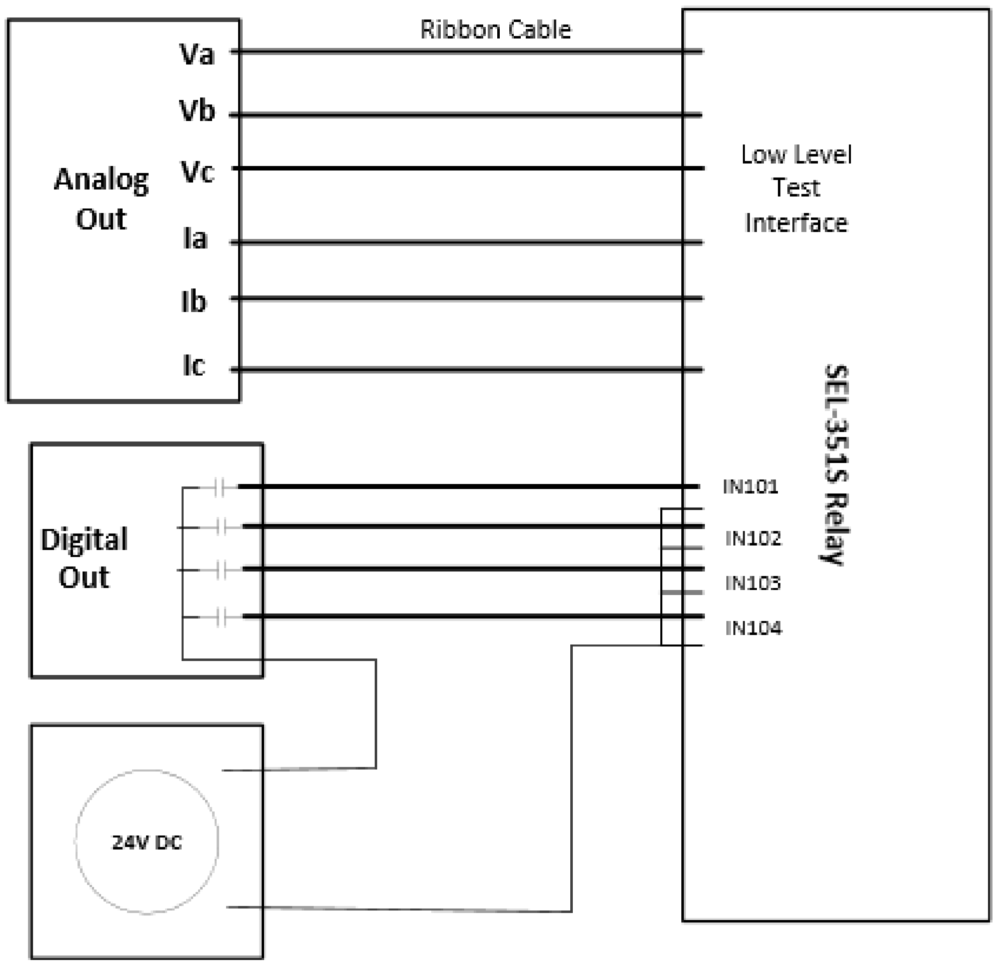

Figure 3.12: Interfacing SEL-351S relay with OPAL-RT

3.4 IEEE 5 Bus with DER

IEEE 5 bus system was chosen as the base test system for this project which was modified further to convert it into a microgrid. Sections 4.1 and 4.2 describe the model development and implementation of this test bus system for real-time time testing with and without distributed generators. Figure 3.13 shows the Single Line Diagram of a modified IEEE 5 bus system to operate as a microgrid. This microgrid can operate in Grid-connected and Islanded mode depending on the state of Circuit Breaker at PCC which is at Bus 2 as shown in Figure 3.13. Protection issue arises when the microgrid state changes from grid-connected to islanded mode as discussed in Section 2.2.

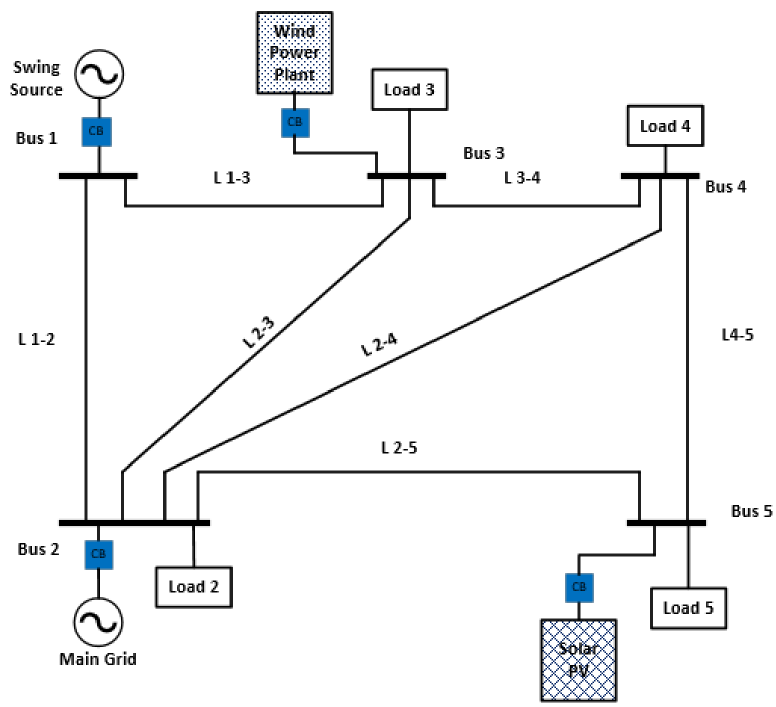

Figure 3.13: Single Line Diagram of Modified IEEE 5 Bus Microgrid

3.5 Algorithm for Adaptive Settings change

To tackle the above mentioned protection issue, different authors proposed different methods which were discussed in Section 2.4. Adaptive protection algorithms are the ones that can solve the protection issue depending on the state of the microgrid. This requires switching relay pickup settings depending on the microgrid states. Thus, for example, the pickup setting for relay should be ‘X’ when it is in grid-connected mode and it should be ‘Y’ during the Islanded mode. This method overcomes the issue of the relay being not able to detect the fault in the Islanded mode of operation. The following sections describe the settings change algorithm.

3.5.1 Settings Group Change

The issue of non-operation during islanded mode and its solution discussed above can only be practically possible if the settings change were to happen in real-time depending upon the status of the microgrid. The status of PCC circuit breaker and DG circuit breakers can be used as an input to the relay to initiate the settings change. This is possible in the SEL-351S relay by taking the status of input contacts and assigning their status to settings group selection setting in the relay. This is shown in Figure 3.14 where the status of input contacts IN101 to IN106 is used to change each corresponding setting group. The input contacts require a DC supply wired in series with them as these are Opto-Isolated Contacts and require an external wetting voltage.

The relay also has a setting called group change delay, where a user can set a time. Although this is highly undesirable in the real-time settings group change it is found

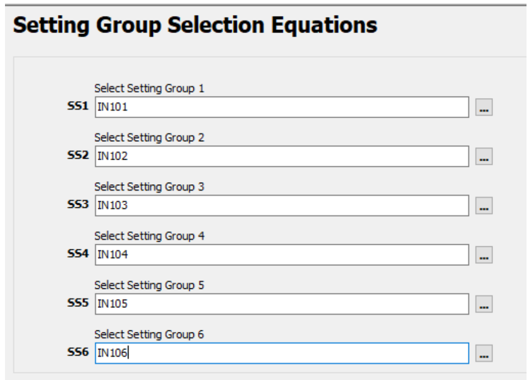

Figure 3.14: Settings Group Change

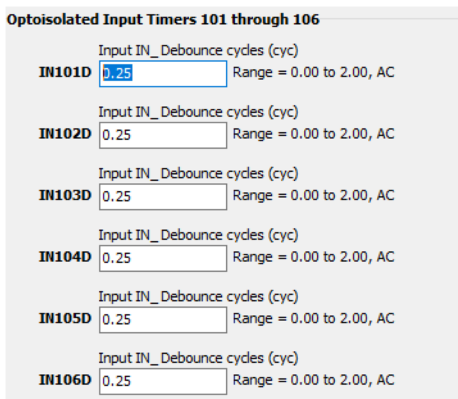

Figure 3.15: Input Debounce

useful for certain other applications. The input contact has a setting called input debounce timer which is shown in Figure 3.15. This is used to avoid nuisance operation of relay logic due to transient assertion of input contact due to noise, radio interference, chattering, etc.

3.5.2 Adaptive Settings without Settings Group Change

A unique approach was implemented and tested to overcome the issue of the system being protection less during settings group change process interval. This method involved the use of different pickup levels of instantaneous overcurrent pickup in the case of the SEL-351S relay. Figure 3.16 shows the multiple pickup settings in the SEL-351S relay. The number of pickups that can be set up are six which are 50P1P to 50P6P. The instantaneous overcurrent (50) element pickup values for Grid Connected, Islanded with Solar, and Islanded with Wind were input into 50P1P, 50P2P, and 50P3P respectively. Also, a time delay can be provided to these pickups to achieve protection coordination in case of downstream relay. The internal logic of these elements was used to create an algorithm to have multiple pickup settings without a need to change the settings group. Each of instantaneous overcurrent element (50) pickups has the internal logic built within the relay as shown in Figure 3.17.

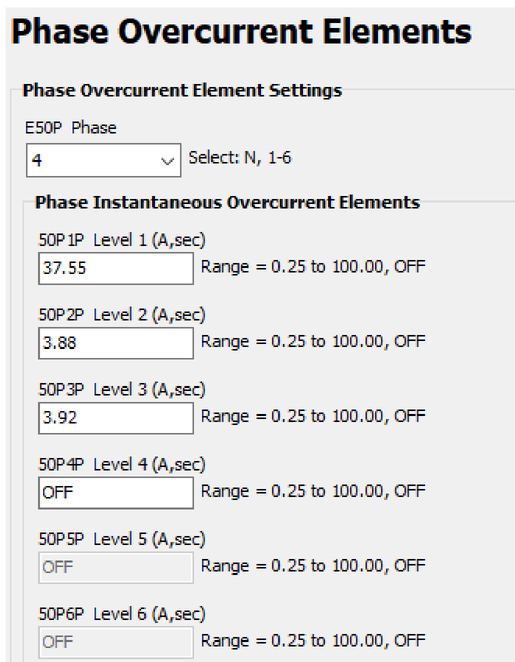

Figure 3.16: Multiple Instantaneous Pickup levels in SEL-351S

The 50P1 bit is logical 'AND' with E32N which is a directional enable bit and 67P1TC which is a directional torque control bit. The value of E32 is set to 1 if it is disabled which means there is no directional supervision over 50P. Torque control (67P1TC) is typically kept to logical 1. With these settings at logic 1 50P1 is the same as 67P1. The torque control bit was put to use to develop an adaptive algorithm. There are in

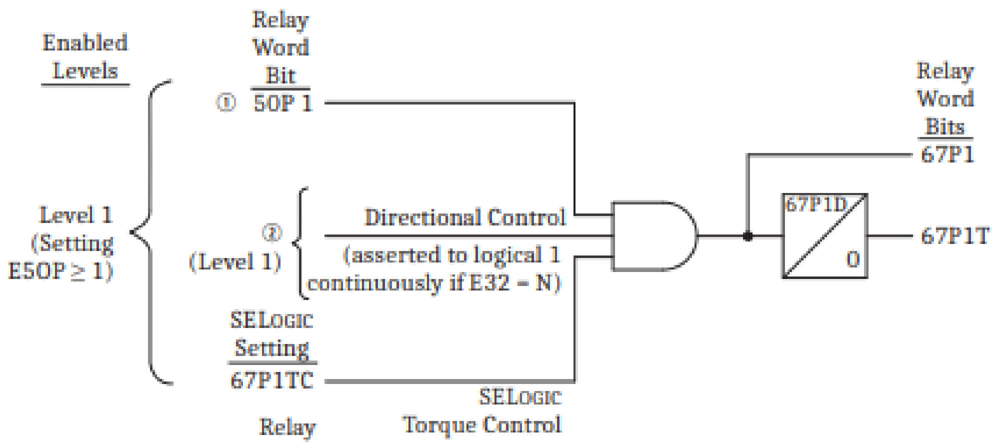

Figure 3.17: Relay Internal logic for Directional Supervision over 50 Element

all four different 'AND' gates within SEL-351S relay which are identical as shown in Figure 3.17. 67P1TC to 67P3TC were given the input contact status bits IN101 to IN103 respectively which is shown in Figure 3.18. The above-discussed method was tested and the results of which are discussed in Chapter 5.

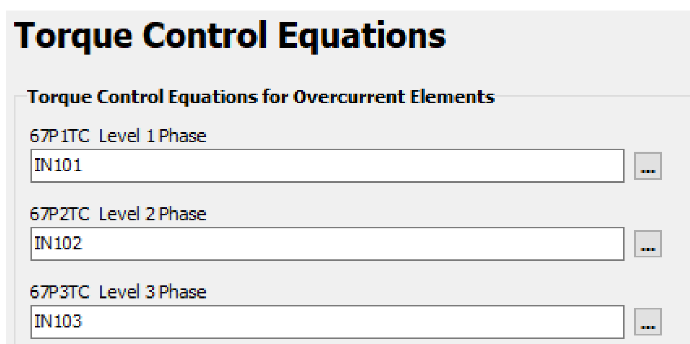

Figure 3.18: Torque Control

Chapter 4

Implementation

This chapter deals with the implementation of IEEE test model for real-time testing of SEL-351S relay using OPAL-RT. The IEEE test models are modified following OPAL-RT requirements and then the relay is interfaced as the hardware in the loop. The same test bus is then modified to include Distributed generators which affect relay operation. Moreover, a settings change algorithm is developed and tested to ensure reliable relay operation during the presence of distributed generators.

4.1 IEEE 5 Bus System

IEEE has developed a standard bus system to test different scenarios in the grid at different voltage levels. IEEE 5 Bus system is shown in Figure 4.1. It consists of two generators, seven lines, 5 buses, and four loads as can be seen from the Figure 4.1. Transmission line parameters connecting the buses are shown in Table 4.1. These values are in per unit with a suitable base power of 100MVA and 10kV as voltage base [57].

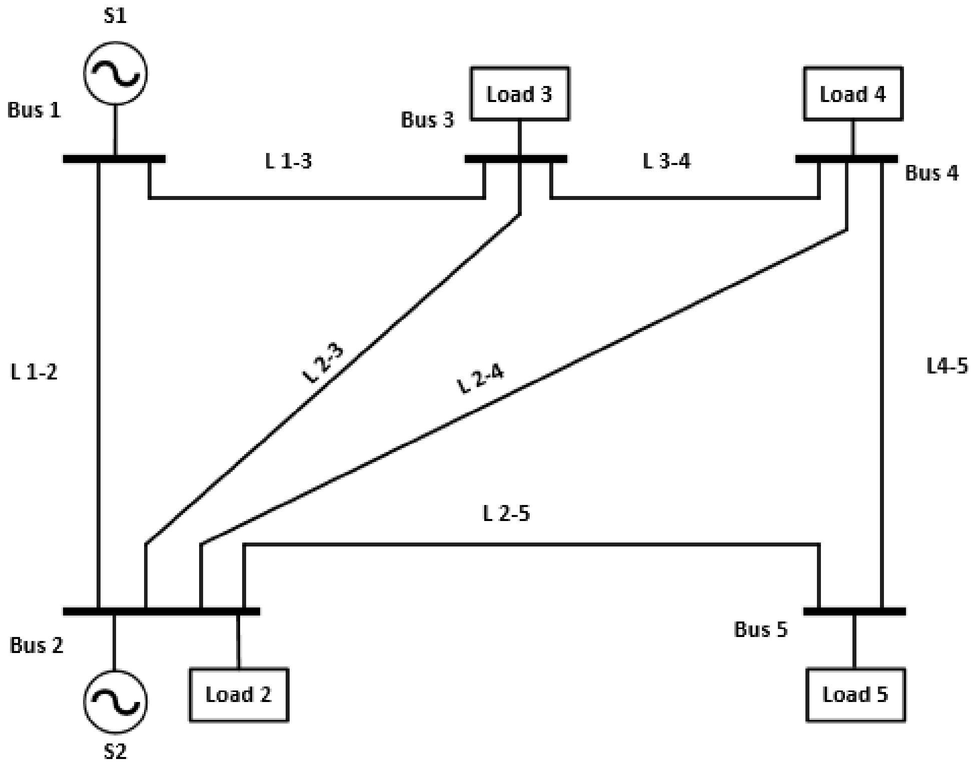

Figure 4.1: IEEE 5 Bus System

Table 4.1
Transmission Line parameters of IEEE 5-Bus system in per Unit

From Bus	To Bus	Resistance	Reactance	Conductance	Susceptance
1	2	0.02	0.06	0	0.06
1	3	0.08	0.24	0	0.05
2	3	0.06	0.18	0	0.04
2	4	0.06	0.18	0	0.04
2	5	0.04	0.12	0	0.03
3	4	0.01	0.03	0	0.02
4	5	0.08	0.24	0	0.05

The 5 Bus test system discussed above was modeled in MATLAB Simulink and was used as a base case for the developments in this project. The 5 bus system was selected as it is a simple system and can be modified into a microgrid which was the main requirement for this project. Table 4.2 shows the bus parameters for IEEE 5

Bus with its sources and loads. Load flow was performed on the developed system. Then the system was modified in order to make it suitable to test on the OPAL-RT interface which is discussed in the following sections.

Table 4.2
Bus Data for IEEE 5-Bus system

Bus No.	Bus Voltage	Generation (MVA)	Load (MVA)
1	1.06+j0.0	0	0
2	1.0+j0.0	40 +j30	20 + j10
3	1.0+j0.0	0	45 + j15
4	1.0+j0.0	0	40 + j5
5	1.0+j0.0	0	60 + j10

4.1.1 Modifications to implement SEL-351S relay in loop

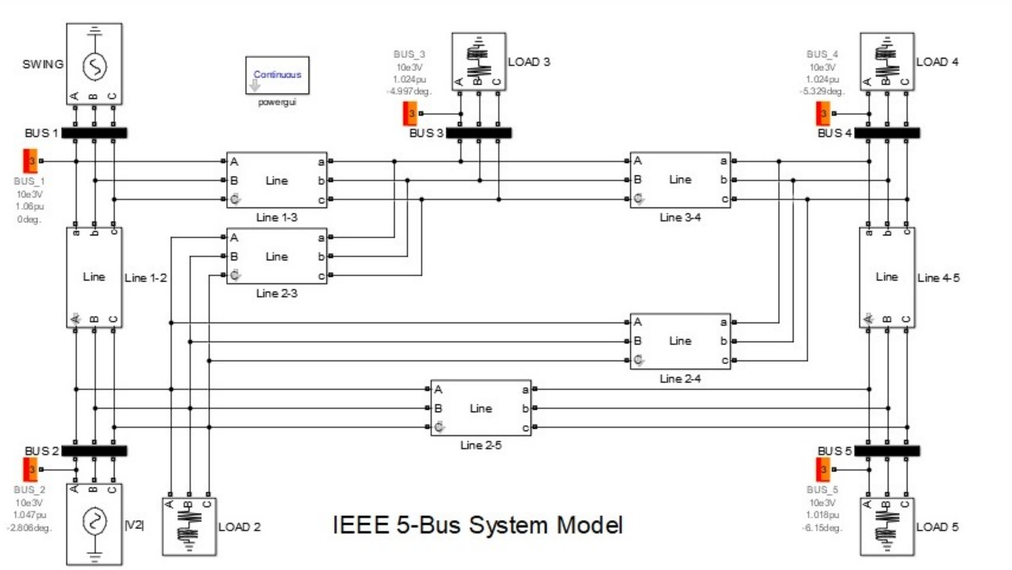

Figure 4.2: IEEE 5 Bus Model Simulink

IEEE-5 Bus system cannot be directly used as a test bench for the relay in loop technique. There are certain modifications that are to be done in order to make the model function properly. First thing is to verify whether the model created in MATLAB Simulink is continuous or discrete. If the model is continuous, it has to be changed to discrete as OPAL-RT works on fixed time steps. Furthermore, the discrete model should have a time step not smaller than 20 microseconds. For this project, a time step of 50 microseconds was chosen in order to not have overruns and long processing time. The IEEE 5 bus model was referred from the MATLAB standard database and was modified to a discrete one.

Figure 4.2 shows the referred model in Simulink. This model was modified to a discrete model as shown in Figure 4.3. Also, the model was modified to include Circuit Breakers at each line as well as V-I measurement blocks. The signals measured were used to send current and voltage input signals to the SEL-351S relay through the

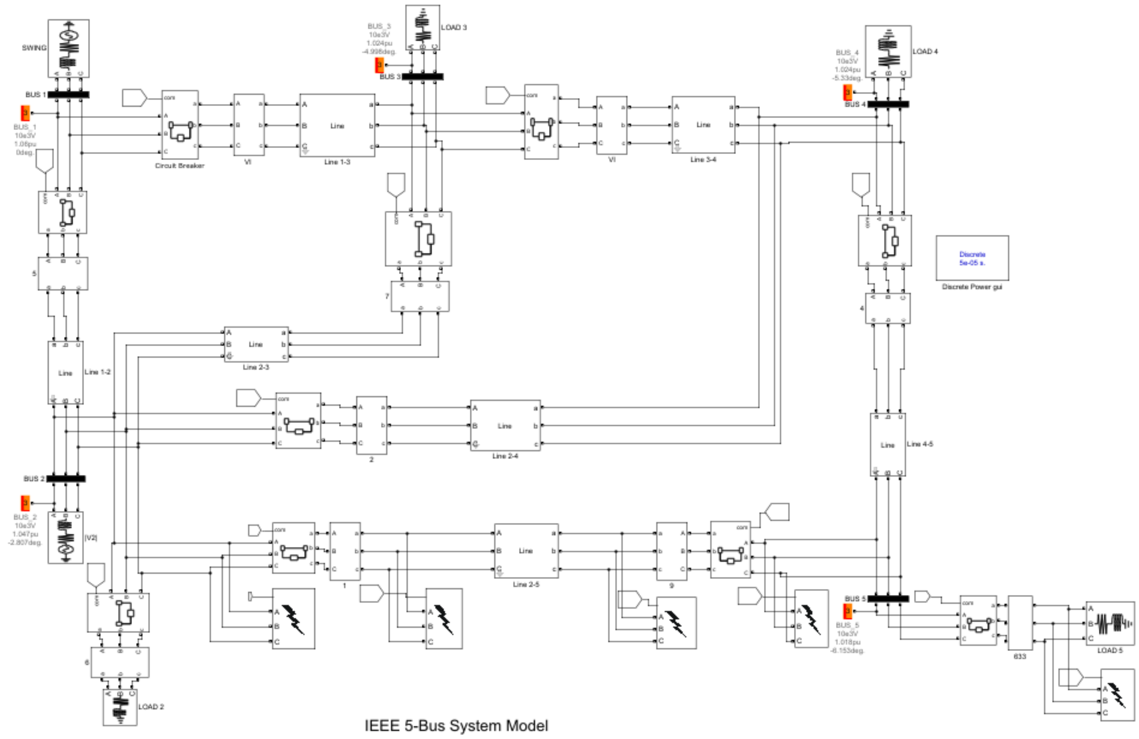

Figure 4.3: IEEE 5 Bus Discrete Model Simulink

OPAL-RT analog output interface. The details of this will follow further in this section. The main modification required to run the model on OPAL-RT target PC is to divide the model into two subsystems. This was done as per the recommendation of OPAL-RT. The two subsystems created had to be named as sm_Master and sc_Console. The sm_Master subsystem is the one that contains the whole IEEE 5 bus model, whereas sc_Console consists of all the display scopes and real-time state control inputs.

Figure 4.4 shows the division of the model into Master and Console along with the interconnection between the two. Figure 4.5 shows the components of the console subsystem which consists of manual switches used for breaker control, mode control, and fault control; analog output and digital input scopes. The OpComm block is used from the RT-Lab module of MATLAB Simulink which is very essential in order

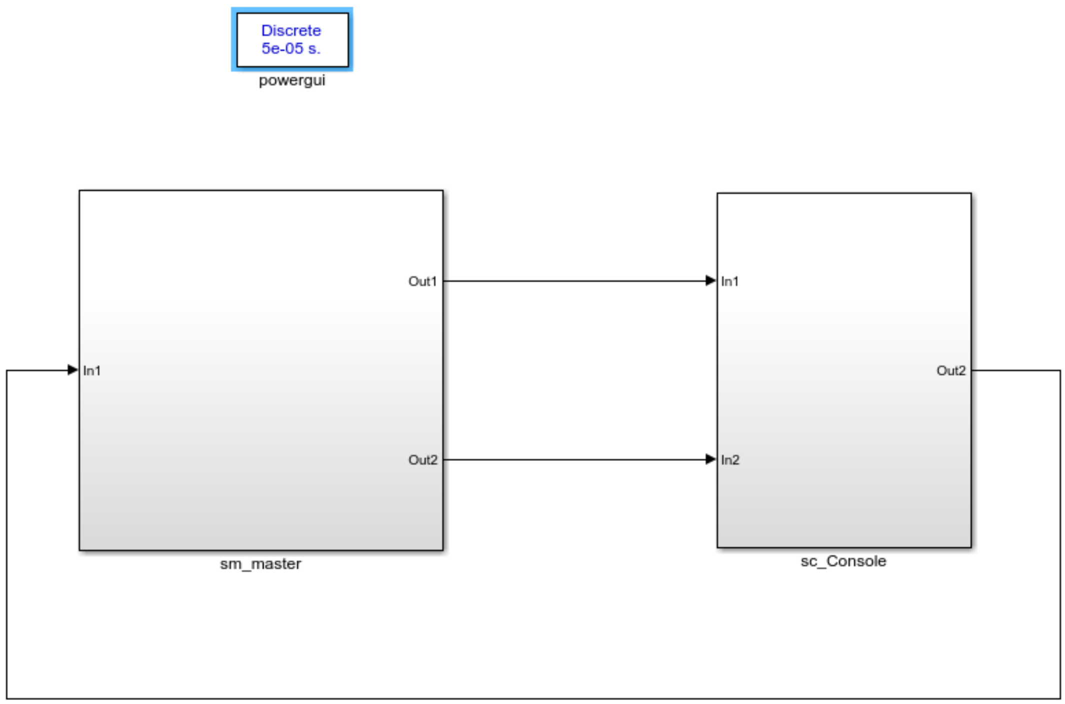

Figure 4.4: Master and Console

to transfer data to and from the separate subsystems (sm_Master and sc_Console).

A three-phase fault block was used to create different types of faults in the system. The trigger for this was provided externally from the signal coming in through sc_Console subsystem. These blocks were placed at different locations in the system.

4.1.2 AIO and DIO configurations

In order to test actual hardware in the loop (SEL-351S relay in this case), the real-time simulation model was selected as hardware synchronized. Input-Output configuration was required for the system to run in hardware synchronized mode. 'OpCtrl' block was used to direct the signals from Simulink to input-output channels of OP5600 (target PC in this project).

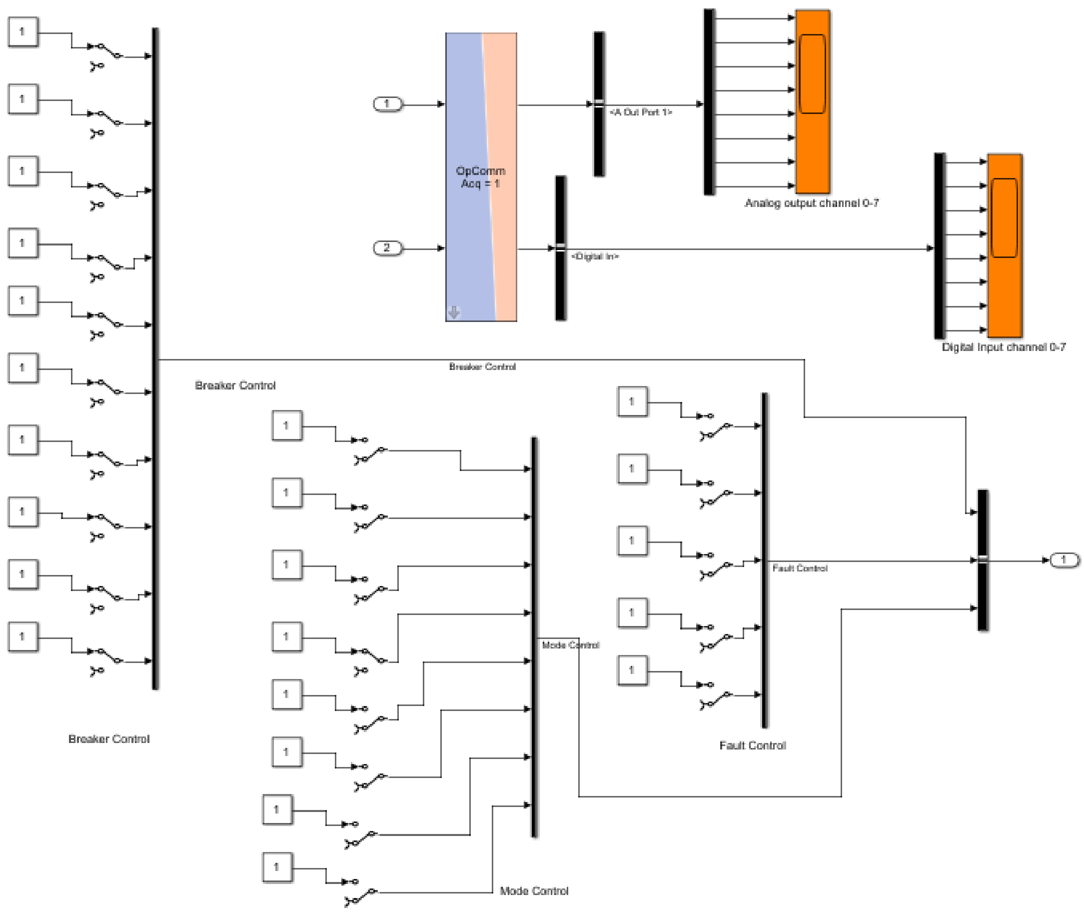

Figure 4.5: Console

OPAL-RT provided a bitstream file and its directory along with the system documentation CD. This bitstream file was copied to the directory where IEEE Bus model was saved on the Host PC. This was very important as the model will not run if the file is missing. Figure 4.6 shows the configuration of OpCtrl block.

OPAL-RT CD also provided a .conf file which consists of analog and digital input-output configuration at different slot, section, and subsection. This is shown in Figure 4.7. This configuration file comes with each OPAL-RT package and is a depiction of the customized user requirements. It shows all the analog and digital input-output configurations in the hardware.

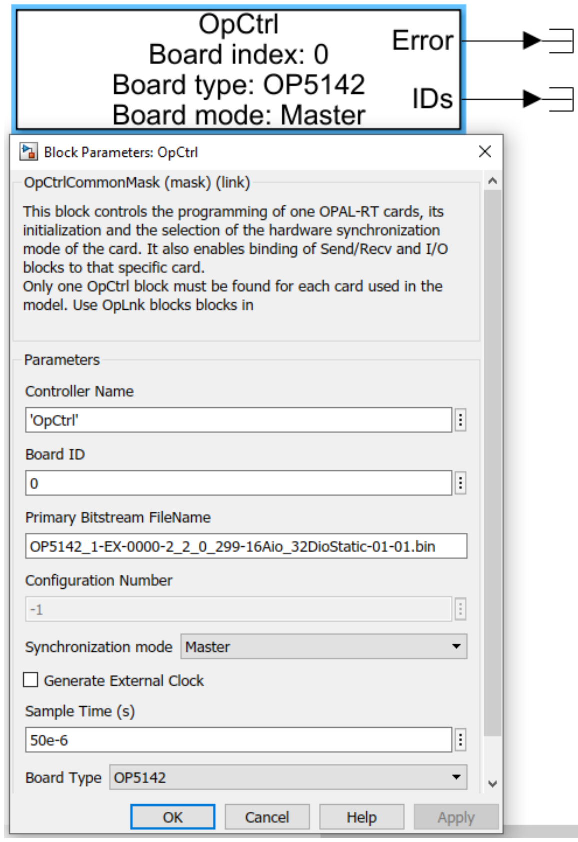

Figure 4.6: OpCtrl

OP5142_1-EX-0000-2_2_0_299-16Aio_32DioStatic-01-01.conf

PortName	Description	Slot	Section	SubSection	Count	Size
DataIn1	AO	1	A	1	8	16
DataIn2	AO	1	A	2	8	16
DataIn3	DO	2	B	1	8	1
DataIn4	DO	2	B	2	8	1
DataIn5	DO	2	B	3	8	1
DataIn6	DO	2	B	4	8	1
DataOut1	AI	1	B	1	8	16
DataOut2	AI	1	B	2	8	16
DataOut3	DI	2	A	1	8	1
DataOut4	DI	2	A	2	8	1
DataOut5	DI	2	A	3	8	1
DataOut6	DI	2	A	4	8	1

Figure 4.7: Input Output Configuration file

Figure 4.8 shows the analog out configuration window in MATLAB Simulink. The controller name is 'OpCtrl' this should be the name given to the 'OpCtrl' block configured previously. Data in port number is the port name assigned to each subsection

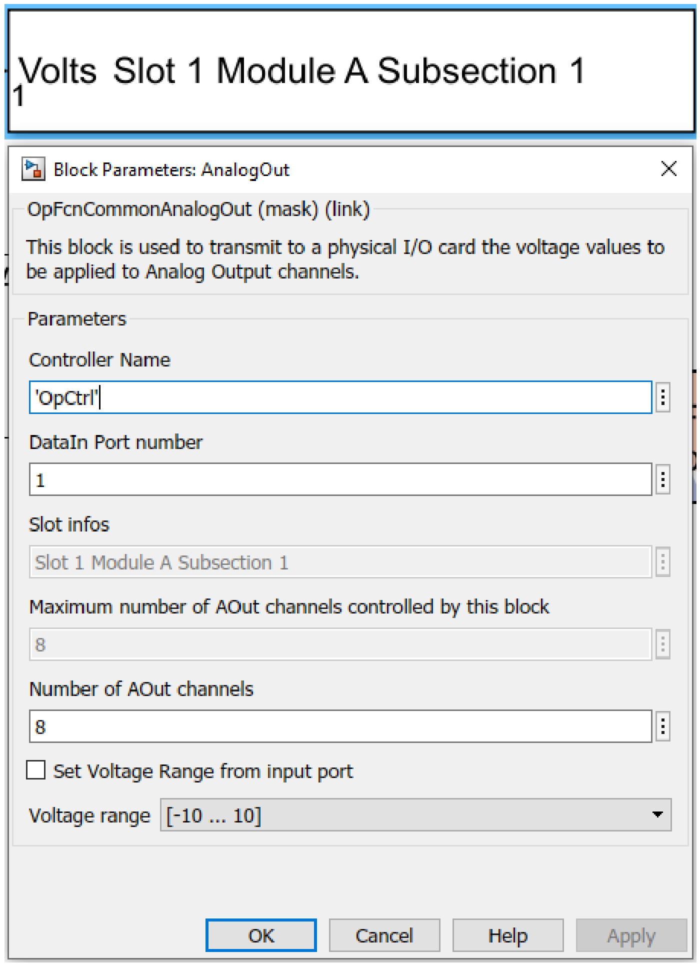

Figure 4.8: Analog Output Configuration

in a particular slot and subsection. This can be chosen from Figure 4.7. The slot information and maximum A out channel are automatically assigned by MATLAB. The quantity of Aout channels can be selected as per the need. The voltage range is to be selected as the maximum voltage that the looped device can handle. In this project, it is an SEL-351S relay that can handle around 9 volts. So, a range from -5 to 5 volts was selected. Similar is the process to configure digital out, digital in, and analog out. The analog output signals from Simulink are sent to the relay via the ribbon cable connection.

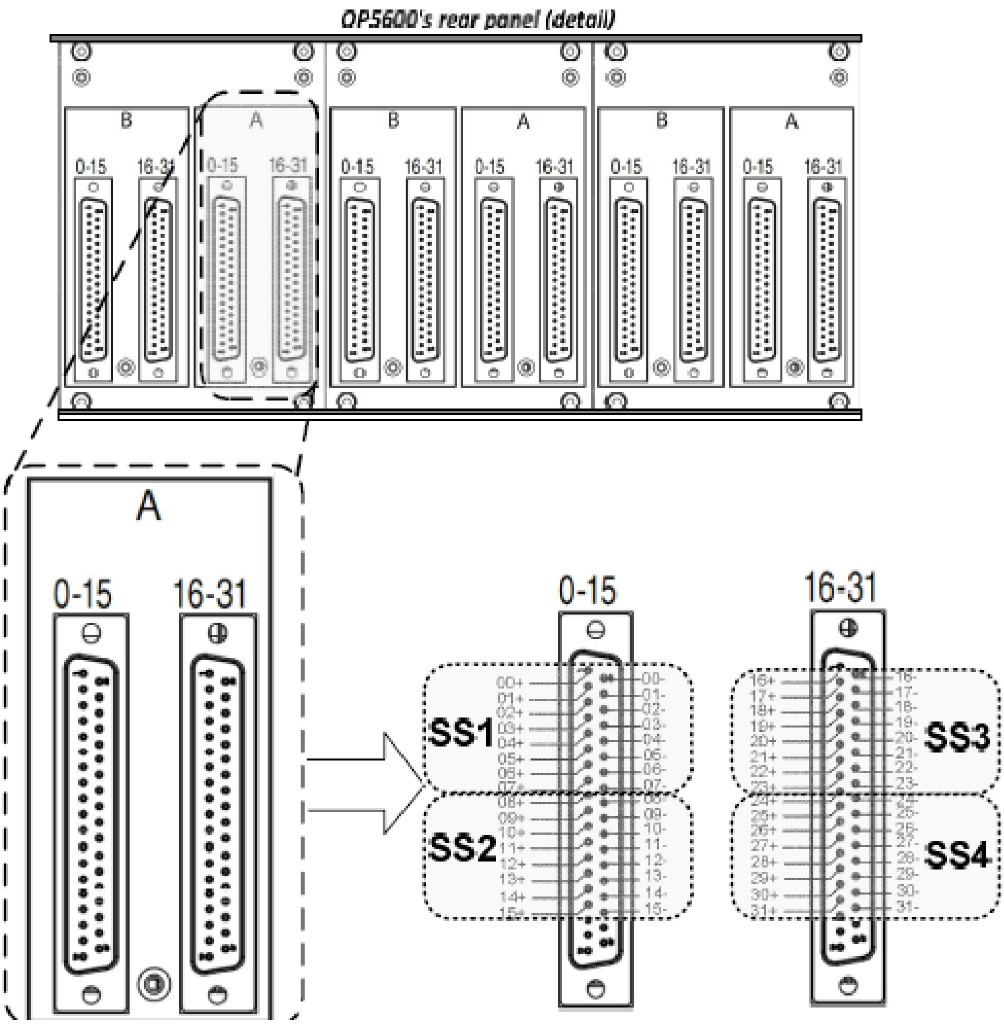

Figure 4.9: Rear Panel View showing AIO and DIO sections

Simulink blocks I/O nomenclature	OP5600 I/O ID nomenclature
Slot	Group
Module A	A
Module B	B
Subsection 1 (SS1)	(0-7)
Subsection 2 (SS2)	(8-15)
Subsection 3 (SS3)	(16-23)
Subsection 4 (SS4)	(24-31)

Figure 4.10: Input Output Nomenclature

Figure 4.9 shows the rear panel detailing of analog input-output and digital input-output. It consists of slot, section then sub-section. Figure 4.10 shows the nomenclature corresponding between Simulink I/O block and OP5600 I/O. To properly link the signals generated by Simulink to the respective I/O pin it is necessary to perform I/O configuration correctly. RT-lab module of Simulink library consists of analog out, analog in, digital out, and digital in blocks.

4.1.3 Analog Output signal scaling

Figure 4.11 shows the connection diagram for analog output channel. The current and voltage signals measured from the test point are input to signal scaling blocks.

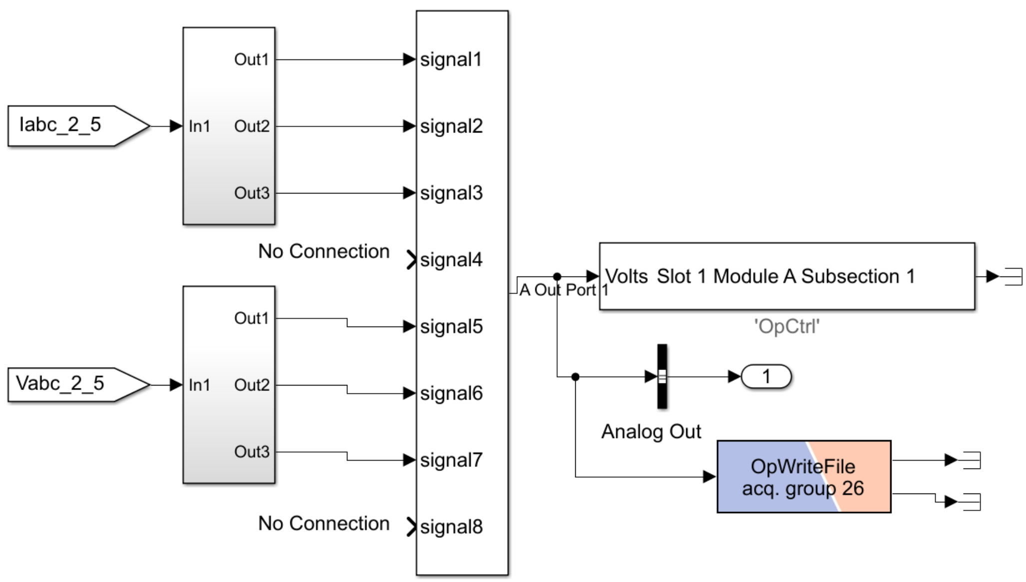

Figure 4.11: Analog Output Connection

Figure 4.12 shows the scaling for current before signals are injected into the relay. The signals are divided by the CT ratio which is 1000 for this bus. Now, the signals are further divided by 50 which is the internal scaling factor for current for SEL-351S relay. This can be found in the low-level test interface section of the SEL-351S instruction manual. The signals are put through a saturation block in order to protect the relay against very high magnitude signals. Similar scaling is performed with voltage signals. The difference being in the value of PT ratio and voltage scaling factor.

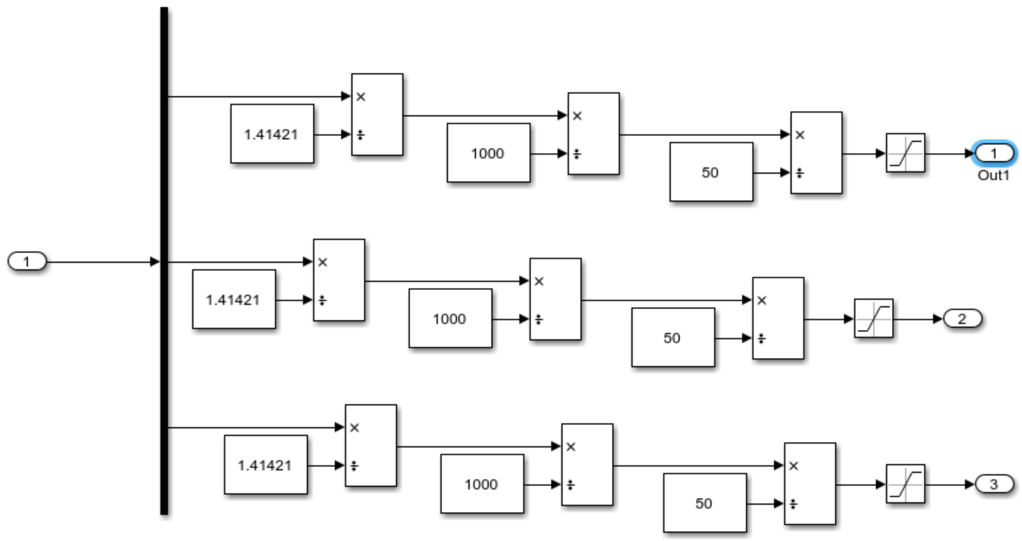

Figure 4.12: Current Scaling

4.1.4 Relay settings for IEEE 5 Bus testing

AcSELerator Quickset was used to do the relay settings for the SEL-351S relay. The settings were done to test faults at the feeder as well as a line. For feeder protection, inverse time overcurrent elements were implemented. Line relays were coordinated with a time delay to serve Directional overcurrent Elements as 5 Bus system is a ring system and has more than one source feeding the fault.

An IEEE 5 Bus system with a base voltage of 10kV was chosen and the loading at different buses as well as a generation at PV bus was set as per the IEEE 5 Bus load flow calculations. A breaker and a VI measurement block were modeled for Each line section and all the sources as well as loads. The breaker operation was externally controlled through the console subsystem which is shown in Figure 4.5.

Referring to Figure 4.3, Relay at Load bus 5 (Relay 1) was chosen to implement a feeder protection scheme, and Relay on line 2-5 looking towards load Bus 5 (Relay 2) was chosen to implement line protection scheme and a backup scheme for Relay 1.

4.1.4.1 Settings for Relay 1

The protection scheme for relay 1 involved setting time overcurrent (51) and instantaneous overcurrent (50) elements to protect and isolate the load during a faulty condition. Performing relay settings require information about maximum load current and minimum fault current. The relay pickup value is set above the maximum load current but below the minimum fault current for its proper operation. To determine maximum load current, 5 Bus system was simulated and the current at maximum load L5 was measured using the VI block. The value of this maximum load current was found out to be 3449 Amperes at 5868 Volts phase to ground voltage. To find out the minimum fault current, a single-phase to ground fault was simulated at load 5 terminals. The value of this fault current was noted as 56.47kA. Then a 3 phase fault was created at the same location to find the maximum fault current value, which was noted to be 58.53kA.

Time Overcurrent pickup (51P1P) = 1.2 X Maximum Load Current = 1.2 X 3450

$$= 4140\ Amperes\ (Primary)$$

CT ratio was selected as 5000/5 which is 1000.

Thus, 51P1P_secondary = 4140/CTR = 4140/ 1000 = 4.140 Amperes

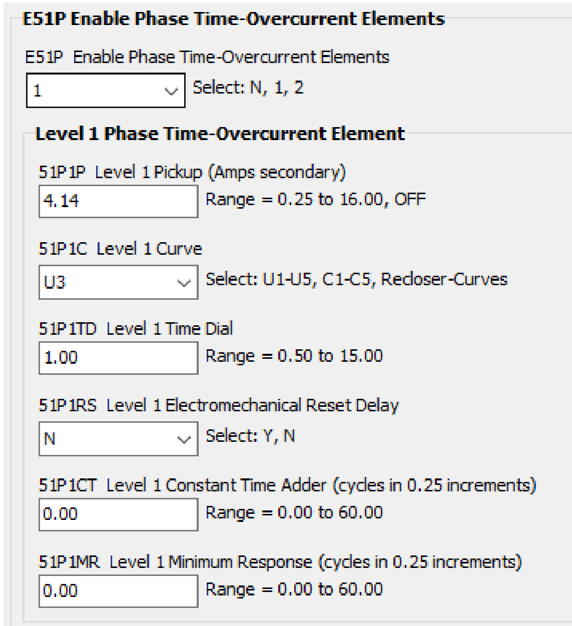

Figure 4.13: 51 Element setting for R1

Figure 4.13 shows the 51 element settings for R1. There are two 51 Elements in the SEL-351S relay and users can enable or disable them using E51P. The 51P1P pickup was set to 4.14 as calculated above. The inverse time curve 51P1C was can be selected from U1 to U5, C1 to C5. In this case, it was set to U3 which is very inverse characteristics. The time dial setting 51P1TD was set to 1. No Electro-mechanical reset time delay was given as there was no Electro-mechanical relay involved.

The time of operation for Relay 1 was calculated using an app-guide [58] which had an excel sheet to calculate the time of operation. This was a useful tool to perform protection coordination between relay R1 and R2. Figure 4.14 shows the steps to calculate the time of operation which in this case for relay 1 was 0.116 seconds. This time was used to find out time dial settings for relay 2.

An instantaneous overcurrent element was used to operate the relay at maximum fault currents. The maximum fault current noted for a three-phase fault was 58.53 kA, so the instantaneous pickup (50P1P) was set to detect 58 kA primary fault current

Relay and Nominal CT Current

Relay	SEL-351S
Nominal CT Current	5

Relay Settings

Nominal Frequency (Hz)	60
Pickup current (A sec)	4.14
Curve type	U3
Time Dial	1.00
Electromechanical Reset (Y, N)	N
Constant Time Adder	0 cycles
Minimum Response Time	0 cycles

Applied Current

Multiples of Pickup (select one)	14.13
Amps secondary	58.50

Results

Operate Time (sec):	0.116
Reset Time (sec):	

Figure 4.14: Time dial and Time of Operation Calculator for Relay 1

which translates to 58 Ampere secondary with a CT ratio of 1000. Figure A.1 in the appendix shows the complete settings for relay 1 along with the CTR, PTR, and line settings.

4.1.4.2 Settings for Relay 2

Relay 2 was located near Bus 2 end of Line 2-5 on the IEEE 5 Bus system. The primary protection zone for this relay was the protection of Line 2-5 and the backup protection zone was to provide coordinated backup for relay 1 which was protecting load 5. This formed a coordination pair and the settings were developed such that these two relays achieved proper coordination.

Line setting calculation was done from the IEEE 5 Bus data given in [57]. For lines 2-5, the per-unit value of R and X were 0.04 and 0.14 pu respectively. With a System base of 100 MVA and 10 kV as the base voltage, the Z_{base} for the system was calculated as 1 ohm.

$$Z = R + jX \tag{4.1}$$

$$|Z_{pu}| = (0.04^2 + 0.12^2)^{0.5} \ = \ 0.1265 \ pu \tag{4.2}$$

$$|Z| = (0.1265) * \ 1 \ ohm \ = 0.1265 \ ohms \tag{4.3}$$

$$CTR = 1000 \ ; PTR = 86 \tag{4.4}$$

$$Z_{1sec} = Z_1 \ (CTR/PTR) \ = 0.1265 \ (1000/86) \tag{4.5}$$

$$Z1MAG = 1.4709 \ Ohms \tag{4.6}$$

The value of Z1ANG was found taking the argument of Z. Zero sequence impedance was considered as three times that of positive sequence impedance. So, Z0MAG was found out to be 4.41 Ohms secondary.

To determine the time overcurrent pickup setting (51P1P) for relay 2, the maximum load current was noted to be 3046 Amps on the primary. To find out the minimum fault current, a single-phase to ground fault was simulated at the remote end of Line 2-5 as seen from relay 2. The value of this fault current was noted as 41.11kA. Then a 3 phase fault was created at the relay 2 terminals to find the maximum fault current value, which was noted to be 49.44kA.

$$Time\ Overcurrent\ Pickup\ (51P1P) = 1.2\ *\ Maximum\ Load\ Current$$

$$= 1.2 * 3046\ = 3655\ Amperes\ (Primary)$$

$$CTR\ = 5000/5\ =\ 1000$$

$$Thus,\ 51P1P\_secondary =\ 3655/\ CTR\ = 3655/1000\ = 3.6\ Amperes$$

To ensure security the pickup was set to 3.55 Ampere secondary. The relay coordination was done by choosing the correct value of the time dial. The time dial setting was calculated by using the app guide [58] and the excel tool for calculating the time of operation. Figure 4.15 shows the time of operation calculation for relay 2. The coordination was done at 42.25kA which was the current seen by the relay during a three-phase fault at L5 terminals. The time of operation for relay 1 was 0.116 seconds as shown in the previous section. Thus, the time dial was selected in such a way that relay 2 operated after 0.3 of relay 1. This ensured proper coordination between the two relays. The time dial was found to be 3.36 which was used in the relay settings.

An instantaneous overcurrent element was used to operate the relay at maximum fault currents. The maximum fault current noted for a three-phase fault at the remote end was 42.5 kA, so the instantaneous pickup (50P1P) was set to detect 42 kA primary fault current which translates to 42 Ampere secondary with a CT ratio of 1000. Figure A.2 shows the complete settings for relay 2 along with the CTR, PTR, and line settings. The relay coordination curves generated as an output of the macro tool is shown in figure 4.16

Relay and Nominal CT Current

Relay	SEL-351S
Nominal CT Current	5

Relay Settings

Nominal Frequency (Hz)	60
Pickup current (A sec)	3.55
Curve type	U3
Time Dial	3.36
Electromechanical Reset (Y, N)	N
Constant Time Adder	0 cycles
Minimum Response Time	0 cycles

Applied Current

Multiples of Pickup (select one)	11.90
Amps secondary	42.25

Results

Operate Time (sec):	0.416
Reset Time (sec):	

Figure 4.15: Time dial and Time of Operation Calculator for Relay at 2-5

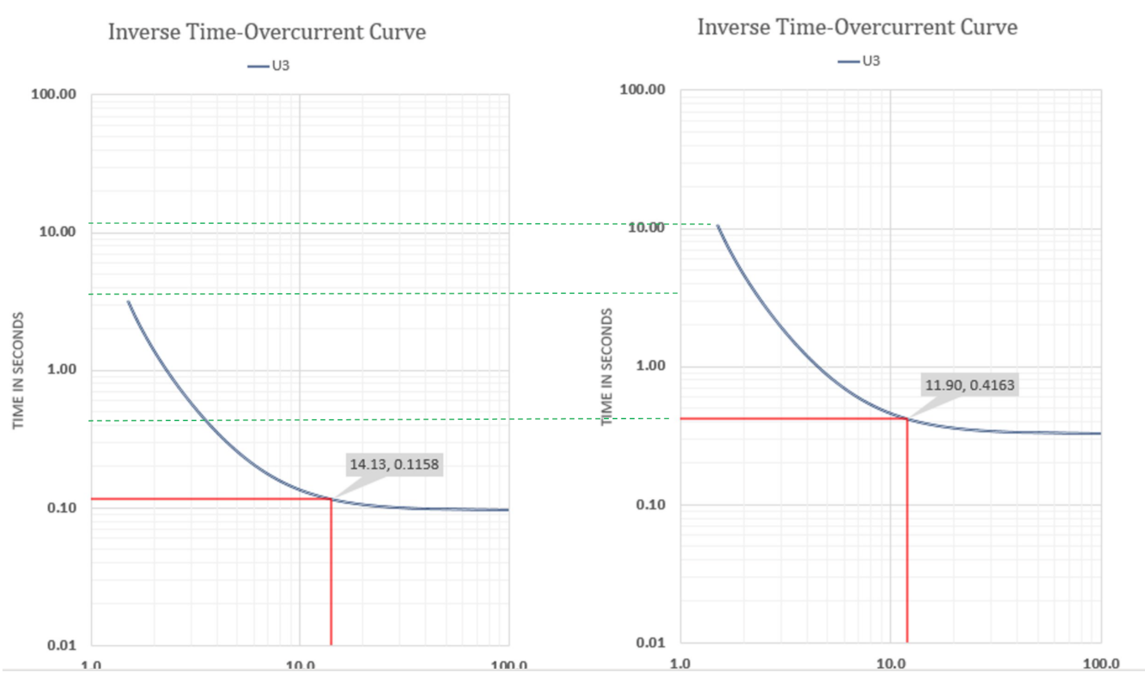

Figure 4.16: Relay Coordination Curves

4.2 Modified IEEE 5 Bus System

IEEE 5 Bus system modes were converted into a microgrid with source S2 being the main grid and the breaker at source 2 as the point of common coupling (PCC). IEEE 5 Bus system model used was at 10kV nominal voltage with S1 as the swing-bus and S2 as the main source. The load was connected to other buses. The model was modified to include solar PV, wind, battery energy storage to match the load demand. The load demand was reduced by a factor of 10 at all the loads to reduce the overall power of the microgrid. This was done to bring the 5 Bus system to depict actual microgrids present in today's scenario. There is a wide range of microgrid capacity; right from kilowatts to several megawatts. NREL has categorized the microgrid types depending on their size in [59]. The categories are campus/institutional; commercial/industrial, community, remote and utility.

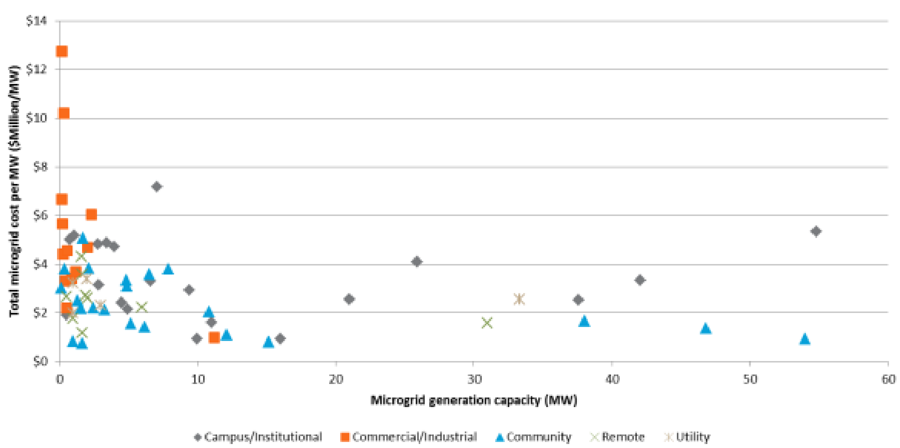

Figure 4.17: Microgrid Capacities as per categories

Figure 4.17 shows the generation cost per MW for different microgrid capacities. For this project, a community-scale microgrid size was chosen to implement on IEEE 5 Bus system. This allows testing the relay protection logic on a standard model modified to depict an actual scale microgrid.

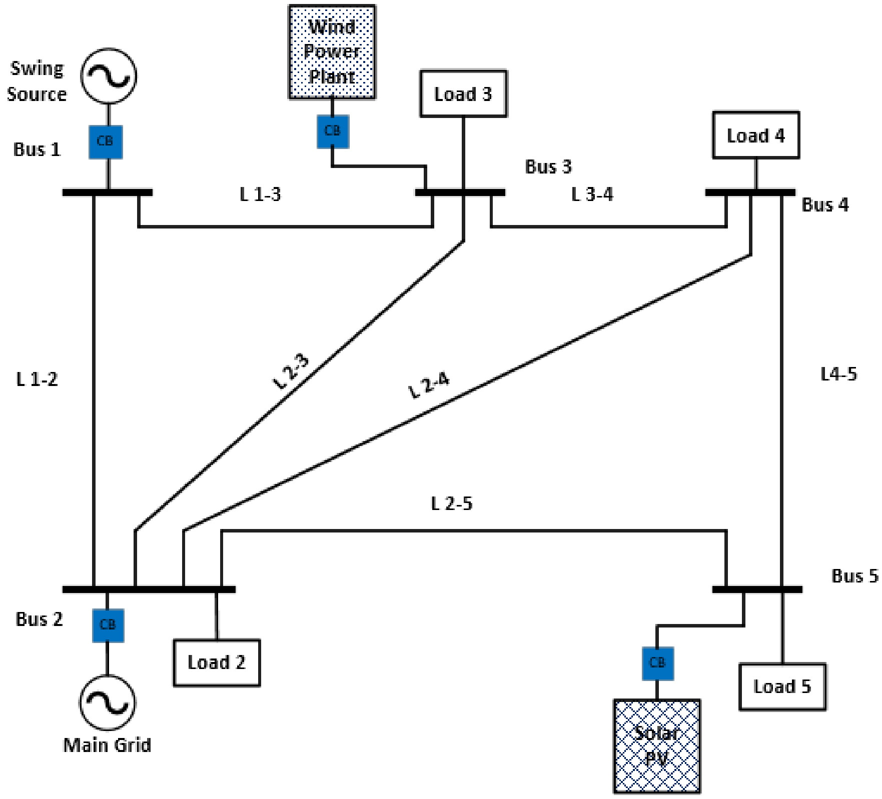

Figure 4.18: Single Line Diagram of Modified IEEE 5 Bus Microgrid

Figure 4.3 shows the single line diagram of the modified 5 Bus microgrid with solar PV, wind, battery, and slack Bus source used as a reactive power controller. The AIO and DIO configurations were used the same as in the case of IEEE 5 Bus system. Also, the console was kept uniform.

4.2.1 Solar PV

Solar PV was modeled using the solar PV module from Simulink library and as an inverter using MOSFET's Figure 4.19 shows the configuration of the PV module. The panels of solar power were selected which gave an output of 414.8 watts and 72.9 volts per module. The total number of series-connected modules was chosen as

10 and parallel modules as 1000. This resulted in a total generated power of 4.15 megawatts. The input to these modules was given through a constant block and a rate limiter block.

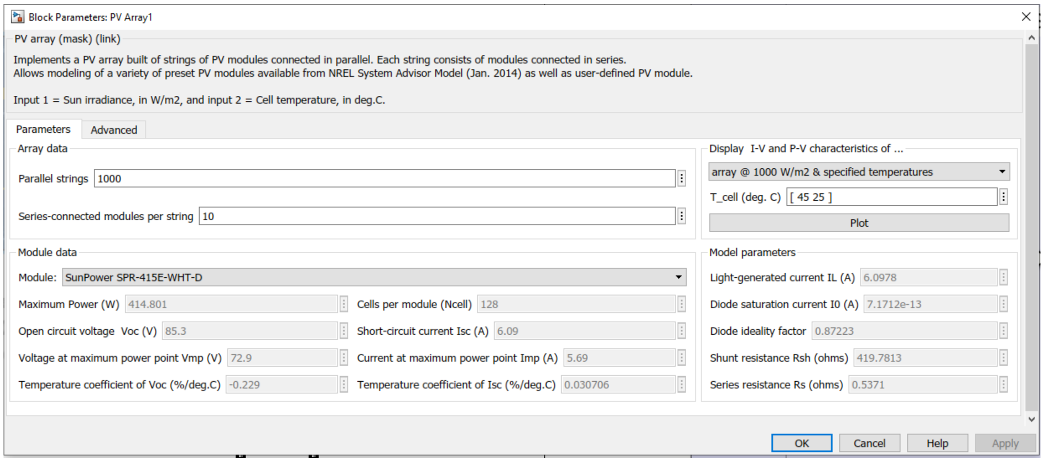

Figure 4.19: Solar PV Module

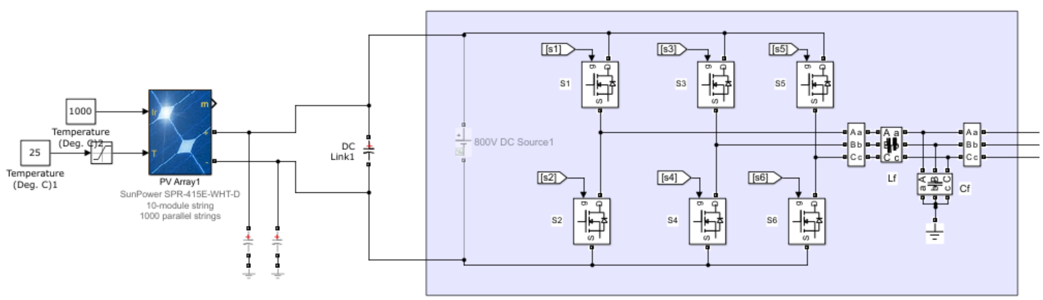

Figure 4.20: Solar Inverter

Figure 4.20 shows the 3 phase inverter connected with solar PV modules. It consists of six MOSFET's triggered through a Gate control circuit as shown in Figure 4.21. At the output of the inverter, a series RL circuit and a parallel capacitor were connected in order to smooth out the ripples in the AC waveform generated by the inverter. The output voltage of the inverter was 800 volts which was then input to a 3 phase transformer to step it up to 10kV line to line voltage in order to connect it with the rest of the microgrid. VI measurement block was connected to measure and label the voltages and currents generated by the solar PV module. Then a circuit breaker

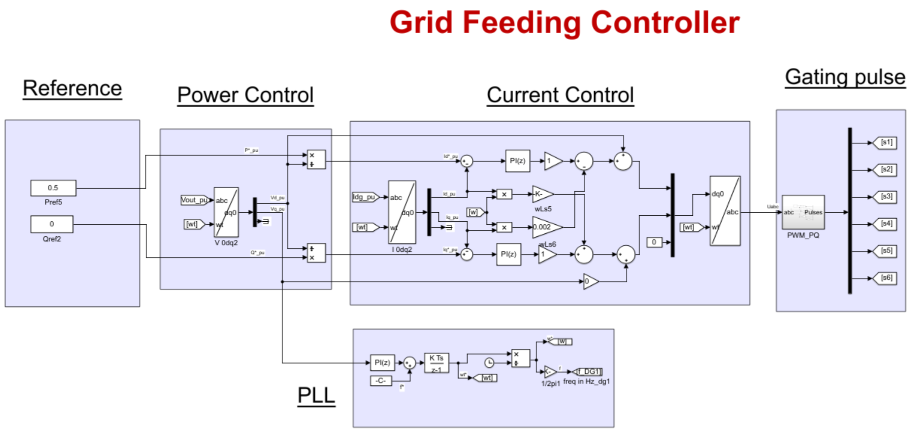

Figure 4.21: GATE Control Mosfet

was connected and its operation was controlled through the manual switch in the console subsystem. Figure 4.22 shows the complete model whose operation was first individually tested without the microgrid.

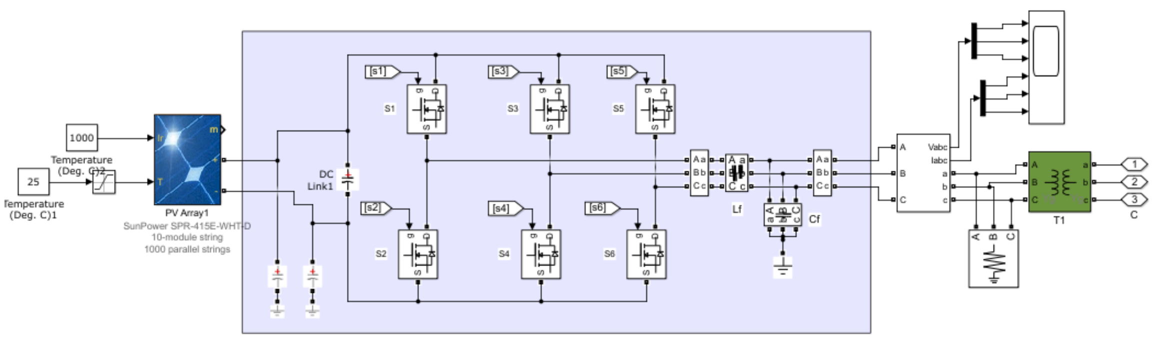

Figure 4.22: Complete Solar PV model

4.2.2 Wind

Wind power plants were modeled in a single subsystem which had the main circuit breaker whose operation was controlled through the console subsystem. Figure 4.23 shows the complete model within the wind power plant subsystem. It consists of a wind energy generator module, a 3 phase transformer, etc.

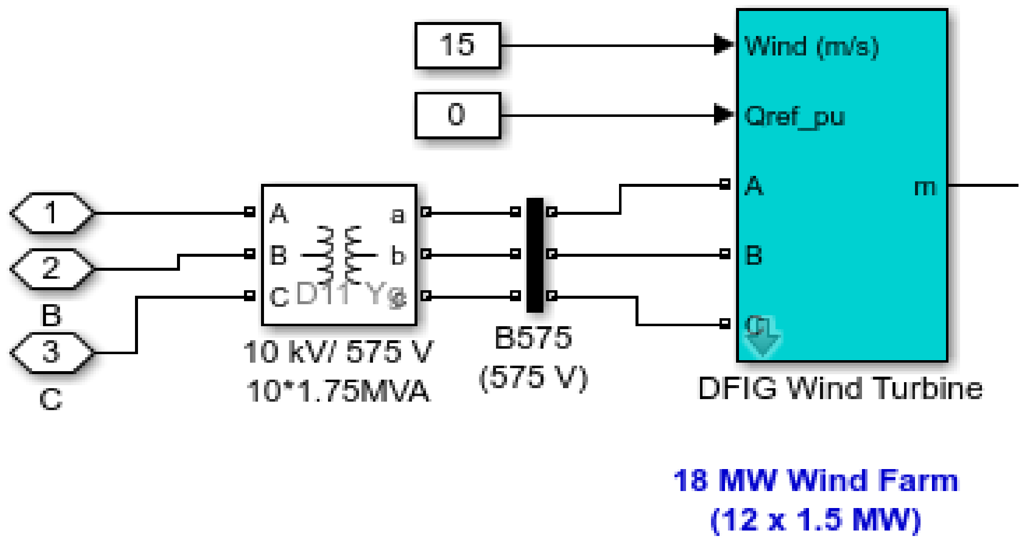

Figure 4.23: Wind Power Plant

Figure 4.24 shows the configuration of the wind energy system. Twelve numbers of 1.5MVA wind energy generator modules were connected in parallel. The nominal voltage of each wind turbine was selected as 575 volts. A setup transformer was used to step up the voltage from 575 volts to 10 kVolts.

Figure 4.25 shows the configuration for transformer. Figure 4.26 shows the under the masked subsystem of the wind turbine. It has an induction generator whose output is fed AC-DC-AC converter whose operation is controlled by a wind turbine control subsystem.

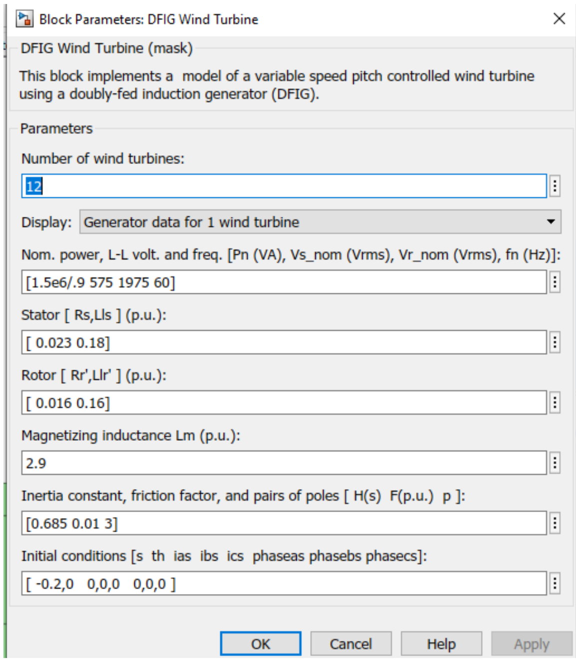

Figure 4.24: Wind Turbine Configuration

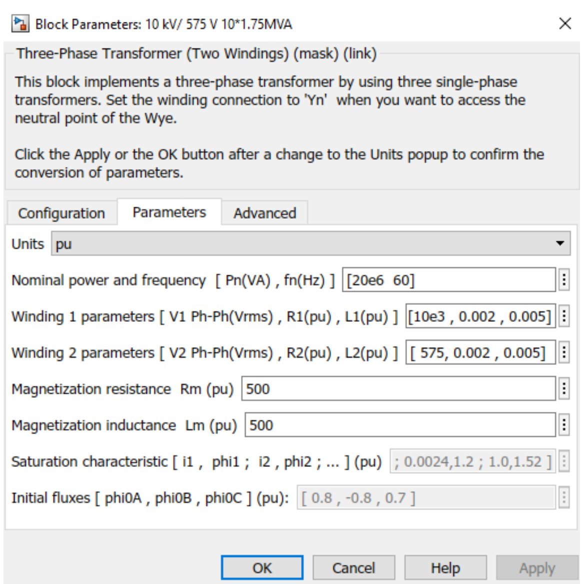

Figure 4.25: Transformer Configuration

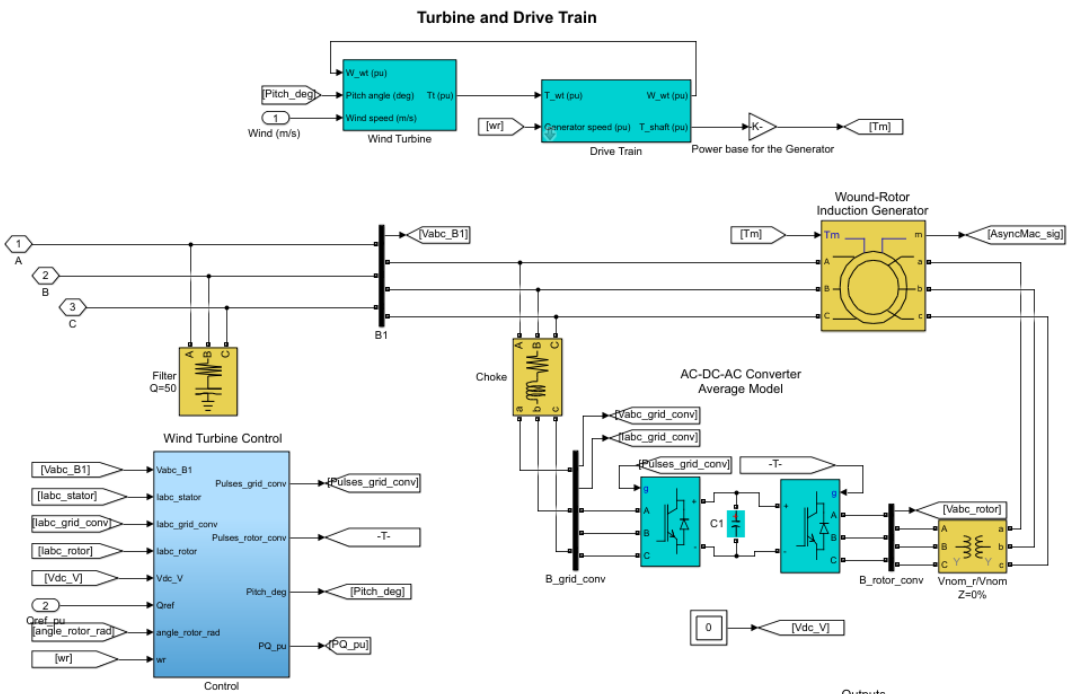

Figure 4.26: Masked Model of Wind Turbine

4.2.3 Relay Settings

IEEE Modified 5 Bus system was modeled to form a microgrid. The power of this microgrid was chosen to be 20 MVA. The loads were adjusted accordingly by reducing them by a factor of 10 so that the distributed sources are able to match this load demand. This was done in order to mimic the actual community grids as described in [59]. The relay settings were changed accordingly by calculating the new pickup values and coordinating the two relays based on these values. The following sections describe the relay settings calculation for the Microgrid in grid-connected and Islanded modes. Furthermore, the settings are developed so that the group change algorithm can be tested as well as the unique approach of multiple pickup settings can be tested.

4.2.3.1 Grid Connected Mode

In this mode of operation, the Circuit Breaker at PCC was closed and all the distributed generators were turned off. This mode involved the presence of a strong source which is the main grid and the fault current contribution during a fault on the microgrid came from the strong sources of the main grid which resulted in the detection of high fault current magnitudes. Relay 1 and relay 2 were again chosen as a protection coordination pair and settings were developed.

Relay 1 Settings

Developing the settings for relay 1 followed the same procedure as described in Section 4.1.4.1. The maximum load current as seen by relay 1 was found out to be 351 Amperes. To find out the minimum fault current, a single-phase to ground fault was simulated at load 5 terminals. The value of this fault current was noted as 31.71kA.

Then a 3 phase fault was created at the same location to find the maximum fault current value, which was noted to be 55.90kA. Following the same calculations as in Section 4.1.4.1, the time overcurrent pickup (51P1P) was found to be 5.26 Amp secondary considering a future load growth of 1.5 times. The instantaneous pickup was set below the minimum fault current which was found out by simulating an SLG fault at L5 terminals. The complete settings are shown in the relay settings sheet in Figure A.3.

Relay 2 Settings

Relay 2 setting procedure followed the same calculation steps as described in Section 4.1.4.2. As the same line (Line 2-5) was selected even in this case and the parameters of IEEE 5 bus didn't change, the line parameter calculations remained the same. CTR was selected as 100 and PTR was maintained at 86 with Vnom as 67 Volts. Time overcurrent pickup (51P1P) was selected as 3.84 Ampere secondary which is 1.5 times the rated secondary current (2.56A). The process for instantaneous overcurrent pickup (50P1P) was the same as explained in previous sections. The time dial calculation was done to have a coordination time interval of 0.3 secs, these calculations are shown in figure 4.27. The complete settings file for Relay 2 in the grid-connected mode for modified IEEE 5 Bus microgrid is shown in figure A.4.

4.2.3.2 Islanded Mode with Solar

During islanded mode, complete load on the system was supplied through a solar power plant and a reactive power source was also switched on in this mode to fulfill the reactive power requirement of the loads and lines. The active and reactive power requirements were scaled down by a factor of 10 to bring down the Microgrid capacity to a near practical microgrid. Transitioning from grid-connected mode to islanded

Relay and Nominal CT Current	
Relay	SEL-351S
Nominal CT Current	5
Relay Settings	
Nominal Frequency (Hz)	60
Pickup current (A sec)	3.84
Curve type	U3
Time Dial	2.46
Electromechanical Reset (Y, N)	N
Constant Time Adder	0 cycles
Minimum Response Time	0 cycles
Applied Current	
Multiples of Pickup (select one)	6.03
Amps secondary	23.16
Results	
Operate Time (sec):	0.507
Reset Time (sec):	

Figure 4.27: Time Dial Calculation for Relay 2

mode reduced the fault current magnitude fed to the fault drastically and the relay pickup settings done for grid connected mode won't be able to detect a fault during this mode. The same load and line were selected to perform protection coordination. The settings for both of these relays are described below.

Relay 1 Settings

Time overcurrent pickup (51P1P) was selected as 3.88 Ampere secondary which is 1.1 times the rated current. This was done as the fault current in a distributed generator with a converter can typically source current 1.1 to 1.5 times the rated current (in exceptional cases this can go to 2 times rated). Instantaneous pickup (50P1P) was also set to 3.88 as the fault current contribution by the inverter will be around this point as the inverters chop the output current to this above-mentioned range. Figure A.5 shows the complete settings for Relay 1 in islanded mode with only Solar as the source.

Relay 2 Settings

Settings for Relay 2 involved measuring the maximum current flowing through lines 2-5 during the maximum loading condition of all the loads in the 5 bus system. The relay settings were developed by following the same methodology as for settings done for relay 1. Only the Time multiplier setting was found out using the app-guide [58]; the value of TOC was found out to be 2.46. The time overcurrent and instantaneous overcurrent settings were calculated using the maximum current flowing through relay 2 and are shown in Figure A.6.

4.2.3.3 Islanded Mode with Wind

In this mode of operation, the microgrid was disconnected from the main grid and a Wind power plant supplied the total power requirement of the grid. The settings procedure for this mode was similar to that of Solar connected mode. The only difference was that the fault current sourcing was a little higher than Solar.

Relay 1 Settings

Instantaneous overcurrent pickup (50P1P) was selected as 3.92 Ampere secondary which is 1.15 times the rated current. This was done as the fault current in Type 4 Wind turbine based distributed generator with a converter can typically source current 1.1 to 1.5 times the rated current (in exceptional cases this can go to 2 times rated) as per NREL in [60].

Relay 2 Settings

Settings for relay 2 involved measuring the maximum current flowing through lines 2-5 during the maximum loading condition of all the loads in the 5 bus system. The relay settings were developed by following the same methodology as for settings done for relay 1. Only the time multiplier setting was found out using the app-guide [58]; the value of TOC was found out to be 2.46. The time overcurrent and instantaneous overcurrent settings were calculated using the maximum current flowing through relay 2.

Chapter 5

Testing and Results Discussion

The scope of this chapter is to present all the results that were generated during testing the relay for different fault scenarios and discuss the outcomes to point out towards the conclusion of the testing. This chapter also goes into describing the various test scenarios and the motivation behind those.

5.1 IEEE 5 Bus testing

IEEE 5 Bus system was chosen as a testbed to develop the relay settings and test the relay operation in real-time using OPAL-RT as a real-time digital simulator. The relay settings were developed as discussed in Section 4.1.4. Testing the relay in real-time involved connecting a relay, SEL-351S in this case to the analog output channels of OPAL-RT as explained in Sections 3.3 and 4.1. The relays R1 and R2 were tested for different fault scenarios and proper operation of the element was verified through these tests.

5.1.1 Fault Scenarios

Relay 1 was tested for terminal fault as it was protecting a load and relay 2 was tested for the terminal as well as line end faults. Also, relay 2 was tested for directionality by creating faults in front and reverse directions. Three-phase faults were created at all the locations to test the operation of a relay at maximum fault current as well as check the coordination between relay R1 and R2.

5.1.1.1 Fault at Load 5 terminals

A three-phase fault was created at load 5 terminals in real-time through the console subsystem by changing the position of the manual switch. This caused a fault current flow through bus 5 towards load 5 and was measured by the VI block on the bus. These measured values of voltage and current were injected into the main board of the SEL-351S relay through analog output channels of OPAL-RT. Figure 5.1 shows the output generated by OPAL-RT which is given to main board of the relay. Channels 1 to 3 generate voltage signals corresponding to the current scaling factor of the relay; whereas channels 5 to 7 generate voltages corresponding to voltage scaling factor. Channels 4 and 8 don't carry any signals as these are for neutral currents and synchronous voltages respectively. This interconnection is described in Chapter 3. Figure 5.2 shows the HMI screen showing injected voltages and currents seen by the relay R1 and the targets displayed on the relay front panel. Figure 5.3 shows the Event Report from relay 1 for this fault. The graph on the top of this image shows the RMS magnitudes of currents plotted with respect to time. This is the RMS calculated by the relay. The bottom graph shows digital bit operation with respect to time.

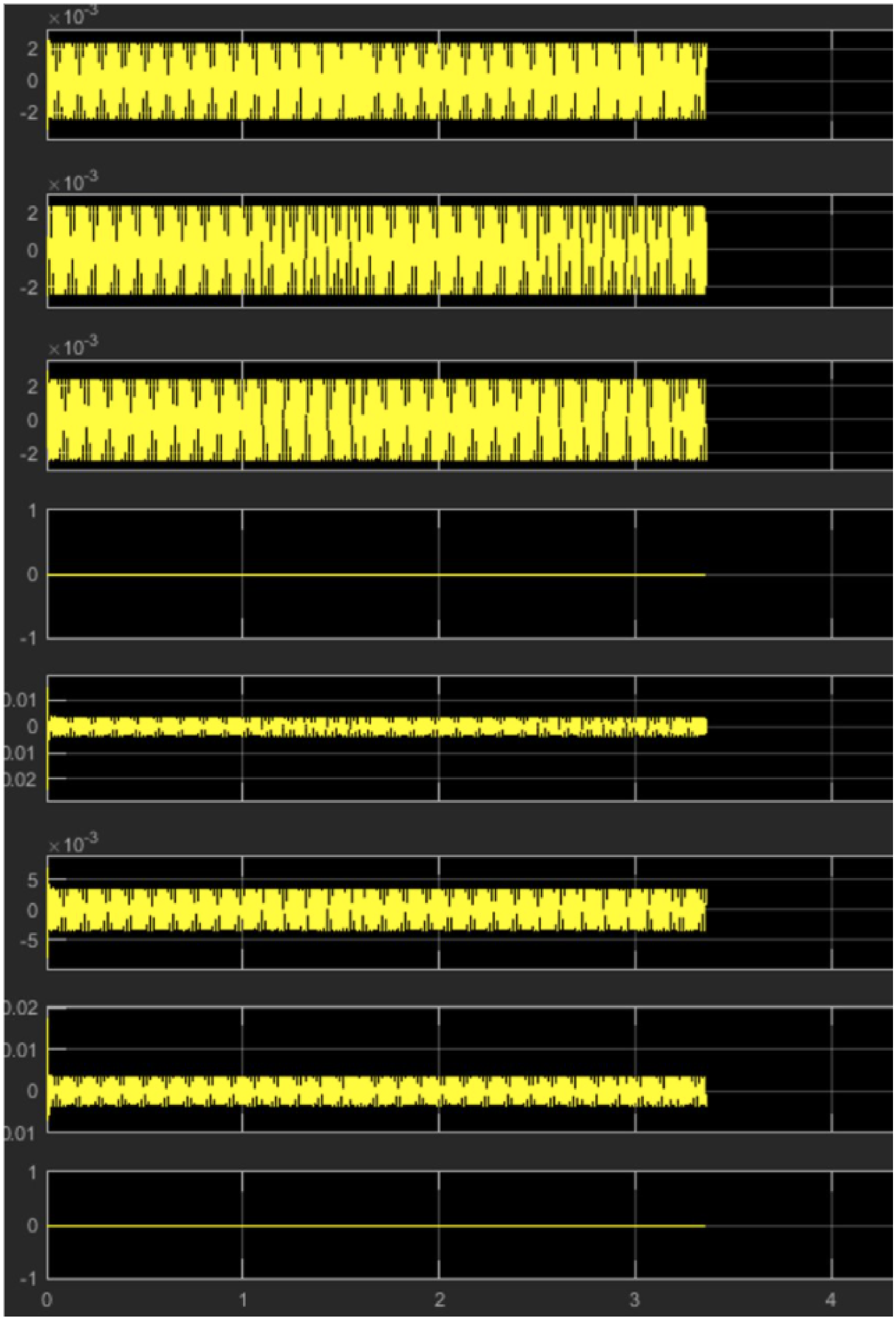

Figure 5.1: Analog Output of OPAL-RT

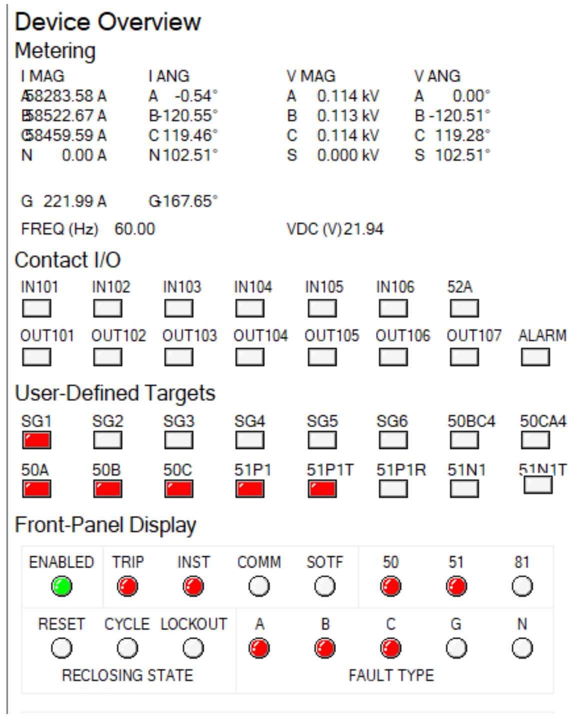

Figure 5.2: Relay 1 HMI Screen for 3phase fault at load 5 terminal

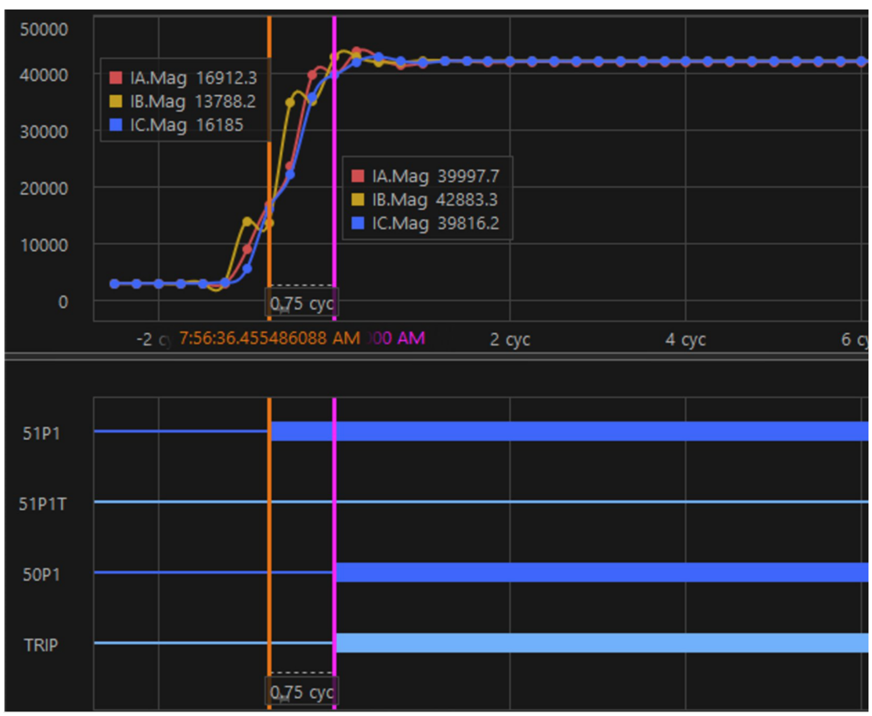

Figure 5.3: Relay 1 Event Report for 3phase fault at load 5 terminal

As seen from the figure 5.2, the time overcurrent, as well as the instantaneous elements operated as both of the pickups, were reached during this fault. Figure 5.4 shows the phasors displayed by the relay HMI interface during this fault. The sequence of operation can be better understood by looking at the timestamps of Sequential Event Records (SER) which is another very good feature of SEL relays. Figure 5.5 shows the SER report for this fault. It is evident that the 50P1 element asserted first and as it did not have any time delay, it was able to trip the relay; whereas the time overcurrent element timed out after the specified time defined by the relay curve and it asserted after the trip was already asserted.

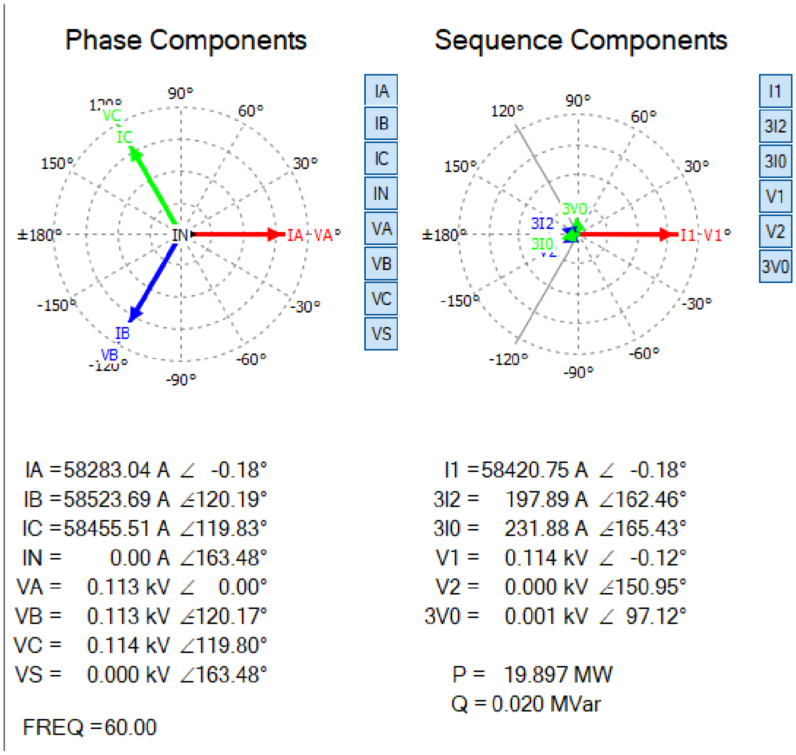

Figure 5.4: Relay 1 Phasors for 3phase fault at load 5 terminal

#	Date	Time	Element	State
4	03/19/21	06:37:30.500	51P1	Asserted
3	03/19/21	06:37:30.517	50P1	Asserted
2	03/19/21	06:37:30.517	TRIP	Asserted
1	03/19/21	06:37:30.600	51P1T	Asserted

Figure 5.5: Relay 1 SER for 3phase fault at load 5 terminals

In order to verify the relay coordination, the fault currents flowing through lines 2-5 as measured by the VI block were injected into the relay to observe its performance. Before doing this the settings developed in Section 4.1.4.2 were sent to the relay. Figure 5.6 shows the HMI screen displaying the currents and voltages seen by the relay during a 3 phase fault at load 5 terminals. Figure 5.7 shows the event report snapshot from Synchrowave software for the fault at load bus 5 and seen by relay 2.

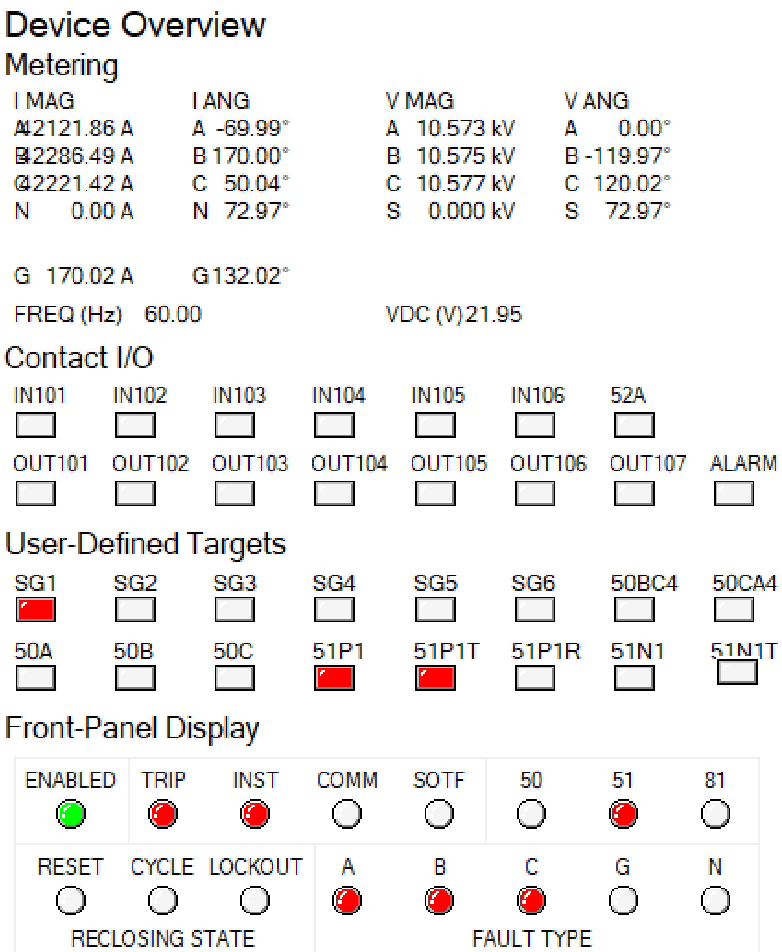

Figure 5.6: Relay 2 HMI Screen for 3phase fault at load 5 terminal

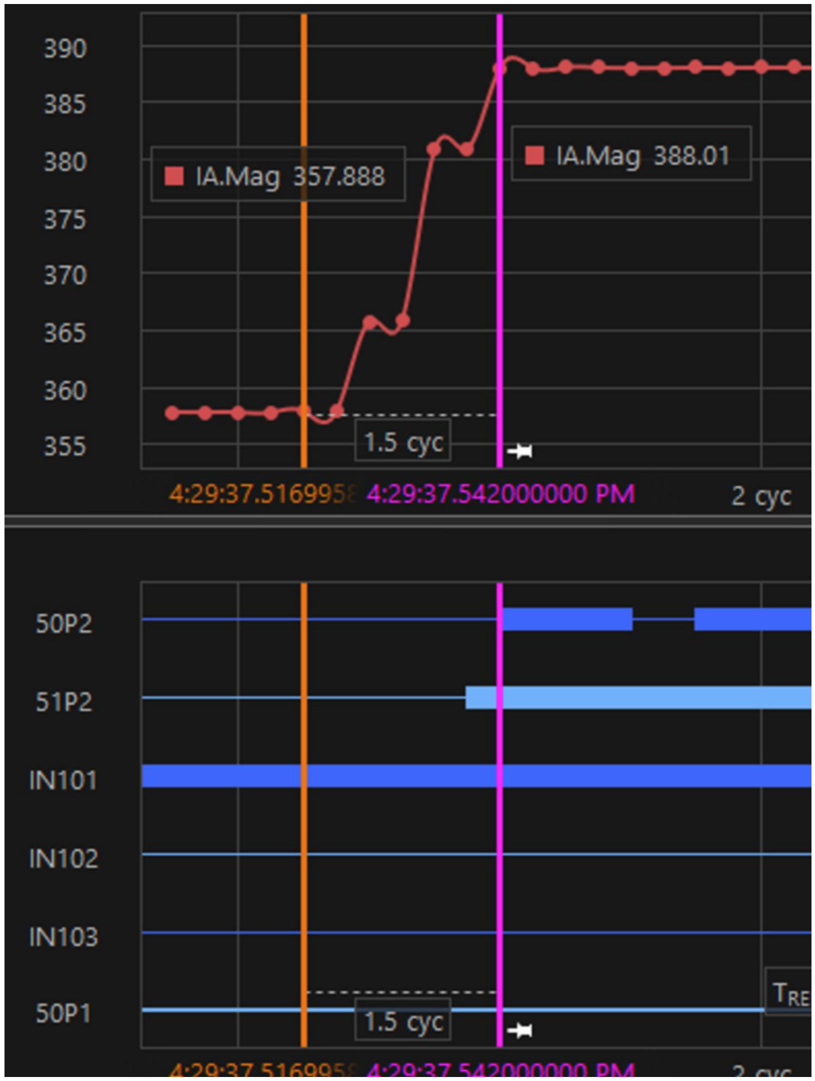

Figure 5.7: Relay 2 Event Report for 3phase fault at load 5 terminal

#	Date	Time	Element	State
13	03/19/21	04:44:26.302	51P1	Asserted
12	03/19/21	04:44:51.095	51P1	Deasserted
11	03/19/21	04:47:38.082	51P1	Asserted
10	03/19/21	04:48:20.962	51P1	Deasserted
9	03/19/21	04:48:20.971	51P1	Asserted
8	03/19/21	04:48:21.354	51P1T	Asserted
7	03/19/21	04:48:21.354	TRIP	Asserted
6	03/19/21	04:49:57.868	51P1	Deasserted
5	03/19/21	04:49:57.885	51P1T	Deasserted
4	03/19/21	04:49:57.885	TRIP	Deasserted
3	03/19/21	04:50:18.783	51P1	Asserted
2	03/19/21	04:50:19.183	51P1T	Asserted
1	03/19/21	04:50:19.183	TRIP	Asserted

Figure 5.8: Relay 2 SER for 3phase fault at load 5 terminal

5.1.1.2 Fault at remote end of line 2-5 in forward direction

In order to ensure the operation of relay R2, a three-phase fault was created at the remote end of lines 2-5 which was in the forward direction as seen from relay R2. The operation of relay R2 was verified for its forward directional supervision. Figure 5.9 shows the HMI for remote end fault; Figure 5.10 shows the phasor and Figure 5.11 shows the SER data for this fault. It can be clearly observed that the 51P1 elements pick up first as current first crossed this pickup setting, but has to wait to time out as per the US3 curve. Then 50P1 pickups and as it does not have any time delay set; it asserts the Trip bit of the relay.

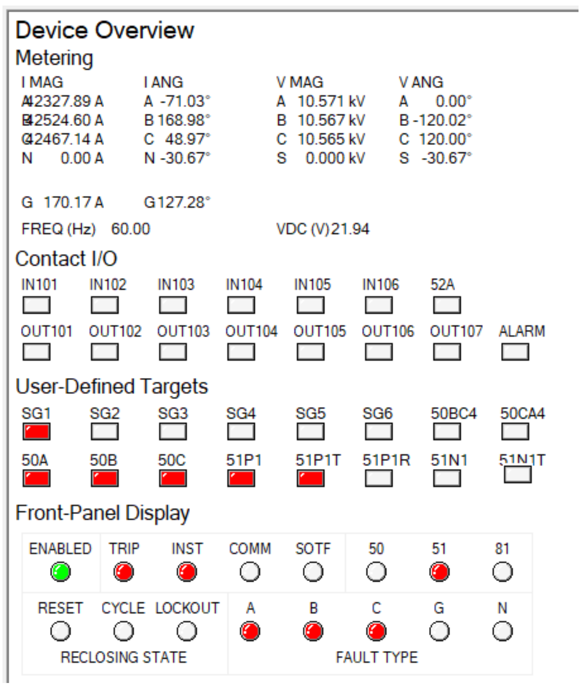

Figure 5.9: Relay 2 HMI Screen for 3phase fault at remote end of line 2-5

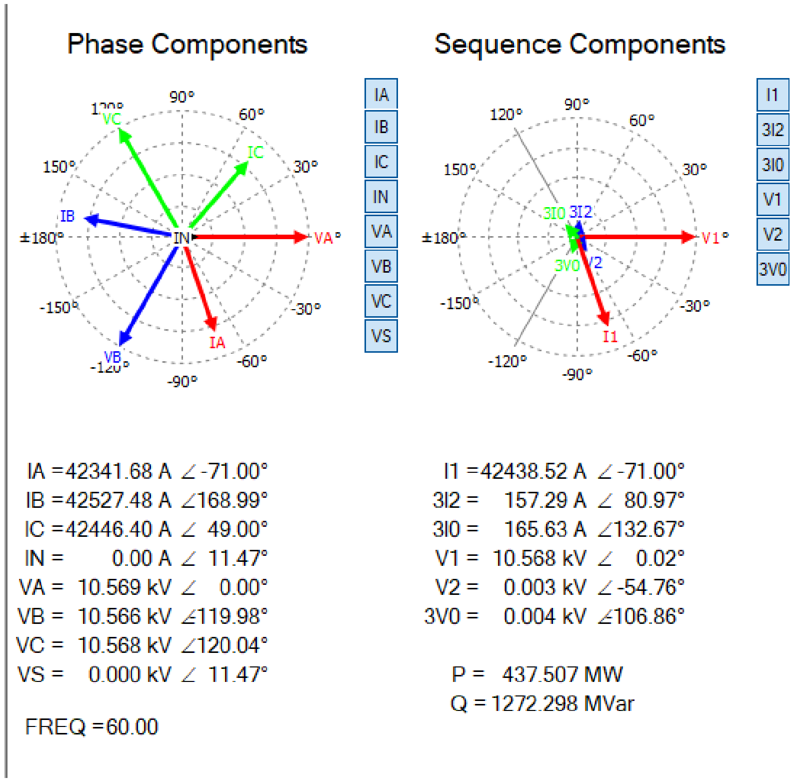

Figure 5.10: Relay 2 Phasors for 3phase fault at remote end of line 2-5

#	Date	Time	Element	State
4	03/19/21	07:51:37.586	51P1	Asserted
3	03/19/21	07:51:37.607	50P1	Asserted
2	03/19/21	07:51:37.607	TRIP	Asserted
1	03/19/21	07:51:38.003	51P1T	Asserted

Figure 5.11: Relay 2 SER for 3phase fault at remote end of line 2-5

5.1.1.3 Fault behind R2 in Reverse direction

Directional element supervision was enabled in the relay by setting the E32 to Y, thus adding directional supervision to the overcurrent elements. This was done to ensure selectivity of relay operation during faults in IEEE 5 Bus system, which is a ring bus. To test this a fault was created just behind the relay R2 and its operation was verified. Figure 5.12 shows the HMI for remote end fault and Figure 5.13 shows the phasor. The relay R2 didn't trip for this fault which means the overcurrent element has enough supervision to make it secure.

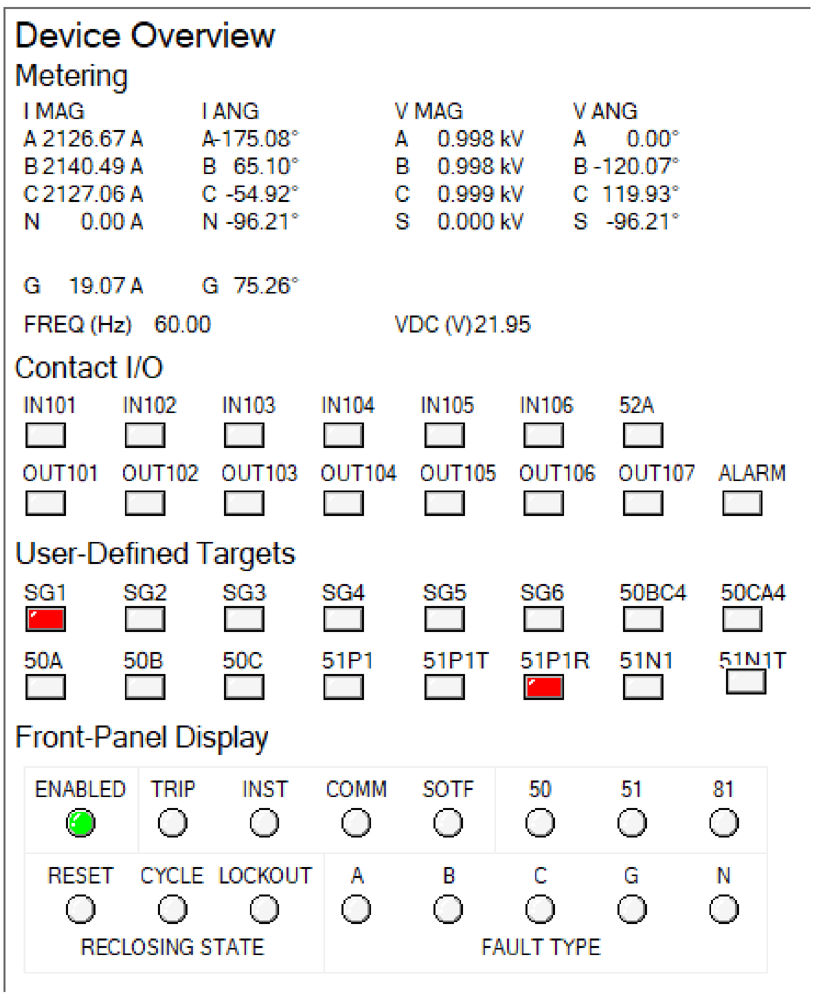

Figure 5.12: Relay 2 HMI Screen for 3phase fault at Reverse of R2

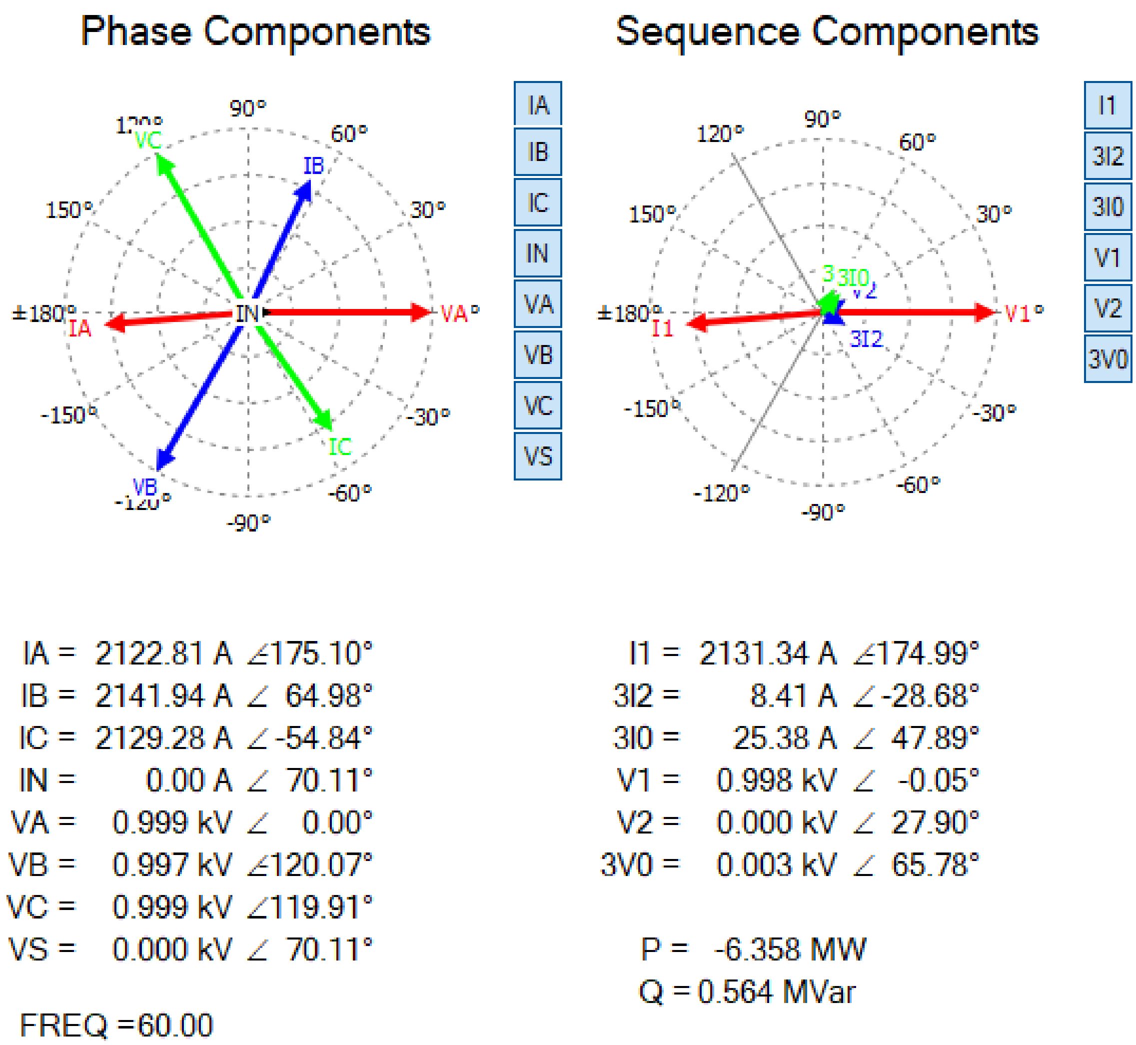

Figure 5.13: Relay 2 Phasors for 3phase fault at Reverse of R2

5.2 Testing of Modified IEEE 5 Bus System Microgrid with Distributed Generators

IEEE 5 Bus system was modified to include distributed generators such as Solar, Wind, etc. which is discussed in 4.2. Testing this microgrid involved tests performed at different modes of operation of the microgrid. The testing and related observation for grid-connected and islanded modes are discussed in the following section. During this testing, all the faults created were single line to ground faults.

5.2.1 Grid Connected Mode

Grid-connected mode is the one when the Point of Common Coupling circuit breaker is closed. This mode of operation has the strongest source, thus the fault current magnitude is very high. The settings for this mode are discussed in Section 4.2.3.1. Testing this mode involved creating an SLG fault at Load 5 Terminals and verifying the relay operation of relay R1 and R2 for the same fault. Figure 5.14 shows the HMI for SLG fault at load 5 terminals; Figure 5.15 shows the metering screen and Figure 5.16 shows the SER data for the same fault. It can be seen that the relay was able to detect and generate a trip for this fault, thus verifying the relay settings.

Figure 5.17 shows the HMI screen of relay 2 for SLG fault at load 5 terminals; Figure 5.18 shows the phasor and Figure 5.19 shows the SER data for the same fault as seen by Relay 2. It can be observed that the relay tripped on 67P1 which means the directional supervision works.

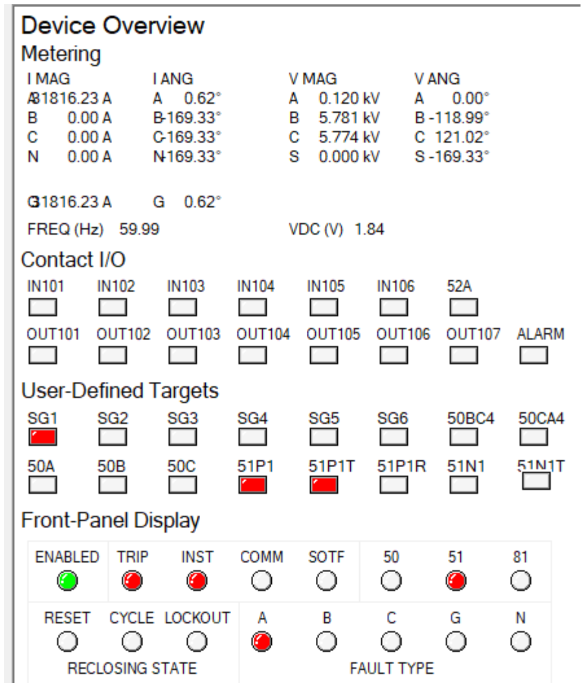

Figure 5.14: Relay 1 HMI Screen for SLG fault at Load 5 terminals

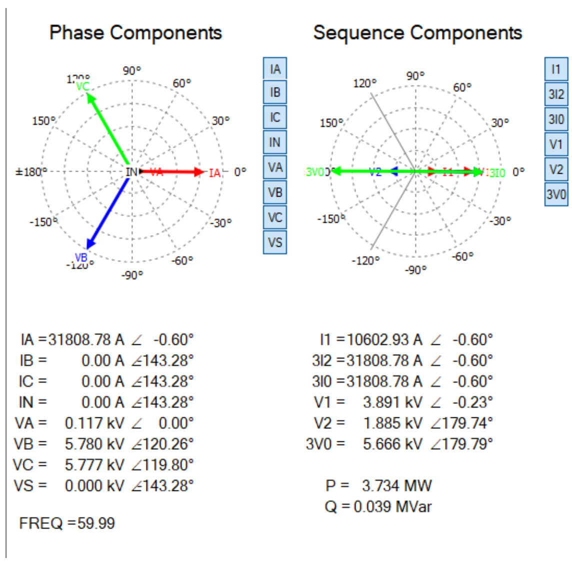

Figure 5.15: Relay 1 MET for SLG fault at Load 5 terminals

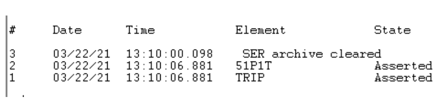

#	Date	Time	Element	State
3	03/22/21	13:10:00.098	SER archive cleared	
2	03/22/21	13:10:06.881	51P1T	Asserted
1	03/22/21	13:10:06.881	TRIP	Asserted

Figure 5.16: Relay 1 SER for SLG fault at Load 5 terminals

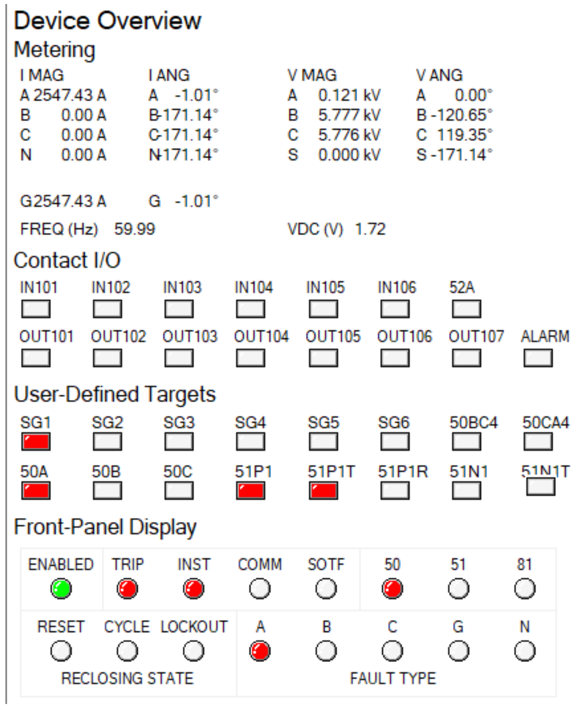

Figure 5.17: Relay 2 HMI Screen for SLG fault at Load 5 terminals

```
=>>met

SEL-351S51HB455421              Date: 03/22/21    Time: 13:31:25.084
MTU-KF-BCNT  9/17/2008

                 A          B          C          N          G
I MAG (A)     2546.224     0.000      0.000      0.000   2546.224
I ANG (DEG)      0.00      0.00       0.00       0.00      -0.00

                 A          B          C          S
V MAG (KV)       0.118      5.781      5.775      0.000
V ANG (DEG)     -0.43   -119.62     120.41       0.00

                 A          B          C          3P
MW               0.300      0.000      0.000      0.300
MVAR            -0.002      0.000      0.000     -0.002
PF               1.000      1.000      1.000      1.000
                 LEAD       LAG        LAG        LEAD

                 I1        3I2        3I0         V1         V2        3V0
MAG            848.741  2546.224  2546.224      3.892      1.886      5.664
ANG   (DEG)     -0.00     -0.00      -0.00       0.39   -179.64   -179.54

FREQ (Hz)      59.99               VDC (V)       1.8
```

Figure 5.18: Relay 2 Phasor for SLG fault at Load 5 terminals

```
4      03/22/21  13:32:34.782    SER archive cleared
3      03/22/21  13:32:49.423   67P1                 Asserted
2      03/22/21  13:32:49.423   TRIP                 Asserted
1      03/22/21  13:32:49.856   51P1T                Asserted
```

Figure 5.19: Relay 2 SER for SLG fault at Load 5 terminals

5.2.2 Islanded Mode

In the islanded mode of operation, the PCC was opened and one distributed generator was feeding the whole microgrid. Only one distributed generator was kept on for a particular mode due to controller tuning issue resulting in power swings in the microgrid. Controller tuning and Optimal load flow were not the scope of this project,thus to verify the relay operation during both modes, one source at a time was brought into the picture. The following section describes the testing performed on the islanded mode of operation of microgrid and only details the operation of solar-powered microgrid state; wind-powered offered similar behavior which is discussed in the succeeding sections.

To understand and mimic the issue of using the same settings while transitioning from grid-connected to islanded mode, the relay settings were kept the same, and mode was changed from grid connected to islanded. An SLG fault was created at the same locations as in grid-connected mode (Load 5 Terminal) and remote end of line 2-5 for which the relay behavior was observed. As it is evident from Figure 5.20 and Figure 5.21 that the relays didn't generate a trip command for both of these faults as the current seen was less than the pickup settings of the relays.

To overcome this issue, new pickup values were calculated which are explained in Section 4.2.3.2 for Solar as well as Section 4.2.3.3 for Wind. These settings were tested which are described in the sections to follow. The same faults were simulated, but this time new settings were sent to the relay before the simulation. It can be seen from the Figure 5.22 and Figure 5.23 that the relay was successfully able to detect and generate a trip for these faults. Figure 5.24 and Figure 5.25 show the SER report for these faults.

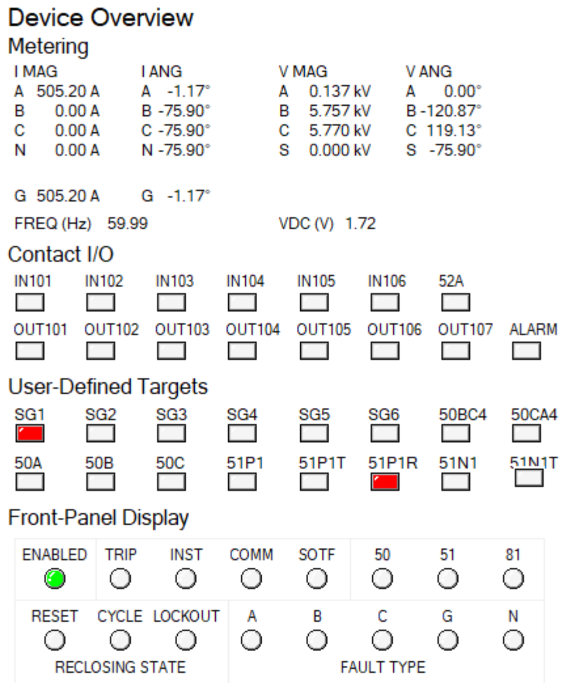

Figure 5.20: Relay 1 HMI for SLG fault at Load 5 terminals in Islanded Mode

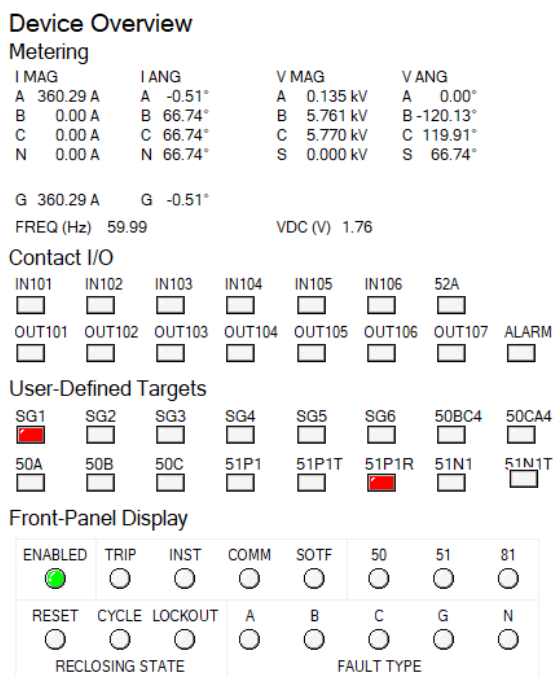

Figure 5.21: Relay 2 HMI for SLG fault at Line 2-5 in Islanded Mode

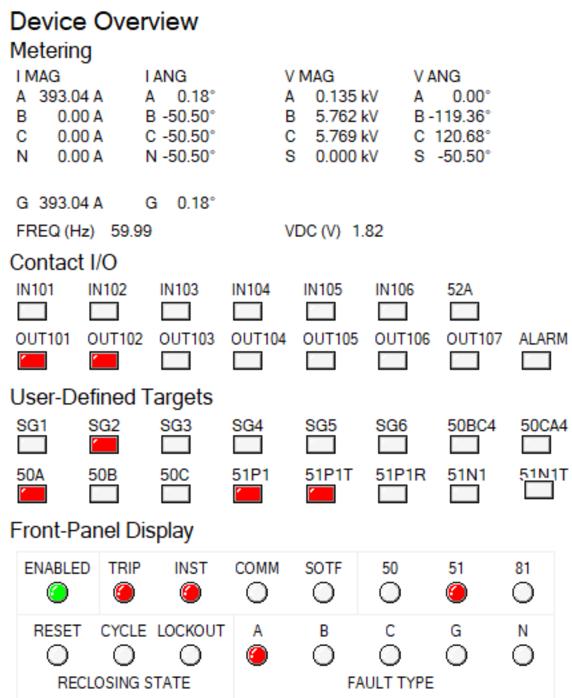

Figure 5.22: Relay 1 Operation HMI for SLG fault at Load 5 in Islanded Mode

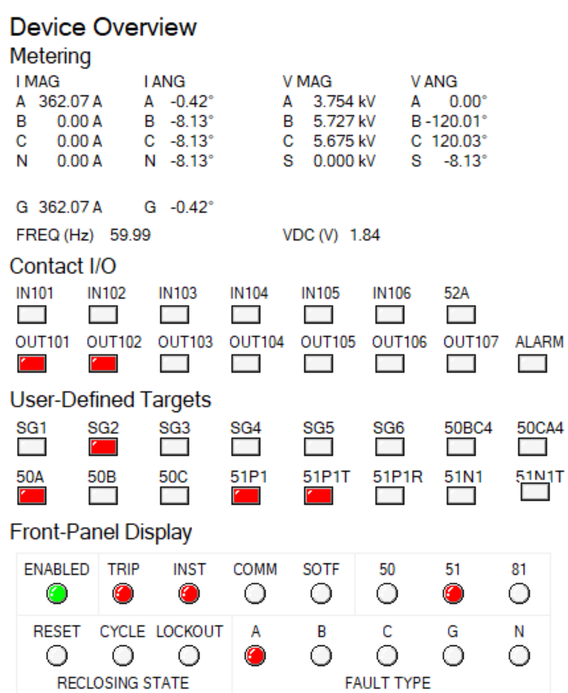

Figure 5.23: Relay 2 Operation HMI for SLG fault at Line 2-5 in Islanded Mode

4	03/22/21	14:27:27.124	SER archive cleared	
3	03/22/21	14:27:34.756	51P1	Asserted
2	03/22/21	14:27:34.756	50P1	Asserted
1	03/22/21	14:27:34.756	TRIP	Asserted

Figure 5.24: Relay 1 Operation SER for SLG fault at Load 5 in Islanded Mode

#	Date	Time	Element	State
5	03/22/21	14:41:43.629	SER archive cleared	
4	03/22/21	14:41:54.120	51P1	Asserted
3	03/22/21	14:41:54.120	50P1	Asserted
2	03/22/21	14:41:54.120	TRIP	Asserted
1	03/22/21	14:42:44.492	51P1T	Asserted

Figure 5.25: Relay 2 Operation SER for SLG fault at Line 2-5 in Islanded Mode

5.2.3 Testing Settings Group Change

Three settings groups were developed for grid-connected, Islanded with Solar, and Islanded with Wind. Each setting group was triggered using input contacts. The status of these input contacts was changed by changing the state of the microgrid. Figure 5.26, Figure 5.27 and Figure 5.28 show the settings group change for the assertion of respective input contact. SER for these group settings changes is shown in Figure 5.29. It can be seen from the SER that there is a time lag of 0.129 secs between the assertion of input contact and settings group change. This issue is switching the settings group in real-time, the system is rendered without protection for the time lag. If a fault occurs during this instant, the system won't be able to detect it and it can create stability issues due to prolonged time requirement for fault clearing.

5.2.4 Testing Adaptive Settings without Settings Group Change

The developed algorithm was tested using the settings developed in the earlier sections for all modes of microgrid operation. The relay R1 was tested and the adaptive

```
=>>TAR IN101

SFAST    SSLOW    IN106    IN105    IN104    IN103    IN102    IN101
0        0        0        0        0        0        0        1

=>>SHO

Group 1
Group Settings:
RID      =SEL-351S51HB455421              TID      =MTU-KF-BCNT  9/17/2008
CTR      = 100        CTRN     = 1        PTR      = 86.00     PTRS     = 1.00
VNOM     = 67.00
Z1MAG    = 1.47       Z1ANG    = 72.00    Z0MAG    = 4.41      Z0ANG    = 68.00
LL       = 47.00
E50P     = 1          E50N     = N        E50G     = N         E50Q     = N
E51P     = 1          E51N     = N        E51G     = N         E51Q     = N
E50BF    = N          EHBL2    = N        E32      = Y         ELOAD    = N
ESOTF    = N          EVOLT    = N        E25      = N         EFLOC    = N
ELOP     = N          ECOMM    = N        E81      = N         E81R     = N
E79      = N          ESV      = 1        EDEM     = THM       EPWR     = N
ESSI     = N
50P1P    = 25.00
67P1D    = 0.00
50PP1P   = OFF
51P1P    = 3.84       51P1C    = U3       51P1TD   = 2.46      51P1RS   = N
51P1CT   = 0.00       51P1MR   = 0.00
DIR1     = F          DIR2     = F        DIR3     = F         DIR4     = R
```

Figure 5.26: Settings Group change to Group 1 due to IN101 assertion

```
=>>TAR IN101

SFAST    SSLOW    IN106    IN105    IN104    IN103    IN102    IN101
0        0        0        0        0        0        1        0

=>>SHO

Group 2
Group Settings:
RID      =SEL-351S51HB455421              TID      =MTU-KF-BCNT  9/17/2008
CTR      = 100        CTRN     = 1        PTR      = 86.00     PTRS     = 86.00
VNOM     = 67.00
Z1MAG    = 1.47       Z1ANG    = 72.00    Z0MAG    = 4.41      Z0ANG    = 68.00
LL       = 47.00
E50P     = 1          E50N     = N        E50G     = N         E50Q     = N
E51P     = 1          E51N     = N        E51G     = N         E51Q     = N
E50BF    = N          EHBL2    = N        E32      = Y         ELOAD    = N
ESOTF    = N          EVOLT    = N        E25      = N         EFLOC    = N
ELOP     = N          ECOMM    = N        E81      = N         E81R     = N
E79      = N          ESV      = 1        EDEM     = THM       EPWR     = N
ESSI     = N
50P1P    = 3.50
67P1D    = 0.00
50PP1P   = OFF
51P1P    = 3.50       51P1C    = U3       51P1TD   = 1.00      51P1RS   = N
51P1CT   = 0.00       51P1MR   = 0.00
DIR1     = N          DIR2     = N        DIR3     = N         DIR4     = N
```

Figure 5.27: Settings Group change to Group 2 due to IN102 assertion

```
=>>TAR IN101

SFAST    SSLOW    IN106    IN105    IN104    IN103    IN102    IN101
0        0        0        0        0        1        0        0

=>>SHO

Group 3
Group Settings:
RID      =SEL-351S51HB455421              TID      =MTU-KF-BCNT  9/17/2008
CTR      = 100        CTRN     = 1        PTR      = 86.00     PTRS     = 86.00
VNOM     = 67.00
Z1MAG    = 99.00      Z1ANG    = 90.00    Z0MAG    = 99.00     Z0ANG    = 90.00
LL       = 999.00
E50P     = 1          E50N     = N        E50G     = N         E50Q     = N
E51P     = N          E51N     = N        E51G     = N         E51Q     = N
E50BF    = N          EHBL2    = N        E32      = N         ELOAD    = N
ESOTF    = N          EVOLT    = N        E25      = N         EFLOC    = N
ELOP     = N          ECOMM    = N        E81      = N         E81R     = N
E79      = N          ESV      = 1        EDEM     = THM       EPWR     = N
ESSI     = N
50P1P    = 66.67
67P1D    = 0.00
50PP1P   = OFF
DMTC     = 60         PDEMP    = OFF      NDEMP    = OFF       GDEMP    = OFF
QDEMP    = OFF
TDURD    = 20.00      CFD      = 60.00    3POD     = 1.00      50LP     = OFF
```

Figure 5.28: Settings Group change to Group 3 due to IN103 assertion

=>>#	Date	Time	Element	State
6	03/22/21	15:09:08.461	IN101	Deasserted
5	03/22/21	15:09:09.586	IN102	Asserted
4	03/22/21	15:09:09.715	Relay group changed	
3	03/22/21	15:09:43.085	IN102	Deasserted
2	03/22/21	15:09:44.335	IN103	Asserted
1	03/22/21	15:09:44.464	Relay group changed	

Figure 5.29: SER for group settings change

algorithm operation was verified. A SLG fault was simulated at Load 5 terminals and the states of microgrid were changed accordingly which automatically altered the pickup. The pickup values seamlessly followed the grid states and there was not a single moment when the system was left without protection. Figure 5.30 and Figure 5.31 show the HMI and SER for relay 1 grid connected mode and IN101 asserted. As IN101 is asserted the active pickup setting is the one that is set for grid connected mode and the relay is able to detect fault as seen from the figures.

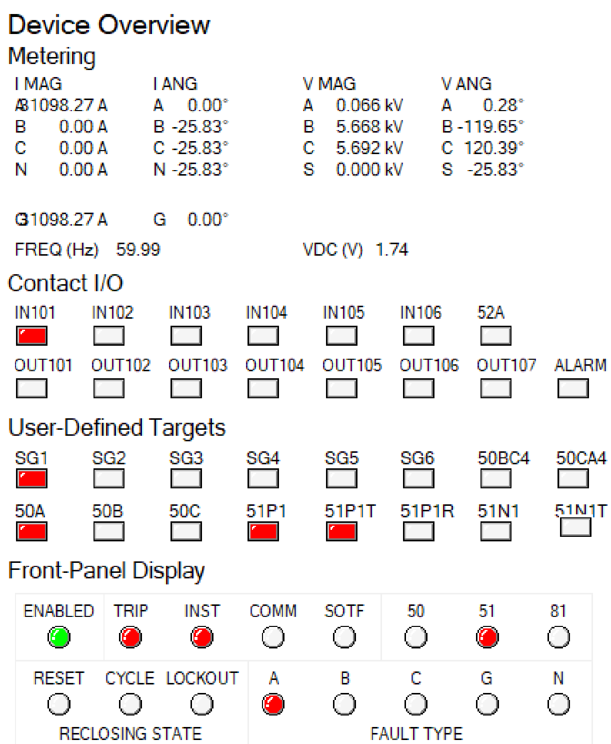

Figure 5.30: Relay 1 HMI for grid connected mode and IN101 asserted

Figure 5.32 and Figure 5.33 show the operation of relay for islanded Solar connected

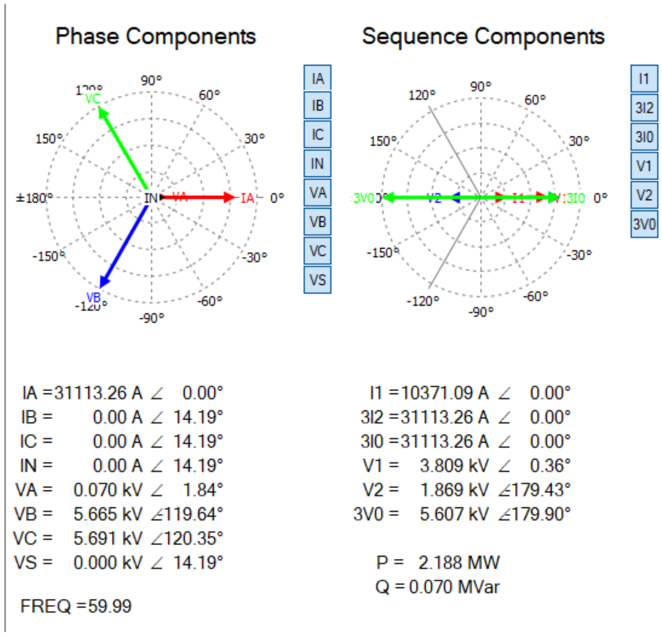

Figure 5.31: Relay 1 Phasor for grid connected mode and IN101 asserted

mode and IN101 asserted. This condition was intentionally created to verify the algorithm. In this case the 50P2 was picked up but as the input IN101 was made one and IN102 was zero, the 67P2 was not able to assert and the relay didn't generate a trip.

To further verify the algorithm, the IN101 was dropped and IN102 was asserted. The relay was able to generate a trip as shown in Figure 5.34. The same was tested with IN103 and Islanded mode with wind Connected, the HMI for which is shown in Figure 5.35.

The complete SER for all the testing performed on the developed algorithm is shown in Figure 5.36. It can be clearly seen that the assertion of input bit controls the trip generation although the relay element is picked up. Thus, the only shortcoming of this scheme is that if the input contact status fails then the relay will not be able to generate a trip.

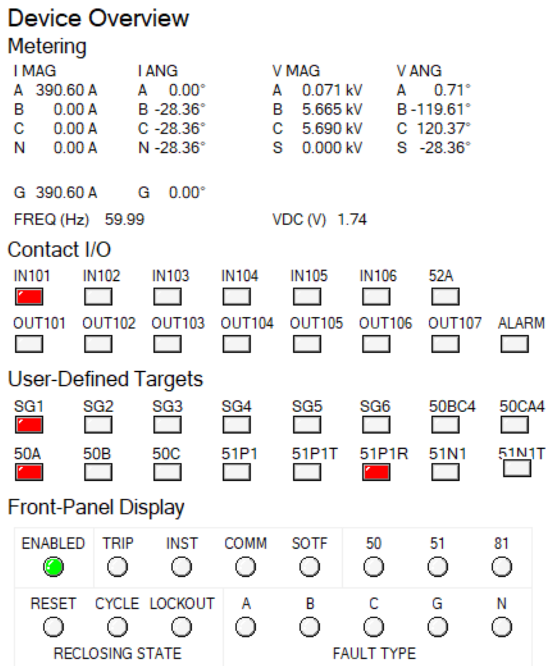

Figure 5.32: Relay 1 HMI for Islanded Solar connected mode and IN101 asserted

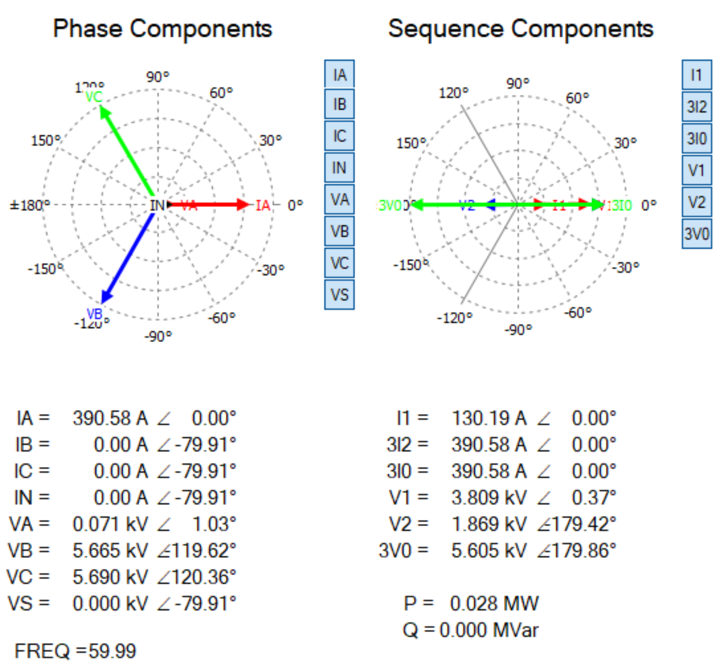

Figure 5.33: Relay 1 Phasor for Islanded Solar connected mode and IN101 asserted

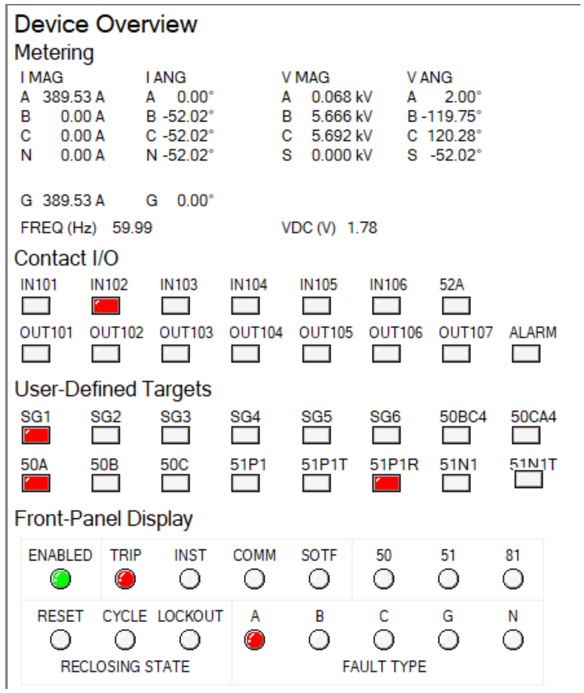

Figure 5.34: Relay 1 HMI for Solar connected mode and IN102 asserted

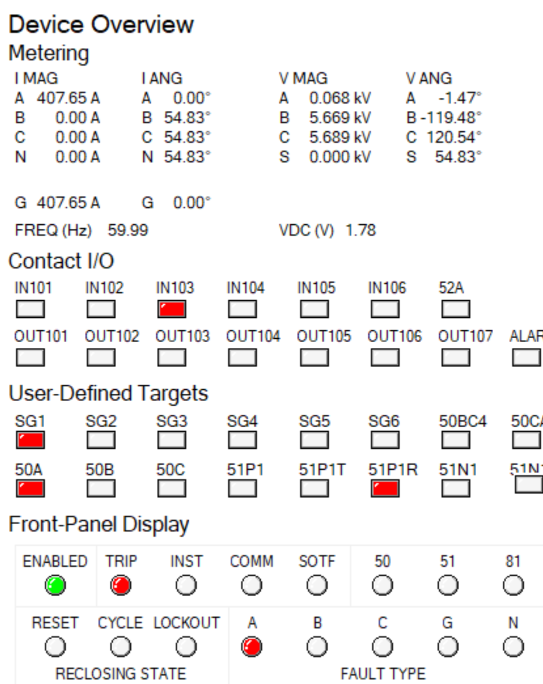

Figure 5.35: Relay 1 HMI for Wind connected mode and IN103 asserted

#	Date	Time	Element	State
17	03/22/21	16:44:19.522	SER archive cleared	
16	03/22/21	16:44:33.629	IN101	Asserted
15	03/22/21	16:44:33.658	51P1	Asserted
14	03/22/21	16:44:33.842	51P1T	Asserted
13	03/22/21	16:44:33.842	TRIP	Asserted
12	03/22/21	16:45:56.632	IN101	Deasserted
11	03/22/21	16:45:56.757	51P1	Deasserted
10	03/22/21	16:45:56.774	51P1T	Deasserted
9	03/22/21	16:46:05.357	TRIP	Deasserted
8	03/22/21	16:47:05.379	IN101	Asserted
7	03/22/21	16:47:19.630	IN101	Deasserted
6	03/22/21	16:47:20.626	IN102	Asserted
5	03/22/21	16:47:20.626	TRIP	Asserted
4	03/22/21	16:48:26.878	IN102	Deasserted
3	03/22/21	16:48:54.222	TRIP	Deasserted
2	03/22/21	16:48:54.501	IN103	Asserted
1	03/22/21	16:48:54.526	TRIP	Asserted

Figure 5.36: Complete SER for Algorithm Testing

Chapter 6

Conclusion

This chapter concludes the findings of this research project. The future scope and work for this project are also described herein in brief.

6.1 Conclusions of Adaptive Protection

The relay settings group change is a good method to address the short circuit level change from grid-connected mode to islanded mode and its operation was successfully verified on IEEE 5 Bus test-bus modified into a microgrid. Settings were developed and the coordination between feeder and line relays was verified on standard 5 Bus as well as modified 5 Bus microgrid system. The issue of the settings group change method which renders the system without protection for a time period while the settings group is being changed was identified and addressed by making use of the internal relay algorithm to develop an algorithm that can have adaptive pickup values depending on the state of microgrid. The developed algorithm was tested using the same pickup settings and the operation was verified for all possible cases. The algorithm successfully passed the testing and shows a promising potential solution for microgrid adaptive protection algorithm.

Following conclusions were derived by testing adaptive algorithm.

- † Adaptive group change in the relay while in service has a time period for which the relay is not protecting the system. This time period depends on relay input contact debounce timer settings (typically 0.25 cycles); group change delay settings and the time required by the relay to switch between protection groups. This can range from 100 ms to 1 s in some cases.

- † The developed adaptive algorithm without group change requirement overcomes the issue with group change algorithm. Also, the maximum settings group that can be switched is 6. This is also overcome and the limiting factor in the developed algorithm is only the relay input contacts (can be up to 16) or remote bits (up to 32)

6.2 Conclusions of Relay in Loop

The relay in the loop method is versatile to test the relay settings and developed algorithms in real-time with near to actual system modeling and testing. It also gives the ability to verify the settings during the dynamic states of the microgrid. This feature is really helpful to study the elements such as out of step and power swing protection algorithms.

Following conclusions were noted for real time testing SEL-351S relay using OPAL-RT as digital simulator.

- † The minimum time step for real time simulation should be 50 microseconds or greater. If it is smaller than this, data overflow occurs in OP5600.
- † There was a data loss seen in the signals read from OP5600 to host PC. This was mainly due to Ethernet connectivity between host PC and OP5600. It can be resolved by using an Ethernet switch and ensuring proper connectivity.

6.3 Future Work

The scope of this project was limited to testing the developed algorithm on SEL-351S relay only which has limited input contacts and doesn't have the feature to create a protection free-form logic.

Following work can be done on this project in future.

- † Real time testing can be performed on the developed logic in SEL-451 relay.The future work on this project is to develop the algorithm in the SEL-451 relay which has the ability to create a protection free form logic. Using this feature, a customized protection element can be created that can implement this algorithm on a wider scale and won't be limited to just 4 pickup values. The limitation, in that case, would only be the hardware limitation, which is the availability of input contacts. The current SEL-451 relays have 16 input contacts which can provide 16 different pickup values for different 16 states of the microgrid.
- † Large systems with multiple pickup settings can be developed using protection free form logic in SEL-451 relay.
- † Number of pickup settings available is equal to number of input contacts or the number of remote bits available. Thus, algorithm with remote bits as can be

developed and verified for larger systems.

† Combined Solar and Wind with diesel simulation can be done by performing control parameter tuning to achieve stable operation then test the system for adaptive settings algorithms.

† Battery Energy Storage was not simulated. It can be done as future work.

References

[1] P. Ray and M. Biswal, *Microgrid Operation, Control Monitoring and Protection.* Springer, Cham, Switzerland, 2020.

[2] D. T. Ton and M. A. Smith, "The U.S. Department of Energy's Microgrid Initiative," *The Electricity Journal*, vol. 25, pp. 84–94, 2012.

[3] N. M. Tabatabaei, E. Kabalci, and N. Bizon, *Microgrid Architectures, Control and Protection Methods.* Springer, Cham, Switzerland, 2020.

[4] B. Patnaik, M. Mishra, R. C. Bansal, and R. K. Jena, "Ac microgrid protection – a review: Current and future prospective," *Applied Energy*, vol. 271, p. 115210, 2020.

[5] P. Gupta, R. S. Bhatia, and D. K. Jain, "Adaptive protection schemes for the microgrid in a smart grid scenario: Technical challenges," in *2013 IEEE Innovative Smart Grid Technologies-Asia (ISGT Asia)*, pp. 1–5, 2013.

[6] D. Liu, D. Tzelepis, and A. Dyśko, "Protection of microgrids with high amounts of renewables: Challenges and solutions," in *2019 54th International Universities Power Engineering Conference (UPEC)*, pp. 1–6, 2019.

[7] M. Dewadasa, A. Ghosh, and G. Ledwich, "Protection of microgrids using differential relays," in *AUPEC 2011*, pp. 1–6, 2011.

[8] M. Dewadasa, A. Ghosh, and G. Ledwich, “Protection of microgrids using differential relays,” in *AUPEC 2011*, pp. 1–6, 2011.

[9] E. Sortomme, S. S. Venkata, and J. Mitra, “Microgrid protection using communication-assisted digital relays,” *IEEE Transactions on Power Delivery*, vol. 25, no. 4, pp. 2789–2796, 2010.

[10] E. Sortomme, J. Ren, and S. S. Venkata, “A differential zone protection scheme for microgrids,” in *2013 IEEE Power Energy Society General Meeting*, pp. 1–5, 2013.

[11] S. R. Samantaray, G. Joos, and I. Kamwa, “Differential energy based microgrid protection against fault conditions,” in *2012 IEEE PES Innovative Smart Grid Technologies (ISGT)*, pp. 1–7, 2012.

[12] E. O. Schweitzer, B. Kasztenny, A. Guzmán, V. Skendzic, and M. V. Mynam, “Speed of line protection - can we break free of phasor limitations?,” in *2015 68th Annual Conference for Protective Relay Engineers*, pp. 448–461, 2015.

[13] X. Li, A. Dyśko, and G. M. Burt, “Traveling wave-based protection scheme for inverter-dominated microgrid using mathematical morphology,” *IEEE Transactions on Smart Grid*, vol. 5, no. 5, pp. 2211–2218, 2014.

[14] A. Zidan, M. Khairalla, A. M. Abdrabou, T. Khalifa, K. Shaban, A. Abdrabou, R. El Shatshat, and A. M. Gaouda, “Fault detection, isolation, and service restoration in distribution systems: State-of-the-art and future trends,” *IEEE Transactions on Smart Grid*, vol. 8, no. 5, pp. 2170–2185, 2017.

[15] X. Li, A. Dyśko, and G. M. Burt, “Traveling wave-based protection scheme for inverter-dominated microgrid using mathematical morphology,” *IEEE Transactions on Smart Grid*, vol. 5, no. 5, pp. 2211–2218, 2014.

[16] S. Gautam and S. M. Brahma, "Overview of mathematical morphology in power systems — a tutorial approach," in *2009 IEEE Power Energy Society General Meeting*, pp. 1–7, 2009.

[17] E. Piesciorovsky, *Relay in the Loop Test Procedures for Adaptive Overcurrent Protection*. PhD thesis, 12 2015.

[18] P. C. Ramaswamy and G. Deconinck, "Relevance of voltage control, grid reconfiguration and adaptive protection in smart grids and genetic algorithm as an optimization tool in achieving their control objectives," in *2011 International Conference on Networking, Sensing and Control*, pp. 26–31, 2011.

[19] I. Abdulhadi, F. Coffele, A. Dysko, C. Booth, and G. Burt, "Adaptive protection architecture for the smart grid," in *2011 2nd IEEE PES International Conference and Exhibition on Innovative Smart Grid Technologies*, pp. 1–8, 2011.

[20] M. V. Sham, K. S. Chethan, and K. P. Vittal, "Development of adaptive distance relay for statcom connected transmission line," in *ISGT2011-India*, pp. 248–253, 2011.

[21] M. R. Islam and H. A. Gabbar, "Analysis of microgrid protection strategies," in *2012 International Conference on Smart Grid (SGE)*, pp. 1–6, 2012.

[22] M. Ojaghi, Z. Sudi, and J. Faiz, "Implementation of full adaptive technique to optimal coordination of overcurrent relays," *IEEE Transactions on Power Delivery*, vol. 28, no. 1, pp. 235–244, 2013.

[23] H. Laaksonen, D. Ishchenko, and A. Oudalov, "Adaptive protection and microgrid control design for hailuoto island," *IEEE Transactions on Smart Grid*, vol. 5, no. 3, pp. 1486–1493, 2014.

[24] N. A. Laway and H. O. Gupta, "A method for adaptive coordination of overcurrent relays in an interconnected power system," in *1993 Fifth International Conference on Developments in Power System Protection*, pp. 240–243, 1993.

[25] M. S. Sachdev, T. S. Sidhu, and B. K. Talukdar, "Topology detection for adaptive protection of distribution networks," in *Proceedings 1995 International Conference on Energy Management and Power Delivery EMPD '95*, vol. 1, pp. 445–450 vol.1, 1995.

[26] Yujie Zhang, J. L. Bastos, and N. N. Schulz, "Model-based design of a protection scheme for shipboard power systems," in *2008 IEEE Power and Energy Society General Meeting - Conversion and Delivery of Electrical Energy in the 21st Century*, pp. 1–9, 2008.

[27] P. Mahat, Z. Chen, B. Bak-Jensen, and C. L. Bak, "A simple adaptive overcurrent protection of distribution systems with distributed generation," *IEEE Transactions on Smart Grid*, vol. 2, no. 3, pp. 428–437, 2011.

[28] C. Liu, Z. Chen, and Z. Liu, "A communication-less overcurrent protection for distribution system with distributed generation integrated," in *2012 3rd IEEE International Symposium on Power Electronics for Distributed Generation Systems (PEDG)*, pp. 140–147, 2012.

[29] B. Matic-Cuka and M. Kezunovic, "Improving smart grid operation with new hierarchically coordinated protection approach," in *8th Mediterranean Conference on Power Generation, Transmission, Distribution and Energy Conversion (MEDPOWER 2012)*, pp. 1–6, 2012.

[30] M. Khederzadeh, "Adaptive setting of protective relays in microgrids in grid-connected and autonomous operation," in *11th IET International Conference on Developments in Power Systems Protection (DPSP 2012)*, pp. 1–4, 2012.

[31] C. Buque, O. Ipinnimo, S. Chowdhury, and S. P. Chowdhury, "Modeling and simulation of an adaptive relaying scheme for a microgrid," in *2012 IEEE Power and Energy Society General Meeting*, pp. 1–8, 2012.

[32] L. A. Montoya, D. Montenegro, and G. Ramos, "Adaptive protection testbed using real time and hardware-in-the-loop simulation," in *2013 IEEE Grenoble Conference*, pp. 1–4, 2013.

[33] V. A. S. Rones and K. P. Vittal, "Adaptive protection schemes for feeders with the penetration of seig based wind farm," in *2013 IEEE Innovative Smart Grid Technologies-Asia (ISGT Asia)*, pp. 1–6, 2013.

[34] R. Jafari, M. S. Naderi, G. B. Gharehpetian, and N. Moaddabi, "Compensation of dgs impact on overcurrent protection system of smart micro-grids," in *22nd International Conference and Exhibition on Electricity Distribution (CIRED 2013)*, pp. 1–4, 2013.

[35] M. Singh, "Protection coordination in grid connected islanded modes of micro-grid operations," in *2013 IEEE Innovative Smart Grid Technologies-Asia (ISGT Asia)*, pp. 1–6, 2013.

[36] P. Gupta, R. S. Bhatia, and D. K. Jain, "Adaptive protection schemes for the microgrid in a smart grid scenario: Technical challenges," in *2013 IEEE Innovative Smart Grid Technologies-Asia (ISGT Asia)*, pp. 1–5, 2013.

[37] Z. C. Li, J. Hu, J. H. He, and T. Yip, "A protection method for microgrids based on information sharing," in *12th IET International Conference on Developments in Power System Protection (DPSP 2014)*, pp. 1–5, 2014.

[38] V. A. Papaspiliotopoulos, G. N. Korres, and N. D. Hatziargyriou, "Protection coordination in modern distribution grids integrating optimization techniques with adaptive relay setting," in *2015 IEEE Eindhoven PowerTech*, pp. 1–6, 2015.

[39] A. Gupta, A. Varshney, O. V. G. Swathika, and S. Hemamalini, "Dual simplex algorithm aided adaptive protection of microgrid," in *2015 International Conference on Computational Intelligence and Communication Networks (CICN)*, pp. 1505–1509, 2015.

[40] M. G. Maleki, H. Javadi, M. Khederzadeh, M. Bayrami, and S. Farajzadeh, "Data exchange standardization in a microgrid protection scheme according to the iec 61850," in *2015 Smart Grid Conference (SGC)*, pp. 130–137, 2015.

[41] Hengwei Lin, J. M. Guerrero, Chenxi Jia, Zheng-hua Tan, J. C. Vasquez, and Chengxi Liu, "Adaptive overcurrent protection for microgrids in extensive distribution systems," in *IECON 2016 - 42nd Annual Conference of the IEEE Industrial Electronics Society*, pp. 4042–4047, 2016.

[42] K. A. Wheeler, S. O. Faried, and M. Elsamahy, "A microgrid protection scheme using differential and adaptive overcurrent relays," in *2017 IEEE Electrical Power and Energy Conference (EPEC)*, pp. 1–6, 2017.

[43] A. I. Atteya, A. M. El Zonkoly, and H. A. Ashour, "Optimal relay coordination of an adaptive protection scheme using modified pso algorithm," in *2017 Nineteenth International Middle East Power Systems Conference (MEPCON)*, pp. 689–694, 2017.

[44] Z. Kailun, D. S. Kumar, D. Srinivasan, and A. Sharma, "An adaptive overcurrent protection scheme for microgrids based on real time digital simulation," in *2017 IEEE Innovative Smart Grid Technologies - Asia (ISGT-Asia)*, pp. 1–6, 2017.

[45] K. Sedghisigarchi and K. T. Sardari, "An adaptive protection strategy for reliable operation of microgrids," in *2018 IEEE International Energy Conference (ENERGYCON)*, pp. 1–6, 2018.

[46] M. Amaratunge, D. U. Y. Edirisuriya, A. L. A. P. L. Ambegoda, M. A. C. Costa, W. L. T. Peiris, and K. T. M. U. Hemapala, "Development of adaptive overcurrent relaying scheme for iidg microgrids," in *2018 2nd International Conference On Electrical Engineering (EECon)*, pp. 71–75, 2018.

[47] M. Singh and A. V. Ravi Teja, "Adaptive over-current protection algorithm for a microgrid," in *2018 IEEE 13th International Conference on Industrial and Information Systems (ICIIS)*, pp. 448–452, 2018.

[48] M. J. Daryani, A. E. Karkevandi, and O. Usta, "Harmonics content and voltage signal based hybrid backup scheme for protection of microgrid under different contingencies," in *2019 IEEE PES Innovative Smart Grid Technologies Europe (ISGT-Europe)*, pp. 1–5, 2019.

[49] N. Kumar and D. K. Jain, "An adaptive inverse-time overcurrent protection method for low voltage microgrid," in *2020 IEEE 9th Power India International Conference (PIICON)*, pp. 1–5, 2020.

[50] A. Ghoor and S. Chowdhury, "Design of adaptive overcurrent protection scheme for a grid-integrated solar pv microgrid," in *2020 IEEE PES/IAS PowerAfrica*, pp. 1–5, 2020.

[51] M. Amirsaman, *Hardware-in-the-loop testing of protection relays in distribution feeders with high penetration of distributed generation.* PhD thesis, 05 2016.

[52] S. S. Noureen, V. Roy, and S. B. Bayne, "An overall study of a real-time simulator and application of rt-lab using matlab simpowersystems," in *2017 IEEE Green Energy and Smart Systems Conference (IGESSC)*, pp. 1–5, 2017.

[53] https://www.opal-rt.com/protection-system overview/, *OPAL-RT website.* (accessed: 02.04.2021).

[54] Schweitzer Engineering Laboratories, *SEL-351S: Distribution Protection System, Flyer*.

[55] Schweitzer Engineering Laboratories, *SEL-351S: Distribution Protection System, Data sheet*.

[56] Schweitzer Engineering Laboratories, *SEL-351S: Distribution Protection System, Instruction Manual*.

[57] A. A. Bhandakkar and L. Mathew, "Real-time-simulation of IEEE-5-bus network on OPAL-RT-OP4510 simulator," *IOP Conference Series: Materials Science and Engineering*, vol. 331, p. 012028, mar 2018.

[58] S. Nick, H. Ariana, and D. Swagata, *Calculating and Testing the Operating Time of an Inverse-Time Overcurrent Curve*. Schweitzer Engineering Laboratories, 2015.

[59] J. Giraldez, F. Francisco, M. Sara, and A. Peter, "Phase 1 microgrid cost study: Data collection and analysis of microgrid costs in the united states," in *Report from National Renewable Energy Laboratory*, 2018.

[60] E. Muljadi, N. Samaan, V. Gevorgian, Jun Li, and S. Pasupulati, "Short circuit current contribution for different wind turbine generator types," in *IEEE PES General Meeting*, pp. 1–8, 2010.

[61] D. Liu, D. Tzelepis, and A. Dyśko, "Protection of microgrids with high amounts of renewables: Challenges and solutions," in *2019 54th International Universities Power Engineering Conference (UPEC)*, pp. 1–6, 2019.

[62] http://wikipedia.org/, *Wikipedia*. The Internet: Wikipedia, 2012.

[63] S. Shi, X. Dong, and S. Wang, "Traveling waves based protection relaying of power lines," in *2011 International Conference on Advanced Power System Automation and Protection*, vol. 3, pp. 2467–2471, 2011.

[64] C. Mishra, D. K. Mohanta, and M. J. B. Reddy, "Impact of adaptive relaying in smart grid," in *2014 14th International Conference on Environment and Electrical Engineering*, pp. 169–174, 2014.

Appendix A

Appendix : Complete Relay Settings

```
=>sho
Group 1
Group Settings:

RID     =SEL-351S51HB455421             TID     =MTU-KF-BCNT  9/17/2008
CTR     = 1000       CTRN    = 1
PTR     = 86.00      PTRS    = 1.00      VNOM    = 67.00
Z1MAG   = 2.14       Z1ANG   = 68.86     Z0MAG   = 6.38      Z0ANG   = 72.47
LL      = 4.84
E50P    = 1          E50N    = N         E50G    = N         E50Q    = N
E51P    = 1          E51N    = N         E51G    = N         E51Q    = N
E32     = N          ELOAD   = N         ESOTF   = N         EVOLT   = N
E25     = N          EFLOC   = N         ELOP    = N         ECOMM   = N
E81     = N          E79     = N         ESV     = 1         EDEM    = THM
EPWR    = N          ESSI    = N
50P1P   = 58.00
67P1D   = 0.00
50PP1P  = OFF
51P1P   = 4.14       51P1C   = U3        51P1TD  = 1.00      51P1RS  = N
51P1CT  = 0.00       51P1MR  = 0.00
DMTC    = 60

Press RETURN to continue
PDEMP   = OFF        NDEMP   = OFF       GDEMP   = OFF       QDEMP   = OFF
TDURD   = 20.00      CFD     = 60.00     3POD    = 1.00      50LP    = OFF
SV1PU   = 5.00       SV1DO   = 0.00
```

Figure A.1: Settings for Relay 1

```
=>>SHO
Group 1
Group Settings:

RID     =SEL-351S51HB455421            TID     =MTU-KF-BCNT  9/17/2008
CTR     = 1000      CTRN    = 1
PTR     = 86.00     PTRS    = 1.00      VNOM    = 67.00
Z1MAG   = 1.47      Z1ANG   = 72.00     Z0MAG   = 4.41      Z0ANG   = 68.00
LL      = 47.00
E50P    = 1         E50N    = 1         E50G    = N         E50Q    = N
E51P    = 2         E51N    = N         E51G    = N         E51Q    = N
E32     = Y         ELOAD   = N         ESOTF   = N         EVOLT   = N
E25     = N         EFLOC   = N         ELOP    = N         ECOMM   = N
E81     = N         E79     = N         ESV     = 1         EDEM    = THM
EPWR    = N         ESSI    = N
50P1P   = 42.00
67P1D   = 0.00
50PP1P  = OFF
50N1P   = OFF
67N1D   = 0.00
51P1P   = 3.55      51P1C   = U3        51P1TD  = 3.36      51P1RS  = N

Press RETURN to continue
51P1CT  = 0.00      51P1MR  = 0.00
51P2P   = OFF       51P2C   = U3        51P2TD  = 3.00      51P2RS  = N
51P2CT  = 0.00      51P2MR  = 0.00
DIR1    = F         DIR2    = F         DIR3    = F         DIR4    = F
ORDER   = OFF       50P32P  = 3.00      Z2F     = 1.08      Z2R     = 1.28
50QFP   = 0.50      50QRP   = 0.25      a2      = 0.10      k2      = 0.20
DMTC    = 60
PDEMP   = OFF       NDEMP   = OFF       GDEMP   = OFF       QDEMP   = OFF
TDURD   = 20.00     CFD     = 60.00     3POD    = 1.00      50LP    = OFF
```

Figure A.2: Settings for Relay at Line 2-5

```
Group 1
Group Settings:
RID     =SEL-351S51HB455421            TID     =MTU-KF-BCNT  9/17/2008
CTR     = 100       CTRN    = 1         PTR     = 86.00     PTRS    = 1.00
VNOM    = 67.00
Z1MAG   = 2.14      Z1ANG   = 68.86     Z0MAG   = 6.38      Z0ANG   = 72.47
LL      = 4.84
E50P    = 1         E50N    = N         E50G    = N         E50Q    = N
E51P    = 1         E51N    = N         E51G    = N         E51Q    = N
E50BF   = N         EHBL2   = N         E32     = N         ELOAD   = N
ESOTF   = N         EVOLT   = N         E25     = N         EFLOC   = N
ELOP    = N         ECOMM   = N         E81     = N         E81R    = N
E79     = N         ESV     = 1         EDEM    = THM       EPWR    = N
ESSI    = N
50P1P   = 37.55
67P1D   = 0.00
50PP1P  = OFF
51P1P   = 5.26      51P1C   = U3        51P1TD  = 1.00      51P1RS  = N
51P1CT  = 0.00      51P1MR  = 0.00
DMTC    = 60        PDEMP   = OFF       NDEMP   = OFF       GDEMP   = OFF

Press RETURN to continue

QDEMP   = OFF
TDURD   = 20.00     CFD     = 60.00     3POD    = 1.00      50LP    = OFF
SV1PU   = 5.00      SV1DO   = 0.00
```

Figure A.3: Settings for Grid Connected mode Relay 1

```
Group 1
Group Settings:
RID     =SEL-351S51HB455421            TID     =MTU-KF-BCNT  9/17/2008
CTR     = 100        CTRN    = 1       PTR     = 86.00      PTRS    = 1.00
VNOM    = 67.00
Z1MAG   = 1.47       Z1ANG   = 72.00   Z0MAG   = 4.41       Z0ANG   = 68.00
LL      = 47.00
E50P    = 1          E50N    = N       E50G    = N          E50Q    = N
E51P    = 1          E51N    = N       E51G    = N          E51Q    = N
E50BF   = N          EHBL2   = N       E32     = Y          ELOAD   = N
ESOTF   = N          EVOLT   = N       E25     = N          EFLOC   = N
ELOP    = N          ECOMM   = N       E81     = N          E81R    = N
E79     = N          ESV     = 1       EDEM    = THM        EPWR    = N
ESSI    = N
50P1P   = 25.00
67P1D   = 0.00
50PP1P  = OFF
51P1P   = 3.84       51P1C   = U3      51P1TD  = 2.46       51P1RS  = N
51P1CT  = 0.00       51P1MR  = 0.00
DIR1    = F          DIR2    = F       DIR3    = F          DIR4    = R

Press RETURN to continue

ORDER   = OFF        50P32P  = 0.50    Z2F     = 1.08       Z2R     = 1.28
50QFP   = 0.50       50QRP   = 0.25    a2      = 0.10       k2      = 0.20
DMTC    = 60         PDEMP   = OFF     NDEMP   = OFF        GDEMP   = OFF
QDEMP   = OFF
TDURD   = 20.00      CFD     = 60.00   3POD    = 1.00       50LP    = OFF
SV1PU   = 5.00       SV1DO   = 0.00
```

Figure A.4: Settings for Grid Connected mode Relay 2

```
=>>sho

Group 2
Group Settings:
RID     =SEL-351S51HB455421            TID     =MTU-KF-BCNT  9/17/2008
CTR     = 100        CTRN    = 1       PTR     = 86.00      PTRS    = 86.00
VNOM    = 67.00
Z1MAG   = 2.14       Z1ANG   = 68.86   Z0MAG   = 6.38       Z0ANG   = 72.47
LL      = 4.84
E50P    = 1          E50N    = N       E50G    = N          E50Q    = N
E51P    = 1          E51N    = N       E51G    = N          E51Q    = N
E50BF   = N          EHBL2   = N       E32     = Y          ELOAD   = N
ESOTF   = N          EVOLT   = N       E25     = N          EFLOC   = N
ELOP    = N          ECOMM   = N       E81     = N          E81R    = N
E79     = N          ESV     = 1       EDEM    = THM        EPWR    = N
ESSI    = N
50P1P   = 3.88
67P1D   = 0.00
50PP1P  = OFF
51P1P   = 3.88       51P1C   = U3      51P1TD  = 1.00       51P1RS  = N
51P1CT  = 0.00       51P1MR  = 0.00
DIR1    = N          DIR2    = N       DIR3    = N          DIR4    = N

Press RETURN to continue

ORDER   = OFF        50P32P  = 3.00    Z2F     = 1.08       Z2R     = 1.28
50QFP   = 0.50       50QRP   = 0.25    a2      = 0.10       k2      = 0.20
DMTC    = 60         PDEMP   = OFF     NDEMP   = OFF        GDEMP   = OFF
QDEMP   = OFF
TDURD   = 20.00      CFD     = 60.00   3POD    = 1.00       50LP    = OFF
SV1PU   = 60.00      SV1DO   = 0.00

=>>
```

Figure A.5: Settings for Relay 1 in Islanded Microgrid with Solar

```
Group 2
Group Settings:
RID      =SEL-351S51HB455421             TID      =MTU-KF-BCNT  9/17/2008
CTR      = 100        CTRN     = 1         PTR      = 86.00     PTRS     = 86.00
VNOM     = 67.00
Z1MAG    = 1.47       Z1ANG    = 72.00     Z0MAG    = 4.41      Z0ANG    = 68.00
LL       = 47.00
E50P     = 1          E50N     = N         E50G     = N         E50Q     = N
E51P     = 1          E51N     = N         E51G     = N         E51Q     = N
E50BF    = N          EHBL2    = N         E32      = Y         ELOAD    = N
ESOTF    = N          EVOLT    = N         E25      = N         EFLOC    = N
ELOP     = N          ECOMM    = N         E81      = N         E81R     = N
E79      = N          ESV      = 1         EDEM     = THM       EPWR     = N
ESSI     = N
50P1P    = 3.50
67P1D    = 0.00
50PP1P   = OFF
51P1P    = 3.50       51P1C    = U3        51P1TD   = 1.00      51P1RS   = N
51P1CT   = 0.00       51P1MR   = 0.00
DIR1     = N          DIR2     = N         DIR3     = N         DIR4     = N

Press RETURN to continue

ORDER    = OFF        50P32P   = 3.00      Z2F      = 1.08      Z2R      = 1.28
50QFP    = 0.50       50QRP    = 0.25      a2       = 0.10      k2       = 0.20
DMTC     = 60         PDEMP    = OFF       NDEMP    = OFF       GDEMP    = OFF
QDEMP    = OFF
TDURD    = 20.00      CFD      = 60.00     3POD     = 1.00      50LP     = OFF
SV1PU    = 60.00      SV1DO    = 0.00
```

Figure A.6: Settings for Relay 2 in Islanded Microgrid with Solar